Institute of Experimental and Clinical Pharmacology, Toxicology and Pharmacology of Natural Products

Head: Prof. Dr. Holger Barth

Characterization of new approaches to inhibit Pertussis toxin based on human peptides and cellular chaperone inhibitors

---

Dissertation

submitted in partial fulfilment of the requirements for the degree of

„Doctor rerum naturalium" (Dr. rer. nat.)

of the International Graduate School in Molecular Medicine Ulm

submitted by

Carolin Kling

born in Heilbronn, Germany

2024

Current dean of the Medical Faculty:

Prof. Dr. Thomas Wirth

Current Chairman of the Graduate School:

Prof. Dr. Bernd Knöll

Thesis advisory Committee

First supervisor:	Dr. Katharina Ernst
Second supervisor:	Prof. Dr. Markus Huber-Lang
Third supervisor:	Prof. Dr. Aswin Mangerich
External reviewer:	Prof. Dr. Harald Genth
Day doctorate awarded:	18.01.2024

Results gained in my thesis have previously been published in the following publications:

1. Ernst K, Mittler AK, Winkelmann V, **Kling C**, Eberhardt N, Anastasia A, Sonnabend M, Lochbaum R, Wirsching J, Sakari M, Pulliainen AT, Skerry C, Carbonetti NH, Frick M, Barth H. **Pharmacological targeting of host chaperones protects from pertussis toxin in vitro and in vivo.** Sci Rep. 2021 Mar 8;11(1):5429. doi: 10.1038/s41598-021-84817-2.
2. **Kling C**, Pulliainen AT, Barth H, Ernst K. **Human Peptides α-Defensin-1 and -5 Inhibit Pertussis Toxin.** Toxins (Basel). 2021 Jul 11;13(7):480. doi: 10.3390/toxins13070480.
3. **Kling C**, Sommer A, Almeida-Hernandez Y, Rodríguez A, Perez-Erviti JA, Bhadane R, Ständker L, Wiese S, Barth H, Pupo-Meriño M, Pulliainen A, Sánchez-Garcia E, Ernst K. **Inhibition of Pertussis Toxin by Human α-Defensins-1 and -5: Differential Mechanisms of Action.** *Int. J. Mol. Sci.* 2023, *24 (13)*, 10557. doi: 10.3390/ijms241310557

Table of Contents

List of Abbreviations ..... **II**

1 Introduction **1**

1.1 Pertussis and Pertussis toxin **1**

1.2 Chaperone inhibitors **5**

1.3 Peptide inhibitors: Defensins **8**

1.4 Aim of this Thesis **12**

2 Results and Discussion **13**

2.1 Pharmacological targeting of host chaperones protects from pertussis toxin in vitro and in vivo **13**

2.1.1 Own contributions 13

2.1.2 Summary of Results 13

2.1.3 Discussion 15

2.2 Human Peptides α-Defensin-1 and -5 Inhibit Pertussis Toxin **36**

2.2.1 Own contributions 36

2.2.2 Summary of Results 36

2.2.3 Discussion 37

2.3 Inhibition of Pertussis Toxin by Human α-Defensins-1 and -5: Differential Mechanisms of Action **52**

2.3.1 Own contributions 52

2.3.2 Summary of Results 52

2.3.3 Discussion 55

3 Summary **78**

4 References **79**

5 Statutory Declaration **88**

List of Abbreviations

A. hydrophila	*Aeromonas hydrophila*
α-def-1-6	α-defensin-1-6
AC	adenylyl cylcase
ADP	adenosine diphosphate
AMP	antimicrobial peptide
ATP	adenosine triphosphate
B. anthracis	*Bacillus anthracis*
B. pertussis	*Bordetella pertussis*
β-def-1-3	β-defensin-1-3
BSA	bovine serum albumin
C.	*Clostridium*
cAMP	cyclic adenosine monophosphate
CDC	cholesterol-dependent cytolysins
CDT	*C. difficile* transferase toxin
CHO-K1	Chinese hamster ovary cells
CsA	cyclosporin A
CT	*Vibrio cholerae* toxin
CTA1	A-subunit of CT
Cyp	cyclophilin
Cyp40	cyclophilin 40

CypA	cyclophilin A
DMEM	Dulbecco's Modified Eagle Medium
DSF	differential scanning fluorimetry
DT	diphtheria toxin
DTA	enzyme domain of diphtheria toxin
EEA1	early endosome antigen 1
ER	endoplasmic reticulum
ERAD	ER associated degradation
ETA	*Pseudomonas* exotoxin A
FKBP	FK506-binding protein
FKBP5	FK506-binding protein 5
G-actin	globular actin
Gαi	α-subunit of inhibitory G-proteins
Gαs	α-subunit of stimulatory G-proteins
GA	geldanamycin
gNarE	gonococcal NarE protein
GPCR	G-protein coupled receptor
hBAEC	human bronchial airway epithelial cell
HBD 1-4	human β-defensin-1-4
HD 5-6	human enteric defensins 5-6
HIV	human immunodeficiency virus
HNP1-4	human neutrophil peptides 1-4
Hsc70	heat shock cognate 70

Hsp70	heat shock protein 70
Hsp90	heat shock protein 90
HSV	herpes simplex virus
iGIST	interference in Gαi-mediated Signal Transduction
MARTX	multifunctional autoprocessing repeats-in-toxin
NAD^+	nicotinamide adenine dinucleotide
PDI	protein disulfide isomerase
PES	2-phenylethynesulfonamide
PLA	proximity ligation assay
PPIase	peptidyl-prolyl *cis/trans* isomerase
PT	Pertussis toxin
PTS1-5	Pertussis toxin subunit 1-5
PVL	Panton-Valentine leukocidin
RT	room temperature
S. aureus	*Staphylococcus aureus*
SPR	surface plasmon resonance
SSTR2	somatostatin receptor 2
TcdA	*C. difficile* toxin A
TcdB	*C. difficile* toxin B
TPR	tetratricopeptide repeat
V. cholerae	Vibrio cholerae
wP	whole cell pertussis vaccine
aP	acellular pertussis vaccine

1 Introduction

1.1 Pertussis and Pertussis toxin

Pertussis, also known as whooping cough is a severe respiratory disease, caused by infection with *Bordetella (B.) pertussis*. This highly contagious disease is transmitted by infected persons via airborne droplets by coughing or sneezing without a distinct seasonality (Kilgore et al., 2016). The typical course of disease is characterized by three stages, spreading over 6 to 12 weeks (Mattoo & Cherry, 2005). First, in the catarrhal stage, symptoms, such as rhinorrhea and mild cough are rather unspecific, making a rapid diagnosis of the disease difficult. The paroxysmal stage, starting in the second week of illness and lasting for 2 to 8 weeks, is characterized by repeated paroxysms with multiple heavy coughs within a single expiration, followed by a strong inspiratory effort, leading to the typical whooping. The paroxysms can be accompanied with cyanosis, exhaustion and posttussive vomiting. When the frequency and severity of the paroxysms decline, patients have reached the third stage of disease, the convalescent stage, which usually lasts for 1 to 2 weeks (Mattoo & Cherry, 2005). For older children and adults, further complications are relatively rare, and asymptomatic infections are also quite common (Long et al., 1990; Mattoo & Cherry, 2005). However, young infants are at highest risk to develop severe complications such as seizures, pneumonia, encephalopathy, and pulmonary hypertension leading to a high risk of fatal outcome (Kilgore et al., 2016; Mattoo & Cherry, 2005; Paddock et al., 2008; Surridge et al., 2007). In Germany, the hospitalization rate of infants < 1 year was 40% compared to 6% in all other age groups in 2020 (RKI, 2020). Globally, the WHO estimated 7 to 40 million cases of pertussis and 38 000 to 670 000 deaths from pertussis in children < 5 years in 2014 (Yeung et al., 2017).

After introduction of vaccination programs in the 1950s, numbers of pertussis cases and deaths declined drastically (WHO, 2016). In 2021, ca. 81% of infants were vaccinated worldwide, but still the disease is endemic in all countries, and one of the leading causes of vaccine-preventable deaths and morbidity worldwide (de Graaf et al., 2020; WHO, 2016; WHO Immunization Coverage). Case numbers even rose in the past decades, particularly in countries, that switched from the initially used inactivated whole cell pertussis vaccines (wP) to acellular pertussis vaccines (aP) (Chiappini et al., 2013). Acellular pertussis vaccines exhibited an improved safety profile and

comparable efficacy to whole cell pertussis vaccines, which is why it is applied in most western countries. But immune protection wanes faster than after vaccination with whole cell pertussis vaccines, and also asymptomatic transmission of *B. pertussis* is quite common in individuals, vaccinated with acellular pertussis vaccines (Althouse & Scarpino, 2015; Locht, 2021; Locht & Antoine, 2021; Wilkinson et al., 2021). In addition to these crucial downsides of acellular pertussis vaccines, also genetic adaptation of circulating *B. pertussis* strains to escape vaccine pressure is discussed as a further reason for the resurgence of pertussis cases (Locht, 2021). Unfortunately, besides symptomatic treatment of complications in intensive care, there is no effective treatment, relieving pertussis symptoms (Carbonetti, 2016; Surridge et al., 2007). Antibiotics, such as erythromycin are broadly used to eradicate *B. pertussis* bacteria in patients, preventing further transmission of the infectious disease (Carbonetti, 2016). However, the clinical course of the patients cannot be improved by antibiotics, except for the rare cases of early administration, which is only possible upon a rapid diagnosis (Altunaiji et al., 2007; Ernst, 2022a). Therefore, novel therapeutic strategies are needed, that target the disease-causing toxins.

Several virulence factors of *B. pertussis* act together to promote the pathogenesis of pertussis in a complex way (Kilgore et al., 2016). For example, surface structure proteins, such as filamentous hemagglutinin, fimbriae and pertactin are responsible for adhesion and colonization of the ciliated epithelia of the human respiratory tract (Kilgore et al., 2016). The adenylyl cyclase toxin protects the bacteria from elimination by the immune system by inhibiting activity of phagocytes. The tracheal cytotoxin induces production of pro-inflammatory cytokines as well as nitric oxide, thereby damaging ciliated cells (Kilgore et al., 2016). Even though many different virulence factors collectively contribute to the course of the disease in a way that is not fully understood yet, pertussis toxin (PT) plays an exceptional role in the disease pathogenesis. PT is produced uniquely by the bacterial species *B. pertussis* and is an integral part of acellular vaccines (Kilgore et al., 2016). Originally, PT was named histamine-sensitizing factor, lymphocytosis- and leukocytosis-promoting factor, or islet-activating protein, indicating its various systemic effects (Carbonetti, 2015). The contribution of PT to respiratory symptoms and severe courses of pertussis has only been elucidated in the past decades. A mutant PT-deficient strain of *B. pertussis* resulted in significantly less fatal outcome in an infant mouse model of pertussis infection (Weiss et al., 1984; Weiss & Goodwin, 1989). A more recent study demonstrated an exacerbated and prolonged airway inflammatory response in a mouse model infected with wildtype *B. pertussis*, compared to infection

with a PT-deficient strain (Connelly et al., 2012). Furthermore, findings in different studies on rats, baboons, and natural and volunteer human *B. pertussis* infection indicate an association between PT production and cough responses (Scanlon et al., 2019b). Severe outcomes of pertussis are associated with high white blood cell counts (leukocytosis) resulting in pulmonary hypertension and cardiac failure. PT has been shown to promote leukocytosis and pulmonary hypertension in several animal studies (Scanlon et al., 2019a). In addition, *in vitro* studies demonstrated that PT transiently disrupts the blood-brain barrier, possibly resulting in encephalopathies and neurological disorders (Kügler et al., 2007). The crucial role of PT in severe courses of the disease makes the toxin a promising target for novel therapeutic strategies.

PT belongs to the family of AB-type protein toxins. This family of highly pathogenic exotoxins can act independently of the secreting bacteria and is responsible for diseases like diphtheria, cholera and enteric diseases (Ernst, Schnell, et al., 2017). AB-type toxins consist of two functional domains, the enzymatically active A-domain, responsible for the specific enzymatic action on the substrate, and the B-domain, responsible for binding to the cell and translocation of the A-domain to the target site. This specific mode of action results in the high toxicity of bacterial exotoxins. PT is composed of the A-protomer pertussis toxin subunit 1 (PTS1) and a pentameric B-subunit, consisting of the four different subunits PTS2, PTS3, PTS4 and PTS5 in a ratio of 1:1:2:1 (see Figure 1) (Stein et al., 1994; Tamura et al., 1982). The B-subunits form a triangular base, topped with PTS1, leading to a pyramid-like structure of the holotoxin (Stein et al., 1994). The holotoxin assembles through non-covalent bonds in the periplasm of the bacteria, which is then actively secreted by a type IV secretion system (Locht et al., 2011).

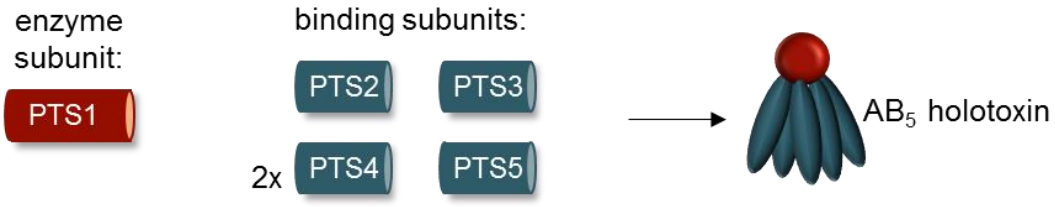

Figure 1: Structure of PT
Pertussis toxin (PT) is composed of the enzyme subunit PTS1 and the binding subunits PTS2-5, forming an AB_5 holotoxin (based on Stein 1984, Tamura 1982)

The B-pentamer enables binding of PT to the cell surface via sialoglycoproteins, found on most mammalian cell types (Armstrong et al., 1988; Hausman & Burns, 1993; Witvliet et al., 1989).

This allows PT to intoxicate a variety of different cell types. After binding, PT is internalized via receptor-mediated endocytosis and follows a retrograde vesicular route through the Golgi to the endoplasmic reticulum (ER) (see Figure 2) (el Bayâ et al., 1997; Teter, 2019).

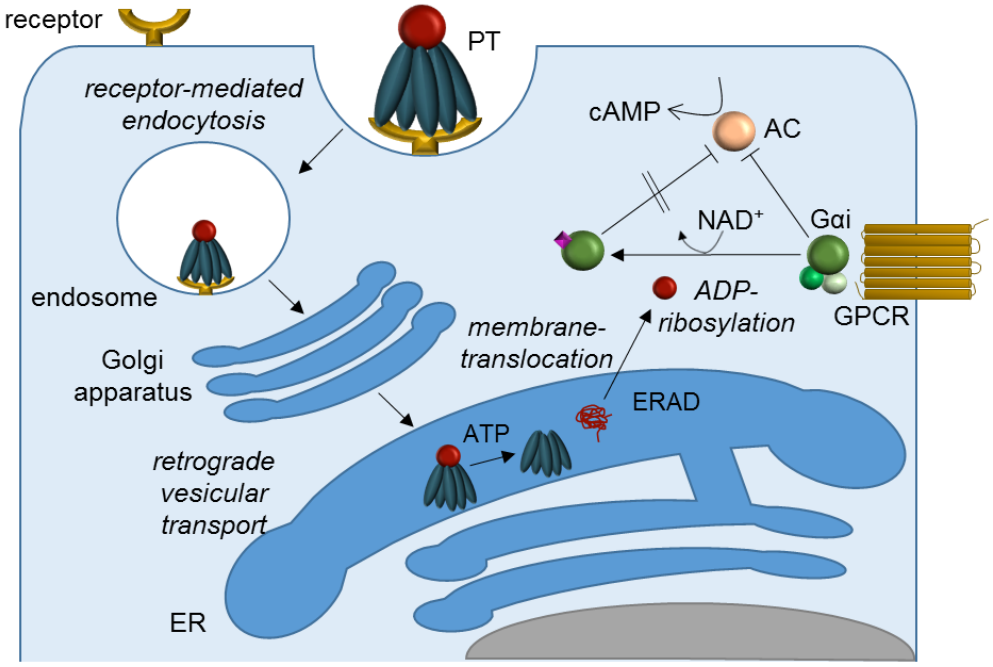

Figure 2: Trafficking and Mode of Action of PT
Pertussis toxin (PT) is taken up into the cell by receptor-mediated endocytosis and follows a retrograde vesicular transport through the Golgi apparatus into the endoplasmic reticulum (ER). There, upon contact with ATP, the A-subunit PTS1 dissociates from the holotoxin and is therefore recognized by the ER-associated degradation (ERAD) pathway and translocated into the cytosol. In the cytosol, PTS1 ADP-ribosylates and thereby inactivates its substrate Gαi, leading to disturbed inhibition of the adenylyl cyclase (AC) and thereby to disturbed cellular cAMP signaling (based on Locht et al., 2011; Teter, 2019).

Interestingly, it was demonstrated, that the cellular uptake is pH- and microtubule-dependent, slowed down by low temperatures and can be inhibited by brefeldin A, an inhibitor of the Golgi apparatus (Punnonen et al., 1998; Schmid & Smythe, 1991; Teter, 2019; Xu & Barbieri, 1995, 1996). Once in the ER, binding of ATP to the central pore of the B-pentamer results in dissociation of PTS1 from the B-pentamer (Burns & Manclark, 1986; Hazes et al., 1996; Plaut et al., 2016). Since ATP is not present in endosomes or the Golgi apparatus, PT first encounters ATP in the ER, making the dissociation site-specific (Hazes et al., 1996). The released and now isolated PTS1 is unstable at 37°C, leading to thermal unfolding in the ER (Pande et al., 2006). As a consequence, holotoxin reassembly is prevented, PTS1 is in a conformation, suitable for translocation through a narrow pore into the cytosol, and PTS1 is recognized by the ER-associated degradation (ERAD)

pathway (Banerjee et al., 2016; Teter, 2019). ERAD physiologically removes misfolded proteins from the ER, followed by ubiquitination at their lysine residues for proteasomal degradation. This pathway is exploited by PT for translocation into the cytosol. The lack of lysine residues in PTS1 leads to an evasion of the subsequent proteasomal degradation (Worthington & Carbonetti, 2007). The exact molecular mechanism of the membrane transport of PTS1 into the cytosol is not fully understood. However, host cell protein folding helper enzymes play an important role in the refolding of PTS1 in the cytosol (see section 1.2) (Ernst, 2022b; Ernst, Eberhardt, et al., 2018; Kellner et al., 2019, 2021). Having reached the cytosol, PTS1 covalently transfers an ADP-ribose moiety from the co-substrate NAD^+ onto α-subunits of inhibitory G-proteins (Gαi) of G-protein coupled receptors (GPCR) (Bokoch et al., 1983; Katada & Ui, 1982). Thus, PT belongs to the group of ADP-ribosylating toxins, a subgroup of AB-type protein toxins. ADP-ribosylated Gαi is in an inactive state and not able anymore, to follow its physiological function as a negative regulator of the adenylyl cyclase (AC) (see Figure 2). This results in increased and thus disturbed signaling of the essential second messenger cAMP. One exemplary consequence is the inhibition of chemotaxis of lymphocytes, monocytes and neutrophils in early stages of infection, leading to a suppression of the immune-mediated clearance of *B. pertussis* in the infected host (Andreasen & Carbonetti, 2008; Kirimanjeswara et al., 2005; Spangrude et al., 1985). However, depending on the affected cell type, consequences of the accumulation of intracellular cAMP by PT are various and not fully understood (Carbonetti, 2010; Teter, 2019).

1.2 Chaperone inhibitors

One approach to avert the serious cytotoxic effects of PT is preventing PTS1 from reaching its cytosolic substrate Gαi. Inhibitors of host cell factors like chaperones and protein folding helper enzymes have been demonstrated over the last years to fulfill this task.

Chaperones and protein folding helper enzymes undertake essential functions in eukaryotic cells. They are mainly responsible for the correct folding of newly synthesized proteins, but also help to prevent protein aggregation under stress conditions. Thus, they maintain the integrity of the cellular protein network (Biebl & Buchner, 2019; Ernst, 2022b). There are different families involved in protein folding including heat shock proteins (Hsps) and peptidyl-prolyl *cis/trans* isomerases (PPIases). Both families have been shown to play a role in the cellular uptake of several ADP-ribosylating toxins (Ernst, 2022b; Ernst, Schnell, et al., 2017). For investigating their requirement

for toxin uptake, specific pharmacological small molecule inhibitors of the host cell factors were utilized (for overview see Figure 3).

Hsp90 was the first host cell factor, which was shown to facilitate the cellular uptake of ADP-ribosylating toxins. Furthermore, as one of the most abundant and conserved cytosolic proteins, Hsp90 is essential for the activation and stabilization of various client proteins, involved in signal transduction, intracellular transport, protein degradation, cell cycle control and cell survival (Li & Buchner, 2013). Radicicol (Rad), a cell-permeable and nucleotide-mimicking compound, prevents the chaperone activity of Hsp90 by binding with high affinity to the ATP-binding pocket of Hsp90 (Arndt et al., 2007; Roe et al., 1999). The accurate function of Hsp90 is regulated by several co-chaperones, including Heat shock protein 70 (Hsp70), as well as PPIases of the FK506-binding protein (FKBP) and cyclophilin (Cyp) families (Li & Buchner, 2013; Scheufler et al., 2000). Hsp70 is one of the first host cell factors, interacting with the client protein in the Hsp90 chaperone machinery (Li et al., 2012). Similarly to Hsp90, Hsp70 was shown to facilitate the cellular uptake of several ADP-ribosylating toxins (Ernst et al., 2016; Ernst, Schmid, et al., 2017; Schuster et al., 2017). The adenosine-derived small molecule VER-155008 (VER) inhibits activity of Hsp70 and its constitutive form Hsc70 by binding to their N-terminal located ATP-binding site (Williamson et al., 2009). The 9-aminoacridizinium-derived small molecule HA9 inhibits only Hsp70 by binding to its C-terminal substrate binding domain, impairing binding of client proteins (Ernst et al., 2016). Like, Hsp90, Hsp70 is also involved in numerous important cellular processes, including protein biogenesis and organization of protein complexes. Remarkably, Hsp70 also facilitates the translocation of several proteins across cellular membranes by interacting with the translocating protein on the *trans* side, to ensure vectorial transport and transfer to chaperones for further maturation and complex assembly (Clerico et al., 2015).

The Hsp70/Hsp90 multichaperone machinery also involves PPIases, which accelerate the *cis/trans* isomerization of proline-peptide bonds, a rate-limiting step in protein folding (Göthel & Marahiel, 1999). PPIases include FKBPs and Cyps. FKBPs are named after their specific pharmacological inhibitor FK506, which is a macrolide with highly potent immunosuppressive activity (Harding et al., 1989). FKBPs are a family of highly conserved proteins involved in various cellular functions like protein folding, cellular signaling, apoptosis and transcription (Tong & Jian, 2015). They have different isoforms with different characteristics. Although it has the highest affinity to FK506, the

single-domain isoform FKBP12 showed no interaction with *Clostridium (C.) botulinum* C2 toxin, *C. perfringens* iota toxin or *C. difficile* transferase toxin (CDT) *in vitro*. The multi-domain isoform FKBP51, however, interacted with the enzymatic A-subunits of C2 toxin, iota toxin and CDT (Kaiser et al., 2012). Interestingly, FKBP5 also competes with cyclophilin 40 (Cyp40), an isoform of Cyps, for the same binding site on Hsp90, when forming multi-chaperone complexes in the cell (Pratt & Toft, 1997). Cyps are the specific intracellular targets of the immunosuppressive drug cyclosporin A (CsA) (Handschuhmacher et al., 1984). CsA binds to the PPIase domain of Cyps, thereby inhibiting their enzymatic activity (Fruman et al., 1994). Like FKBPs, Cyps are well conserved and ubiquitous proteins with many important cellular functions. The single-domain isoform cyclophilin A (CypA) is the most abundant member of the Cyp family and is involved in protein folding, trafficking, T-cell activation and cell signaling (Nigro et al., 2013). The multi-domain isoform Cyp40 contains three tetratricopeptide repeat (TPR) domains responsible for interaction with the MEEVD-motif of Hsp90 (Ratajczak et al., 1993). Both CypA and Cyp40 have been shown to directly interact with PTS1 *in vitro* (Ernst, Eberhardt, et al., 2018).

The involvement of host cell chaperones and PPIases in PT intoxication has only recently been evaluated. CsA and its non-immunosuppressive derivative VK112 protected cells from PT intoxication (Ernst, Eberhardt, et al., 2018). This was shown by analyzing the morphology of intoxicated cells, as well as the amount of ADP-ribosylated Gαi in those cells. Additionally, fluorescence microscopy revealed that less PTS1 was detected in the cytosol of PT-intoxicated cells when treated with CsA (Ernst, Eberhardt, et al., 2018). Furthermore, Hsp90 was shown to play a role in PT intoxication. PTS1 was found to share a binding motif for Hsp90 with other ADP-ribosylating toxins (Kellner 2019). Binding of Hsp90 to PT was confirmed by a surface plasmon resonance (SPR)-based assay, and demonstrated to be relevant by inhibition of Hsp90 with geldanamycin (GA), which resulted in reduced cytosolic PTS1 in PT-treated cells (Kellner et al., 2019). By expressing PTS1 directly in the ER of transfected CHO-K1 cells, the ER-to-cytosol export could be specifically investigated. Incubation of these cells with GA or CsA, resulted in a reduction of the cytosolic amount of PTS1, suggesting an involvement of Hsp90 and Cyps in the membrane translocation of PTS1 into the cytosol (Kellner et al., 2019, 2021).

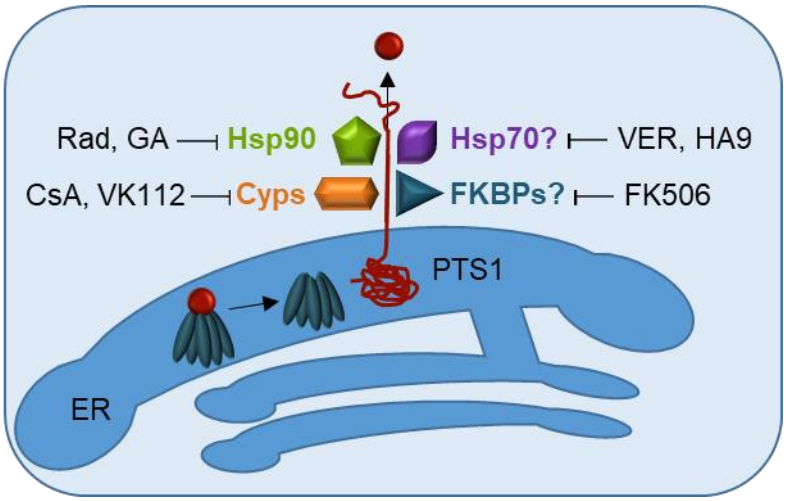

Figure 3: Role of Host cell Factors and their Inhibitors in Translocation of PTS1
Heat shock protein 90 (Hsp90) and cyclophilins (Cyps) have been shown to facilitate cellular uptake of PTS1. Heat shock protein 70 (Hsp70) and FK506 binding proteins (FKBPs) might also facilitate uptake of PTS1. The chaperones and protein folding helper enzymes can be inhibited by their specific pharmacological inhibitors as indicated (based on Ernst, 2022b). Rad = Radicicol, GA = Geldanamycin, CsA = cyclosporin A

In conclusion, there is profound evidence, that chaperones and protein folding helper enzymes play an important role for PTS1 to reach its cytosolic target (see Figure 3). For Hsp90 and Cyps, this role has already been demonstrated, whereas for Hsp70 and FKBPs their role in the uptake of PTS1 still has to be evaluated. Therefore, already established pharmacological inhibitors hold an immense potential as novel therapeutic options against pertussis.

1.3 Peptide-based inhibitors: Defensins

Besides small molecule inhibitors, peptides gained substantial attention as pharmacological inhibitors of various cellular functions over the last years. To date, over 60 peptide drugs have been approved in Europe and 20 new peptide-based clinical trials are performed each year (Lee et al., 2019). With their short amino acid sequence, peptides lie between small molecules and proteins regarding their size, thus they form a unique class of pharmaceutical compounds (Lau & Dunn, 2018). The small size of peptides compared to proteins favors their ability to bind deep into folding pockets of proteins and to reach cellular targets (Lee et al., 2019). The human proteome comprises more than 1 million proteins and peptides, generated by proteolytic processing of larger precursors (Bosso et al., 2018). As endogenous signaling molecules, human peptides serve several physiological functions, opening the possibility to access novel targets and mechanisms of action (Lau & Dunn, 2018). Their size and conformational flexibility make them promising candidates

for targeting challenging protein-protein-interactions, which has been difficult for small molecules (Lee et al., 2019). Furthermore, human peptides are less prone to the emergence of microbial resistance than classical antibiotics, and usually are less immunogenic, and therefore better tolerated by patients than foreign agents (Bosso et al., 2018; Pachón-Ibáñez et al., 2017). Therefore, peptides form an interesting class of novel drug candidates against pertussis.

Human defensins are an important class of human antimicrobial peptides (AMPs). They are arginine-rich and thus cationic peptides with around 30 amino acids. They carry six cysteines, forming three intramolecular disulfide bonds, which stabilize their characteristic triple-stranded β-sheet structure (see Figure 4).

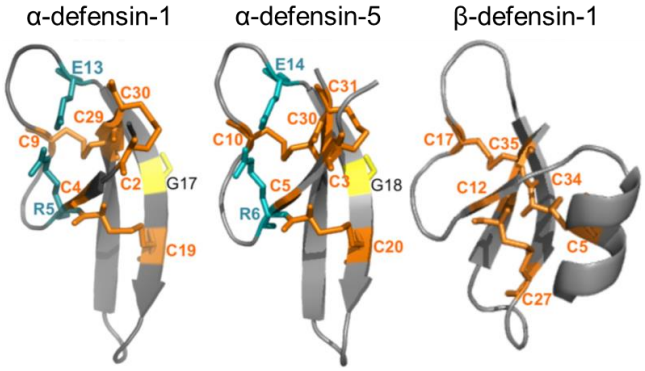

Figure 4: Structure of Human Defensins
Exemplary structures of human α-defensin-1, -5 and β-defensin-1. Cysteines (C) are shown in orange, invariant glycine (G) residues are shown in yellow and a salt bridge between oppositely charged arginine (R) and glutamate (E) residues is shown in blue (taken from Kudryashova et al., 2017).

The length of the peptide segments between the cysteines and their pairing differ in the two human defensins' subfamilies, the α- and β-defensins (Ganz, 2003) (see Table 1). The human α-defensins are further divided by their localization: α-defensin-1 to -4, also known as human neutrophil peptides 1-4 (HNP 1-4) are produced in neutrophil precursor cells in the bone marrow, and found in primary granules of mature neutrophils, circulating in the blood or invading inflamed tissues (Cederlund et al., 2011; Ganz, 2003). α-Defensin-5 and -6, also known as human enteric defensins 5 and 6 (HD 5-6) are produced in Paneth cells, which are highly specialized epithelial cells in the small intestine. α-Defensin-5 and -6 are secreted into the crypts of the small intestine. Human β-defensin-1 to -4, also abbreviated as HBD 1-4, are expressed in several epithelial cells, for example in the respiratory and gastrointestinal tract, cornea, skin and kidney (Cederlund et al., 2011).

Table 1: Groups of Human Defensins

Group	Synonym	Site of production
α-defensin-1-4	Human neutrophil peptides (HNP) 1-4	Neutrophil precursor cells in bone marrow
α-defensin-5-6	Human enteric defensins (HD) 5-6	Paneth cells in the small intestine
β-defensin-1-4	Human beta defensin (HBD) 1-4	Several epithelial cells

The term "defensin" originated from their antibiotic activity against different pathogens (Ganz et al., 1985). Also today, defensins are commonly known for their broad antimicrobial activity. Defensins are active against Gram-positive and Gram-negative bacteria, enveloped and non-enveloped viruses as well as different fungi. Additionally to their role in innate immunity, they have functions in adaptive and antitumor immunity. Furthermore, they play a role in regulating wound repair, inflammation, histamine production, cytokine release, chemotaxis and proliferation (Mattar et al., 2016; Zhao & Lu, 2014).

As "swiss army knives" of innate immunity, defensins also interfere with a variety of bacterial effector proteins like pore-forming, non-enzymatic as well as enzymatic toxins (Kudryashova et al., 2017). The bacterial toxins, found to be inhibited by human defensins are listed in Table 2. Several studies investigated the inhibitory mechanism of human defensins on various bacterial toxins. They found many common mechanisms, like the direct inhibition of the enzyme activity, for example of *B. anthracis* lethal factor (LF), *Diphtheria* toxin (DT), *Pseudomonas exotoxin* A (ETA), and *C. difficile* toxin B (TcdB) by α-defensin-1-3 (Giesemann et al., 2008; Kim et al., 2005, 2006), or the inhibition of pore formation, for example of *S. aureus* Panton-Valentine leukocidin (PVL) by α-defensin-3 (Cardot-Martin et al., 2015) and CDT by α-defensin-1 and -5 (Fischer et al., 2020; Korbmacher et al., 2020). They also found unique strategies, such as a complex formation of α-defensin-6 with TcdB (Barthold et al., 2022) or the interaction of α-defensin-1 with the B-component of iota toxin (Fischer et al., 2018). Notably, the α-defensins showed varying mechanisms of inhibition on different toxins. For instance, α-defensin-1 was found to inhibit pore formation of CDT (Fischer et al., 2020), while also targeting the enzyme activity of DT (Kim et al., 2006). Also, the same toxin could be inhibited by different defensins with different mechanisms of inhibition, for example TcdB, which was inhibited by α-defensin-1 via binding to the toxin (Fischer et al., 2020), by α-defensin-5 via inhibition of enzyme activity and by α-defensin-6 via complex formation (Barthold et al., 2022). Furthermore, some investigated defensins did not show any inhibition of the investigated toxin, for example β-defensin-1, which did not inhibit TcdB

(Giesemann et al., 2008), cholesterol-dependent cytolysins (CDCs) (Lehrer et al., 2009) or iota toxin (Fischer et al., 2018). A concept for a common pattern, predicting the toxins, targeted by the defensins or their respective mechanisms of inhibition, could not be determined so far. Besides a short mention of finding no effect of α-defensin-1, -2, or -3 on cAMP levels of PT-treated cells (Kim et al., 2006), no thorough study, investigating the effects of human defensins on PT has been performed and published to my knowledge.

Table 2: Bacterial Toxins inhibited by Human Defensins
(derived and modified from Kudryashova et al., 2017)

Toxin	Defensin	Mechanism of inhibition	References
B. anthracis lethal factor (LF)	α-def-1/-2/-3 β-def-3	inhibit enzyme activity inhibit enzyme activity	(Kim et al., 2005) (Wei et al., 2009)
Diphtheria toxin (DT)	α-def-1/-2/-3	inhibit enzyme activity	(Kim et al., 2006)
Pseudomonas exotoxin A (ETA)	α-def-1/-2/-3	inhibit enzyme activity	(Kim et al., 2006)
C. perfringens iota toxin	α-def-1 **not** β-def-1	interacts with B-component no inhibition	(Fischer et al., 2018)
C. difficile transferase toxin (CDT)	α-def-1 α-def-5	inhibit pore formation inhibit pore formation	(Fischer et al., 2020) (Korbmacher et al., 2020)
C. difficile toxin A (TcdA)	α-def-5 α-def-1 α-def-6	aggregate formation binding to toxin unknown	(Korbmacher et al., 2020) (Fischer et al., 2020) (Barthold et al., 2022)
C. difficile toxin B (TcdB)	α-def-1/-3/-5 **not** β-def-1 α-def-5 α-def-1 α-def-6	inhibit enzyme activity no inhibition inhibits enzyme activity binding to toxin complex formation	(Giesemann et al., 2008) (Barthold et al., 2022) (Fischer et al., 2020) (Barthold et al., 2022)
Cholesterol-dependent cytolysins (CDCs)	α-def-1/-2/-3 **not** α-def-4/-6 **not** β-def-1/-2/-3	inhibit hemolysis no inhibition no inhibition	(Lehrer et al., 2009)
V. cholerae and *A. hydrophila* MARTX	α-def-1/-5	inhibit enzyme activity	(Kudryashova et al., 2014)
S. aureus Panton-Valentine leukocidin (PVL)	α-def-3 **not** α-def-1/-2	inhibits pore formation no inhibition	(Cardot-Martin et al., 2015)
Neisseria gonorrhoeae gNarE	β-def-1/-2/-4	inhibit enzyme activity	(Rodas et al., 2016)

1.4 Aim of this Thesis

Pertussis is a serious childhood disease with very limited therapeutic options. As a major virulence factor of the disease, PT qualifies as a starting point for developing new therapeutics. To carry out its toxic effect, the enzyme subunit PTS1 has to reach its cytosolic target Gαi. For this, the holotoxin binds to cellular receptors, is taken up by endocytosis, follows a retrograde vesicular transport from the Golgi to the ER, where PTS1 dissociates and translocates into the cytosol. This mechanism of uptake and action of PT offers many possible target points for pharmacological inhibitors, such as blocking receptor binding, cellular trafficking or enzyme activity in the cytosol.

This thesis aims to identify and characterize novel pharmacological inhibitors of PT. The present studies focused on two different classes of inhibitors.

On the one hand, small molecule inhibitors against cellular chaperones and protein folding helper enzymes were investigated. For CsA, the specific inhibitor of Cyps, and for GA, an inhibitor of Hsp90, there was already evidence, that they reduced cytosolic levels of PTS1 in cells, intoxicated with PT, and protect them from the effects of PT intoxication. Other inhibitors of chaperones and PPIases, such as VER and FK506 targeting Hsp70 and FKBPs, as well as Rad and CsA showed protective effects against other ADP-ribosylating toxins. Therefore, in this thesis, the protective effect of pharmacological inhibitors of Hsp90, Cyps, as well as Hsp70 and FKBPs was investigated and characterized. The hypothesis, that they inhibit the effects of PT intoxication, by interfering with the uptake of PTS1 into the cytosol was studied in-depth.

On the other hand, peptides, particularly defensins were investigated as novel inhibitors of PT. Human defensins are known as antimicrobial peptides, acting mainly in innate immunity. Different human defensins have been shown to inhibit other bacterial toxins with various mechanisms of inhibition. This thesis focused on α-defensin-1, α-defensin-5 and β-defensin-1. After identifying α-defensin-1 and -5, but not β-defensin-1 as inhibitors of PT intoxication, the distinct underlying mechanisms of inhibition were further examined.

Taken together, the present study aims at characterizing new approaches to inhibit pertussis toxin based on cellular chaperone inhibitors and human peptides, to provide a starting point for novel therapeutic strategies for treatment of severe whooping cough.

2 Results and Discussion

2.1 Pharmacological targeting of host chaperones protects from pertussis toxin *in vitro* and *in vivo*

Scientific Reports (2021) 11 (1), 5429. https://doi.org/10.1038/s41598-021-84817-2

Katharina Ernst*[#], Ann-Katrin Mittler*, Veronika Winkelmann, Carolin Kling, Nina Eberhardt, Anna Anastasia, Michael Sonnabend, Robin Lochbaum, Jan Wirsching, Moona Sakari, Arto T. Pulliainen, Ciaran Skerry, Nicholas H. Carbonetti, Manfred Frick & Holger Barth[#]

*authors contributed equally

[#]corresponding authors

The reuse of the present article in my dissertation is permitted by the Creative Commons Attribution 4.0 International License (CC BY 4.0) (https://creativecommons.org/licenses/by/4.0/).

2.1.1 Own contributions

- Data and Figures of **Figure 2b** (Effect of chaperone inhibitors on intracellular cAMP levels in PT-treated cells), **Figure 2c** (Effect of Rad, CsA, FK506 and VER on enzyme activity in vitro), **Figure 2d** (Influence of Rad, CsA, FK506 and VER on receptor binding of PT to CHO-K1 Cells)
- Data and Figure of **Figure 4d** (FKBP51, Hsp70 and Hsp90 interact with PTS1 in cells)
- Data and Figure of **Figure 5a** (Rad and CsA inhibit ADP-ribosylation of Giα in PT-treated basal cells)
- Preparation of parts of the manuscript and revision

2.1.2 Summary of Results

In the present publication, the role of the cellular chaperones Hsp90, Hsp70, Cyps and FKBPs for the uptake of PTS1 into the cytosol of target cells was investigated. For this purpose, their specific pharmacological inhibitors were employed.

First, in a morphology-based assay, it was shown that the specific pharmacological inhibitors of Hsp90, Hsp70, Cyps and FKBPs, which are Rad, VER, HA9, CsA and FK506, respectively, protect

CHO-K1 cells from PT-induced clustering. Furthermore, the protective effect of the pharmacological inhibitors was shown in a reduction of the ADP-ribosylation of the cytosolic substrate Gαi in PT-treated CHO-K1 cells. Additionally, CsA and FK506 reduced PT-mediated increase of intracellular cAMP levels, as investigated by the iGIST (interference in Gαi-mediated Signal Transduction) bioassay (Paramonov et al., 2020) (see Figure 5).

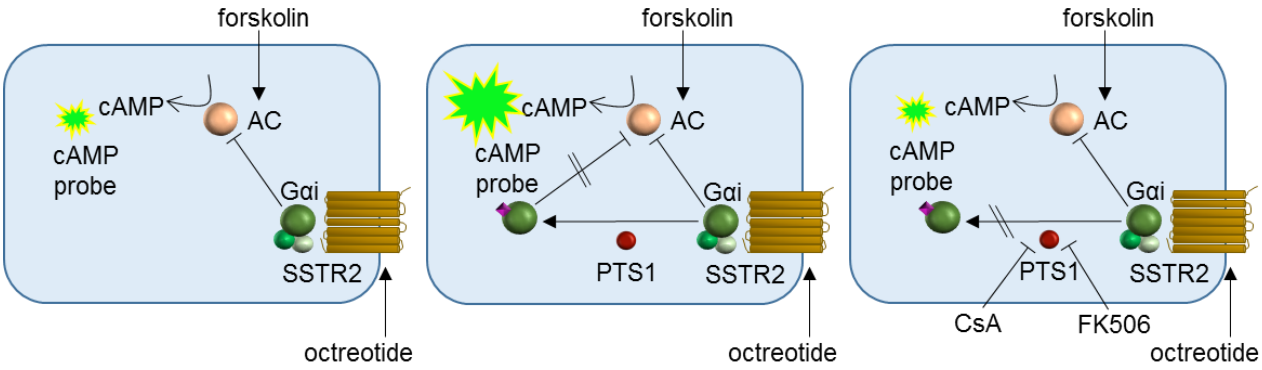

Figure 5: Principle of iGIST Bioassay
iGIST sensor cells recombinantly express the Gαi-coupled somatostatin receptor 2 (SSTR2) and a luminescent cAMP probe. Activation of adenylyl cyclase (AC) by forskolin and activation of SSTR2 by octreotide results in moderate levels of cAMP, since Gαi inhibits AC (see left image). ADP-ribosylation of Gαi by PTS1 is preventing Gαi from inhibiting AC, which results in a strong increase of cAMP levels, and thus high luminescence of the cell (see center image). When PTS1 uptake is inhibited by CsA or FK506, it leads to decreased cAMP levels, as Gαi can freely inhibit AC without hindrance (see right image).

To investigate the mechanism of inhibition of PT by Rad, VER, HA9, CsA and FK506, different steps of intoxication were examined in an isolated manner. The enzyme activity of PTS1 was not inhibited by the chaperone/PPIase inhibitors, which was shown in an *in vitro* assay, detecting ADP-ribosylated Gαi. Also, receptor binding of PT to cells was not impaired by the inhibitors. The same amount of PT was detected on cells, incubated on ice with PT and then washed, with or without pre-incubation with the inhibitors. Fluorescence microscopy showed that in the presence of Rad, VER, CsA and FK506, less free PTS1 was detected in CHO-K1 cells. These findings indicate that chaperones and PPIases play a role in the uptake of PTS1 to the cytosol. The interaction of PTS1 with chaperones was investigated with two different assays. In a dot blot experiment, purified chaperones and PPIases were immobilized on a nitrocellulose membrane and incubated with PTS1. After extensive washing, bound PTS1 was detected with a specific antibody. This *in vitro* assay revealed direct binding of PTS1 to Hsp90, Hsp70, Hsc70, CypA, Cyp40, FKBP51 and FKPB52. The proximity ligation assay (PLA) detects interaction of two binding partners within cells. CHO-

K1 cells were intoxicated with PT for 3 h or 24 h. For detection of binding to Cyp40, even more time points (0.5 h, 3 h, 6 h, 48 h) were tested exemplarily. Then, cells were fixed and the fluorescence-based PLA was performed, which launches a signal amplification reaction that only occurs, if two antibodies against the investigated binding partners come into close proximity. All investigated chaperones and PPIases interacted with PTS1 at all investigated time points in cells.

Next, to get closer to the physiological site of action of PT, experiments were conducted in a model of a primary human bronchial airway epithelium. Rad and CsA reduced the ADP-ribosylation of Gαi in PT-treated human primary basal cells. When basal cells were differentiated to ciliated and secretory cells of the airway epithelium at air-liquid interface condition, and incubated with PT, PTS1 was only detected in secretory, but not ciliated cells by fluorescence microscopy. CsA, but not Rad or FK506 reduced the uptake of PTS1 into human bronchial airway epithelial cells (hBAECs). In functional experiments, it was shown, that PT does not impair the barrier function of hBAECs but did increase their apical surface liquid. This increase of apical surface liquid was not impaired by Rad, CsA or FK506. Finally, it was shown that the Cyp-inhibitor CsA and its non-immunosuppressive derivative NIM811 reduced leukocytosis *in vivo* in an infant mouse model of pertussis, without reducing the bacterial burden.

2.1.3 Discussion

PTS1 unfolds upon dissociation from the B-pentamer, translocates through a narrow pore into the cytosol and necessarily has to be refolded to exert its cytotoxic effect, causing the clinical symptoms. Other AB-type toxins require chaperones and protein folding helper enzymes for this step of intoxication. For example, uptake of *Clostridium (C.) botulinum* C2 toxin has been shown to be assisted by Hsp90 (Haug et al., 2003), Hsp70 (Ernst, Schmid, et al., 2017), FKBPs (Kaiser et al., 2012), and Cyps (Ernst et al., 2015; Ernst, Kling, et al., 2018; Kaiser et al., 2009). Moreover, *C. perfringens* iota toxin, and CDT have also been shown to require Hsp90 (Haug et al., 2004; Kaiser et al., 2011), Hsp70 (Ernst et al., 2016; Ernst, Schmid, et al., 2017), FKBPs (Kaiser et al., 2012), and Cyps (Ernst et al., 2015; Kaiser et al., 2011) for their intoxication. Pre-incubation of mammalian cells with Rad, VER, CsA, or FK506 resulted in a significant delay of cell morphology induced by the respective toxin. Furthermore, membrane translocation of the toxins was impaired but not receptor-binding or enzyme activity. Similarly, uptake of the enzyme subunit of DT has been shown to depend on Hsp90 (Dmochewitz et al., 2011; Ratts et al., 2003; Schuster et al., 2017),

Hsp70, FKBPs, and Cyps (Schuster et al., 2017). Additionally, *Vibrio cholerae* toxin (CT) has been shown to be assisted by Hsp90 (Burress et al., 2014, 2019; Taylor et al., 2010) and Hsp70 (Burress et al., 2019). This led to the hypothesis, that chaperones and protein folding helper enzymes might also play a role in the uptake of PTS1 into the cytosol.

Previous work demonstrated the requirement of Cyps for PT intoxication (Ernst, Eberhardt, et al., 2018). PTS1 was shown to directly interact with CypA and Cyp40 *in vitro* and the Cyp-inhibitors CsA and VK112 protected CHO-K1 cells from PT-induced clustering and ADP-ribosylation of Gαi. Additionally, less PTS1 was detected in the cytosol of CHO-K1 cells, in the presence of CsA, compared to incubation with PT only. The present work confirms the previously obtained results and extends the findings to other chaperones and chaperone inhibitors: Here, PTS1 was shown to interact not only with CypA and Cyp40, but also Hsp90, Hsp70, Hsc70, FKBP51 and FKPB52 *in vitro* and with Cyp40, Hsp90, Hsp70 and FKBP51 in cells. PT-induced clustering and ADP-ribosylation of Gαi in CHO-K1 cells was inhibited by CsA, but also Rad, VER, HA9 and FK506. Also, the amount of free PTS1 in CHO-K1 cells was reduced by the same chaperone inhibitors. Furthermore, the downstream effect of PT, which is an elevated intracellular cAMP level, was reduced by CsA and FK506.

Hsp90, Hsp70, Cyps and FKBPs, all demonstrated to be involved in PT intoxication, also cooperate in other contexts, for example the activation of steroid receptors (Pratt & Toft, 1997). Assembly of Hsp90 with co-chaperones is facilitated by the conserved MEEVD motif at the C-terminus of Hsp90, which is bound by a TPR motif, found in Hsp70, Cyps and FKBPs (Scheufler et al., 2000). The interplay is described as a co-chaperone cycle of the Hsp90 machinery. Briefly, in this cycle, Hsp70 and Hsp40 form an early complex with a client protein, which is then transferred to Hsp90 through the adaptor protein Hop/Sti1. PPIases, ATP and other proteins join the complex until the hydrolysis of ATP and the release of the folded client protein (Li et al., 2012). This known interplay of chaperones and PPIases on folding of different client proteins suggests a possible interplay also for the refolding of PTS1 after translocation into the cytosol.

In the context of the ADP-ribosylating toxins C2 and CDT, a combination of the four pharmacological inhibitors Rad, VER, CsA and FK506 resulted in an enhanced protective effect for intoxicated cells compared to the application of the individual inhibitors (Ernst, Kling, et al., 2018; Ernst, Sailer, et al., 2021) Thus, the concentrations of the individual inhibitors can be

reduced. These findings support the approach to focus on Hsp90, Hsp70, Cyps and FKBPs in the same study, as executed here. When PTS1 was directly expressed in the ER of transfected CHO-K1 cells, the translocation from the ER to the cytosol could be inhibited with GA (Kellner et al., 2019). These findings demonstrate the role of Hsp90 in the translocation step of PTS1 into the cytosol. This has not been shown this specifically for Hsp70, Cyps and FKBPs, so an inhibition of endocytosis or transport to the Golgi or to the ER cannot be excluded. Still, their role in the same step of intoxication as Hsp90 is very likely.

The findings, that Hsp90, Hsp70, Cyps and FKBPs are required by PT for intoxication of cells is in line with other AB-type toxins, which depend on these chaperones and PPIases. A common feature of the ADP-ribosylating toxins PT, CT, ETA, *Escherichia coli* heat-labile toxin and *Salmonella enterica serovar Typhimurium* ADP-ribosylating toxin, is a recently found binding motif to Hsp90 (Kellner et al., 2019). Remarkably, all these toxins are taking the long-trip route through the cell and translocate through the ER. CTA1, the enzyme subunit of CT, is also sharing this common binding motif to Hsp90 and has been shown to continue binding to Hsp90 even after translocation and refolding into its active conformation (Burress et al., 2014). This stabilization of the enzyme subunit by chaperones and PPIases after translocation is also conceivable for PTS1, as the present study showed an interaction between PTS1 and Hsp90, Hsp70 and FKBP at 24 h after PT incubation, and Cyp40 even after 48 h. Moreover, both CTA1 and PTS1 are thermally unstable, as they unfold at 37°C after dissociation from the B-pentamer (Pande et al., 2006, 2007). Therefore, release of the A-subunits from the chaperones and PPIases after translocation would probably again result in their unfolding. In fact, a recent publication showed an increase in enzyme activity of PTS1 in the presence of Hsp90, Hsp70 or Hsc70 at room temperature and 37°C, which could be prevented by the respective chaperone inhibitors (Jia et al., 2023). Similarly, Hsp90 restored enzyme activity of a disordered conformation of CTA1 after incubation at 37°C (Burress et al., 2014).

A substantial advantage of implementing the inhibition of chaperones and PPIases as a treatment of pertussis in clinical use, is that specific pharmacological inhibitors are already identified, studied, and partly even already used for other indications. Hsp90 and Hsp70 inhibitors have been in clinical trials for their anti-tumor activity but the efficacy was too low at the tolerated doses (Biebl & Buchner, 2019; Dhingra et al., 1994; Schlecht et al., 2013). However, FK506, also known

as tacrolimus, and CsA are licensed immunosuppressive drugs that are applied for example to avoid organ rejection after organ transplantation (Liu et al., 1991). This effect is mediated by inhibiting Cyps and FKBPs, binding to the protein phosphatase calcineurin, which is then prevented from indirectly activating T-lymphocytes. Certainly, the immunosuppressive effect of CsA and FK506 is not wanted in patients with a bacterial infection with *B. pertussis*. Thus, the development of non-immunosuppressive derivatives of CsA and FK506 is all the more important. The non-immunosuppressive derivative of CsA, VK112 still inhibits Cyps and thereby intoxication of cells with various toxins (Ernst, Eberhardt, et al., 2018; Ernst et al., 2015; Schuster et al., 2017). Another non-immunosuppressive derivative of CsA, NIM811 (Rosenwirth et al., 1994) was shown in the present study to protect *B. pertussis*-infected infant mice from leukocytosis, a hallmark of severe pertussis. The gained knowledge about the safety profile and pharmacokinetics of already tested chaperone inhibitors is useful for their further development. Moreover, development of chaperone inhibitors for clinical use might not only benefit patients suffering from pertussis, but also patients with other diseases, such as diphtheria, cholera and enteric diseases, caused by the various bacterial toxins, dependent on chaperones and PPIases.

www.nature.com/scientificreports

scientific reports

Check for updates

OPEN

Pharmacological targeting of host chaperones protects from pertussis toxin in vitro and in vivo

Katharina Ernst[1,5]✉, Ann-Katrin Mittler[1,5], Veronika Winkelmann[2], Carolin Kling[1], Nina Eberhardt[1], Anna Anastasia[1], Michael Sonnabend[1], Robin Lochbaum[2], Jan Wirsching[1], Moona Sakari[3], Arto T. Pulliainen[3], Ciaran Skerry[4], Nicholas H. Carbonetti[4], Manfred Frick[2] & Holger Barth[1]✉

Whooping cough is caused by *Bordetella pertussis* that releases pertussis toxin (PT) which comprises enzyme A-subunit PTS1 and binding/transport B-subunit. After receptor-mediated endocytosis, PT reaches the endoplasmic reticulum from where unfolded PTS1 is transported to the cytosol. PTS1 ADP-ribosylates G-protein α-subunits resulting in increased cAMP signaling. Here, a role of target cell chaperones Hsp90, Hsp70, cyclophilins and FK506-binding proteins for cytosolic PTS1-uptake is demonstrated. PTS1 specifically and directly interacts with chaperones in vitro and in cells. Specific pharmacological chaperone inhibition protects CHO-K1, human primary airway basal cells and a fully differentiated airway epithelium from PT-intoxication by reducing intracellular PTS1-amounts without affecting cell binding or enzyme activity. PT is internalized by human airway epithelium secretory but not ciliated cells and leads to increase of apical surface liquid. Cyclophilin-inhibitors reduced leukocytosis in infant mouse model of pertussis, indicating their promising potential for developing novel therapeutic strategies against whooping cough.

Whooping cough is a highly transmissible respiratory disease caused by droplet infection of the respiratory tract with *Bordetella* (*B.*) *pertussis*. This bacterium mediates disease through several virulence factors including adhesion factors and the enzymatically active pertussis toxin (PT)[1]. Characteristic symptoms include severe paroxysmal coughing, which typically lasts for several weeks and can cause secondary complications like vomiting, rib fractures and pneumothorax. In severe cases, further complications such as pneumonia, encephalopathy, seizures and apnea can lead to death especially in newborns and infants[2]. Leukocytosis, the rapid, unregulated expansion of circulating leukocytes, is a hallmark of severe infant disease[3,4]. High levels of leukocytosis are associated with poor disease outcome and death[3]. In 2008, whooping cough caused death in 195,000 of an estimated 16 million cases worldwide according to the world health organization (WHO)[5]. Despite widespread vaccine coverage, disease incidence is at its highest since the 1950s[6].

B. pertussis infects humans and colonizes the ciliated epithelium of the respiratory tract. Adhesion factors like filamentous hemagglutinin (FHA) and fimbria are required for efficient infection. Moreover, *B. pertussis* produces several toxins that directly influence physiological functions. The precise role of PT for the pathogenesis of *B. pertussis* is still not completely elucidated. In mouse models, PT causes exacerbated and prolonged airway inflammation[7]. Mutant strains of *B. pertussis* that do not express PT, do not cause severe symptoms such as leukocytosis or death in animal models[8]. This observation clearly indicates that PT promotes disease severity and represents an attractive drug target[7,9,10].

PT is an AB_5-type protein toxin, consisting of one enzyme subunit, the A protomer PTS1, and four different binding (B) subunits PTS2, PTS3, PTS4 and PTS5 occurring in the ratio 1:1:2:1, respectively[11,12]. In *B. pertussis*, PTS1 and the B pentamer are assembled in a non-covalent manner as PT holotoxin in the periplasm prior to secretion by type IV secretion system[11,13]. The B oligomer facilitates binding of PT to sialic acid-containing glycoproteins present on most mammalian cell types. PT does not appear to bind a single unique receptor, instead it binds in a non-saturable, non-specific manner[14]. PT is endocytosed and follows a retrograde route of intracellular

[1]Institute of Pharmacology and Toxicology, University of Ulm Medical Center, Ulm, Germany. [2]Institute of General Physiology, University of Ulm, Ulm, Germany. [3]Institute of Biomedicine, Research Unit for Infection and Immunity, University of Turku, Turku, Finland. [4]Department of Microbiology and Immunology, University of Maryland School of Medicine, Baltimore, MD, USA. [5]These authors contributed equally: Katharina Ernst and Ann-Katrin Mittler. ✉email: katharina.ernst@uni-ulm.de; holger.barth@uni-ulm.de

trafficking travelling through the Golgi apparatus to the endoplasmic reticulum (ER). Consequently, brefeldin A (BFA), which leads to disassembly of the Golgi apparatus, inhibits intoxication of CHO cells with PT[15–17]. In the ER, binding of ATP to PT destabilizes interaction between PTS1 and B oligomer, which contributes to the release of PTS1[18,19]. ATP-mediated release occurs in the ER because it is one of the few cellular compartments besides the cytosol and lysosomes/lysosome-related organelles that contains ATP[20]. Released PTS1 is thermally unstable and therefore in its unfolded conformation, which makes it susceptible for transport from the ER into the cytosol via the ER-associated degradation (ERAD) pathway[21,22]. ERAD is responsible for transport of misfolded proteins from the ER into the cytosol where they become ubiquitinated and degraded by the proteasome system[22]. PTS1 is able to utilize this transport pathway and simultaneously evade subsequent degradation since it contains no lysine residues, which are required for ubiquitination[23]. The molecular mechanism underlying membrane transport and refolding of PTS1 and a possible role of host cell factors in this process are not sufficiently understood. In the cytosol, PTS1 covalently transfers ADP-ribose from NAD^+ onto the α-subunit of trimeric inhibitory G proteins (Giα)[24,25]. This ADP-ribosylation inhibits the activity of Giα as a negative regulator of membrane-bound adenylate cyclase, hence leading to increased intracellular cAMP levels and therefore disturbed signal transduction.

Consequences of cAMP increase depend on the target cells. Presence of the PT-receptor on a wide range of different cell types might explain the various effects of PT during infection with *B. pertussis*. PT inhibits recruitment of neutrophils, monocytes and lymphocytes to the respiratory tract up to 1 week after infection[26,27]. PT leads to decreased amounts of pro-inflammatory chemokines and cytokines and increased bacterial burden in early stages of infection in a mouse model[28]. The current therapeutic regimen only comprises antibiotic treatment, which is important to inhibit rapid spreading of disease via droplet infection but impacts course of disease only if administered in very early stages of infection. Moreover, antibiotic treatment does not improve symptoms including typical paroxysmal cough and in severe manifestations pneumonia, seizures, encephalopathy, apnea and death[2]. Resurgence of pertussis disease and lack of effective treatments necessitates development of novel therapeutics for treatment of severe whooping cough. The PT-dependent nature of severe disease suggests that targeting PT should be an effective strategy for drug development.

We recently demonstrated that specific members of the cyclophilin (Cyp) family, namely CypA and Cyp40 are involved in uptake of PTS1 into the cytosol of target cells[29]. Cyps are members of the peptidyl prolyl cis/trans isomerases (PPIases), which are protein folding helper enzymes that catalyze the rotation of peptide bonds in proteins, assist chaperones such as heat shock protein (Hsp) 90 in protein folding/refolding and are involved in regulating mitochondrial function and permeability (Cyp40)[30–33]. Both CypA and Cyp40 directly bound to PTS1 in vitro and application of pharmacological Cyp inhibitors such as cyclosporine A (CsA) protected CHO-K1 cells from intoxication with PT. In the presence of Cyp inhibitor, less PTS1 reached the cytosol and there was less ADP-ribosylated Giα, implicating that Cyps are required for uptake of PTS1 into the cytosol[29,34].

Here, the role of chaperones and PPIases for the uptake of PT into target cells was investigated and Hsp90, Hsp70, as well as specific Cyps and FK506 binding proteins (FKBPs) were identified as novel interaction partners of PTS1. Application of specific pharmacological inhibitors revealed their crucial functional role for the transport of PTS1 into the cytosol of target cells, protected cells, including primary human airway cells, from intoxication with PT and reduced leukocytosis in an infant mouse model of pertussis.

Results

Specific pharmacological inhibition of chaperone and PPIase activities protects cells from intoxication with PT. A previously established morphology based assay of cellular intoxication was used to determine the functional role of host cell chaperones and PPIases during PT-intoxication[29,35]. CHO-K1 cells show a characteristic clustering morphology if treated with PT (Fig. 1). CHO-K1 cells were pre-incubated prior to PT-treatment with radicicol (Rad) to block Hsp90-activity, and FK506 or CsA to inhibit FKBP or Cyp activity, respectively. Presence of Rad, CsA or FK506 robustly reduced CHO-K1 cell clustering compared to cells treated with PT (Fig. 1a). BFA was used as an inhibitor of PT-induced CHO-K1 cell clustering[17,29,36]. Additionally, fewer cells were observed in wells treated with PT (Fig. 1a). This effect was also inhibited by Rad, CsA and FK506. Hsp70 inhibitors VER-155008 (VER) and HA9[37] both inhibited PT-intoxication (Fig. 1b). The inhibitors alone had no effect on cell morphology or cell number (Supplemental Fig. 1a,b). Taken together, the results indicate a functional role of Hsp90, Hsp70, Cyps and FKBPs for PT-intoxication.

Inhibition of chaperone/PPIase activities leads to reduced ADP-ribosylated Giα without interfering with enzyme activity of PTS1 or binding of PT to cells. After incubation of CHO-K1 cells with PT in the presence or absence of the chaperone and PPIase inhibitors, cells were lysed and incubated with fresh PTS1 in the presence of biotin-labeled NAD^+. During this incubation, the portion of Giα, which has not been modified by PTS1 during the previous treatment of living cells with PT, was ADP-ribosylated in vitro[29]. This results in biotin-labeling of Giα due to the covalent transfer of the biotin-labeled ADP-ribose moiety from NAD^+. Biotin-labeled i.e. ADP-ribosylated Giα was then detected by Western blotting. A strong signal was obtained from control samples, whereas a weaker signal was observed in the presence of PT, showing that in PT-treated cells a substantial amount of Giα was already ADP-ribosylated and could not serve as substrate in the subsequent in vitro ADP-ribosylation reaction. Pre-treatment of cells with chaperone/PPIase inhibitors reduced the ADP-ribosylation of Giα compared to cells treated with PT alone (Fig. 2a). Treatment of cells with the inhibitors only did not affect the subsequent in vitro ADP-ribosylation of Giα by PTS1 (Supplemental Fig. 1c).

Inhibition of Cyps and FKBPs prevented PT-mediated cAMP increase in the iGIST bioassay (Fig. 2b). This assay is based on HEK293 cells that express the Giα-coupled somatostatin receptor 2 (SSTR2) as well as a luminescent cAMP probe[38]. Control samples treated with forskolin to stimulate adenylate cyclase activity and

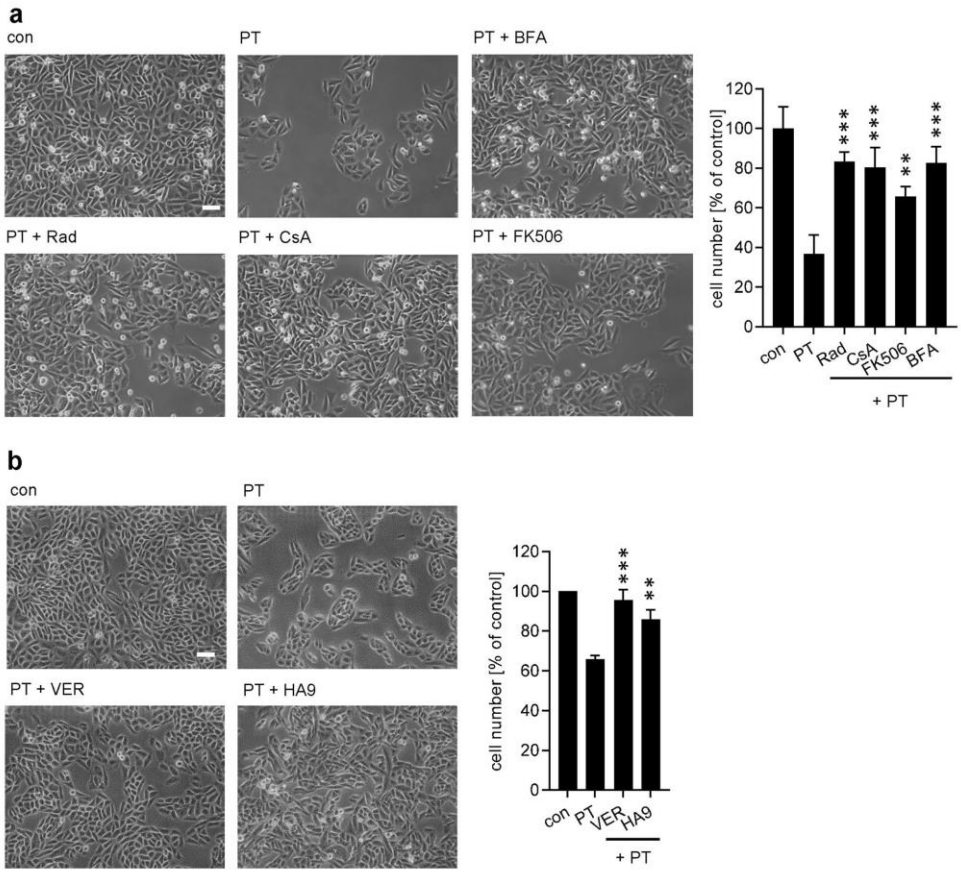

Figure 1. (**a**) Effect of BFA, Rad, FK506 and CsA on the intoxication of CHO-K1 cells with PT. CHO-K1 cells were pre-incubated with 10 µM BFA, Rad, FK506 or CsA or left untreated for control. After 30 min 10 ng/ml PT were added. 1.5 h later the culture medium was removed, and cells were further incubated at 37 °C and 5% CO_2 in fresh medium that did not contain PT or any inhibitor. Pictures were taken after 18 h. A quantitative analysis of total cell number of CHO-K1 cells is shown, values are normalized on control cells (n = 3, mean ± SD). (**b**) Pharmacological inhibition of Hsp70 activity protects cells from PT-intoxication. CHO-K1 cells were treated with VER (30 µM) or HA9 (20 µM) for 30 min and then intoxicated with PT (10 ng/ml) for 18 h. Pictures were taken, and cell numbers were determined as described in A. Significance was tested by one-way ANOVA with Dunnett's multiple comparisons test and refers to samples treated with PT only (*p < 0.05, **p < 0.01, ***p < 0.001). Scale bar = 50 µm.

octreotide to activate SSTR2 which inhibits adenylate cyclase activity show a moderate increase in luminescence signal, i.e. intracellular cAMP (Fig. 2b). In contrast, in samples treated with PT, an enhanced increase in cAMP levels was detected because SSTR2-mediated inhibition of the adenylate cyclase through Giα was impaired. If cells were treated only with forskolin, a comparable increase in cAMP levels was detected with or without PT-treatment (Supplemental Fig. 2b). CsA and FK506 prevented the PT-mediated increase while only marginally affecting cAMP levels in the absence of PT (Fig. 2b). Rad, VER and BFA reduced cAMP levels in the absence of PT (Supplemental Fig. 2a). An inhibitory effect of Rad, VER and BFA on PT-mediated cAMP increase could therefore not be detected with this assay. Solvents of inhibitors had no effect on cAMP levels (Supplemental Fig. 2a).

Taken together, these results suggest that inhibition of chaperones/PPIases reduced PTS1-mediated cytosolic ADP-ribosyltransferase activity. To explain this, we have developed competing hypotheses: (1) the inhibitors reduce the enzyme activity of PTS1 or (2) the inhibitors interfere with the transport of PTS1 into the cytosol.

None of the inhibitors impaired the ADP-ribosylation of Giα by PTS1 in vitro (Fig. 2c, Supplemental Fig. 2c), suggesting that the inhibitors prevent uptake of PTS1 into the cytosol. Binding of PT was not inhibited by

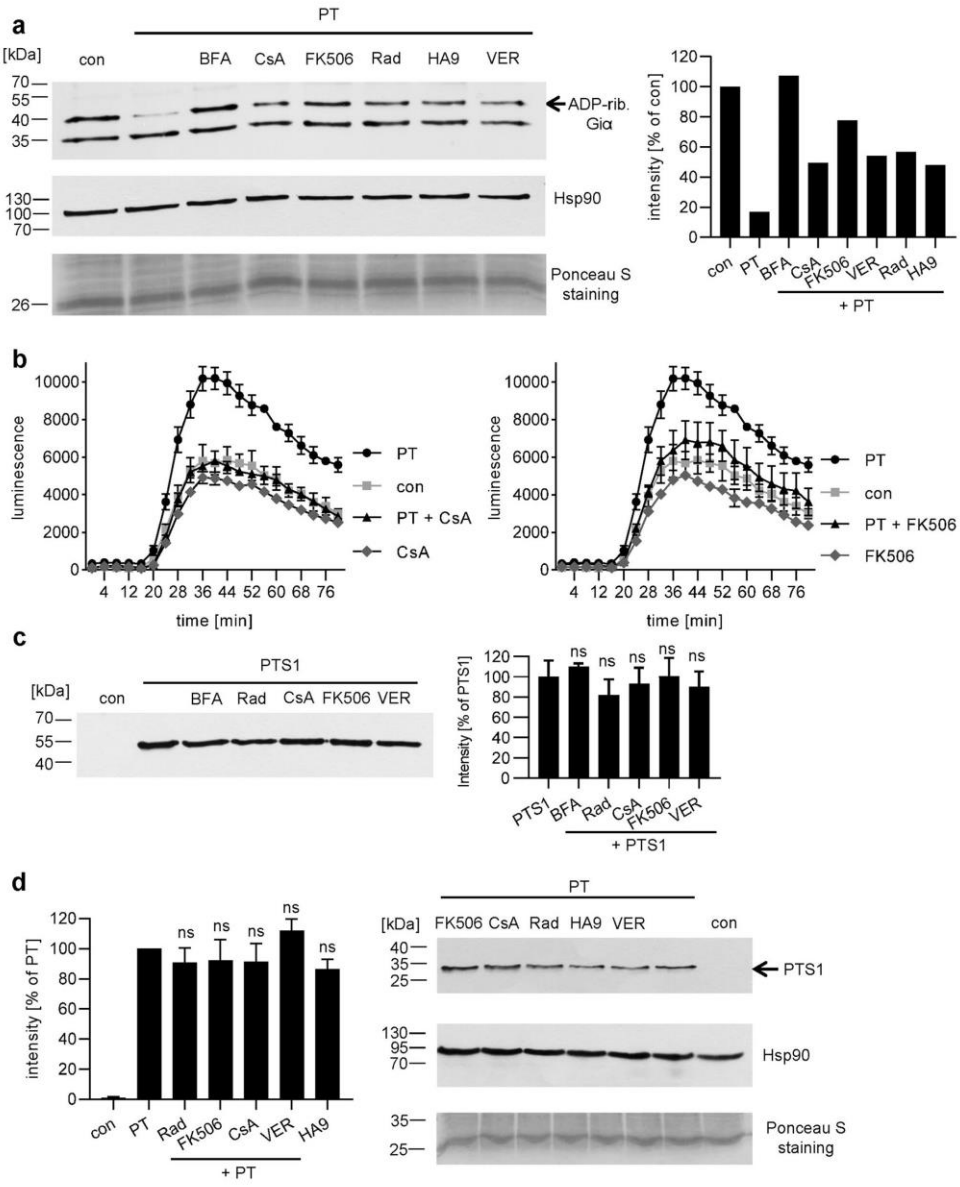
a
PT
[kDa]
con
BFA
CsA
FK506
Rad
HA9
VER
70
55
40
35
ADP-rib. Giα
130
100
70
Hsp90
26
Ponceau S staining
intensity [% of con]
120
100
80
60
40
20
0
con
PT
BFA
CsA
FK506
VER
Rad
HA9
+ PT
b
luminescence
10000
8000
6000
4000
2000
0
4 12 20 28 36 44 52 60 68 76
time [min]
PT
con
PT + CsA
CsA
PT + FK506
FK506
c
PTS1
[kDa]
con
BFA
Rad
CsA
FK506
VER
70
55
40
Intensity [% of PTS1]
ns
PTS1
+ PTS1
d
intensity [% of PT]
con
PT
Rad
FK506
CsA
VER
HA9
+ PT
[kDa]
FK506
CsA
Rad
HA9
VER
con
40
35
25
PTS1
130
95
70
Hsp90
Ponceau S staining

◂**Figure 2.** (**a**) Effect of Rad, CsA, FK506, VER and HA9 on the ADP-ribosylation status of Giα in PT-treated CHO-K1 cells. Cells were pre-incubated with 20 µM of Rad, CsA or FK506, 30 µM VER, 100 µM HA9 or 20 µM BFA for control for 30 min or left untreated. Then, cells were challenged with 20 ng/ml PT for 3 h. Cells were lysed and ADP-ribosylation status of Giα was analyzed. Biotin-labeled (i.e., ADP-ribosylated) Giα was detected. Comparable protein loading was confirmed by Hsp90 and Ponceau S staining. Western blot signals were quantified and normalized to protein loading (Ponceau S). One representative result is shown (n = 3). For uncropped blots see Supplemental Fig. S10. (**b**) Effect of chaperone inhibitors on intracellular cAMP levels in PT-treated cells. iGIST sensor cells (HEK293 cells expressing SSTR2 and luminescent cAMP probe) were incubated with CsA or FK506 (5 µM) or left untreated for control for 30 min. 500 ng/ml PT were added for 3 h and afterwards inducing medium was added to start the luminescence reaction. A baseline was recorded for 15 min. Then, cells were treated with forskolin to activate adenylate cyclase and with octreotide to activate SSTR2. Luminescence was recorded for 1 h. Values are given as mean ± SD. Results from one representative experiment are shown. (**c**) Effect of Rad, CsA, FK506 and VER on enzyme activity in vitro. Recombinant Giα (0.5 µM) was pre-incubated with 10 µM Rad, CsA, 20 µM FK506 or VER for 30 min or with buffer for control. After 30 min rPTxS1 (50 nM) and 1 µM biotin-labeled NAD^+ were added and incubated for 40 min at room temperature. Samples were subjected to SDS-PAGE, blotted and ADP-ribosylated Giα was detected with Strep-POD. Western blot signals were quantified. Values are given as percent of samples treated with PTS1 only (n = 3 values from 3 independent experiments, mean ± SD). Significance was tested one-way ANOVA with Dunnett's multiple comparisons test and refers to samples treated with PTS1 only (*ns* not significant). For uncropped blot see Supplemental Fig. S11. (**d**) Influence of Rad, CsA, FK506 and VER on receptor binding of PT to CHO-K1 cells. CHO-K1 cells were pre-incubated with 20 µM Rad, CsA, FK506 or 30 µM VER or left untreated. After 30 min cells were cooled to 4 °C for 15 min. Then 500 ng/ml PT were added for 30 min at 4 °C. After washing, cells were lysed with Laemmli buffer at 95 °C. Cell-bound PT was detected via an anti-PTS1 antibody in Western Blot. Comparable protein loading was confirmed with Hsp90 and Ponceau-S-staining. Quantification of Western blot signals and one representative Western blot is shown. Values were normalized on the amount of loaded protein (Ponceau S) and are given as percent of PT binding (second bar from left). (n = 4, mean ± SEM). Significance was tested by one-way ANOVA with Dunnett's multiple comparisons test and refers to samples treated with PT only (*ns* not significant). For uncropped blots see Supplemental Fig. S12.

chaperone/PPIase inhibitors (Fig. 2d). This implies that another step of toxin uptake, such as the intracellular membrane transport of PTS1 into the cytosol is the target of these inhibitors.

In the presence of chaperone/PPIase inhibitors, less free PTS1 is detectable in cells. Previously we used fluorescence microscopy to demonstrate that a monoclonal PTS1-antibody recognizes preferably PTS1 when it is detached from the B-subunit pentamer, i.e. cytosolic PTS1[29]. Detection of free PTS1 is decreased following incubation with chaperone/PPIase inhibitors compared to cells challenged with PT only (Fig. 3, Supplemental Fig. 3). This suggests that the inhibitors interfere with uptake of PTS1 into the cytosol. The reason for that might be that endocytosis, retrograde transport to the ER or translocation from the ER to the cytosol are affected. Clustering of cells was still observed in some samples (Rad- and CsA-treated), which might be caused by a small amount of PTS1 that still reached the cytosol in these cells. Notably, the PT-concentration needed for fluorescence experiments is higher than for intoxication experiments in Fig. 1. This might explain why protection by inhibitors against clustering is not as strong as shown in Fig. 1. A reduced PTS1 signal was also observed with BFA, which prevents transport of PT from the Golgi apparatus to the ER and the results are in line with our earlier findings that CsA inhibits uptake of PTS1 into the cytosol[29]. Hence, the reduction of the PTS1 signal in the presence of chaperone/PPIase inhibitors suggests that chaperones/PPIases are involved in uptake of PTS1 to the cytosol.

PTS1 directly and specifically interacts with chaperones and PPIases in vitro. To determine if PTS1 interacts directly with chaperones and PPIases, recombinant chaperones/PPIases were immobilized on a nitrocellulose membrane and overlaid with PTS1. Results in Fig. 4a show specific and concentration-dependent binding of PTS1 to Hsp90, Hsp70 and Hsc70 as well as to CypA, Cyp40, FKBP51 and FKBP52. Previously, we showed that other toxin subunits like the lethal factor of *B. anthracis* or the transport component of *C. botulinum* C2 toxin do not interact with these chaperones/PPIases in the same assay indicating its specificity[39,40]. Ponceau S-staining confirmed transfer of recombinant proteins onto the membrane. Moreover, no interaction was observed with a control protein C3bot from *C. botulinum* or the small isoform FKBP12. FKBP12 consists of only one PPIase domain. FKBP51 and FKBP52 also contain a PPIase domain and have additional domains that facilitate the interaction with potential client proteins[32]. Here, we investigated the binding of PTS1 to FKBP-fragments that only comprise the conserved PPIase domains i.e. FKBP51 FK1 and FKBP52 FK1. Results shown in Fig. 4b indicate that there still is an interaction of PTS1 with the fragments, but it is obviously weaker, compared to full-length FKBPs. This suggests that the PPIase domain, as well as the other domains of FKBPs, are involved in binding of PTS1.

Cyp40, FKBP51, Hsp70 and Hsp90 interact with PTS1 in cells for at least 24 h post intoxication. After demonstrating a direct interaction of chaperones/PPIases with PTS1 in vitro and establishing a functional role of these factors during uptake of PT into the cytosol, the duration of the PTS1-Cyp40 interaction was investigated in cells. The proximity ligation assay (PLA) technology encompasses an internal amplification reaction that only occurs if two antibodies against the potential binding partners come into close proxim-

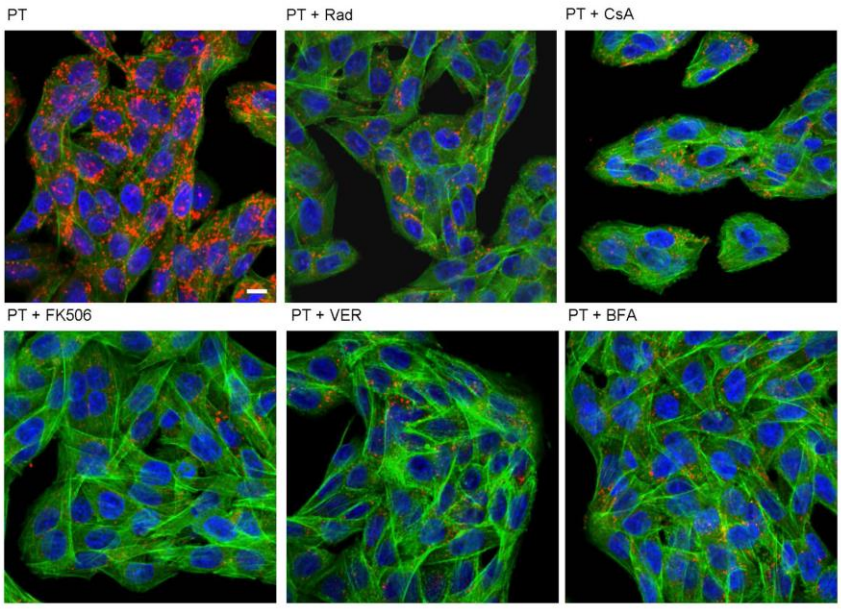

Figure 3. In the presence of inhibitors of Hsp90/Hsp70 and PPIases less free PTS1 is detected in CHO-K1 cells. CHO-K1 cells were pre-incubated with CsA, FK506, Rad (20 µM) or VER (30 µM) for 30 min. 20 µM BFA were used as control. Then, cells were challenged with 1 µg/ml PT and 1 h later medium was exchanged. After 24 h, cells were fixed, permeabilized and blocked. Subsequently, cells were probed with an anti-PTS1 antibody, Hoechst and phalloidin-FITC for F-actin staining. Pictures were taken with a Zeiss LSM-710 confocal microscope. Red = PTS1, green = F-actin, blue = nucleus, scale bar = 10 µm.

ity. Every PLA signal detected by fluorescence microscopy represents one interaction event between PTS1 and Cyp40. The interaction between PTS1 and Cyp40 was detected from 30 min up to 48 h after incubation of cells with PT (Fig. 4c, Supplemental Fig. 4). CsA or BFA did not inhibit interaction of Cyp40 with PTS1 i.e. the PLA signal, most likely due to high PT concentration (Supplemental Fig. 5). Notably, under these conditions CsA and BFA did not reduce the PTS1 signal per se as shown before with lower concentrations of PT in Fig. 3 (Supplemental Fig. 5). Moreover, interaction between PTS1 and Hsp90, Hsp70 and FKBP51 was demonstrated after 3 h and 24 h of PT intoxication (Fig. 4d, Supplemental Fig. 6).

PT invades secretory but not ciliated cells in a human airway epithelium. To determine if the phenomenon of chaperone/PPIase requirement for PT uptake is recapitulated in a model of primary human bronchial airway epithelium, we first demonstrated that PT intoxicates human primary basal cells from airway epithelium in a concentration-dependent manner (Supplemental Fig. 7). Although clustering was not observed in these cells upon PT-treatment, impairment of cell morphology was noted (Supplemental Fig. 7) suggesting some cell damage induced by PT. Application of Rad or CsA reduced ADP-ribosylation of Giα in PT-treated basal cells (Fig. 5a), as analyzed by sequential ADP-ribosylation. Inhibitors alone had no significant effect on ADP-ribosylation of Giα (Supplemental Fig. 8). Mechanistic studies performed in CHO-K1 cells demonstrated that Rad and CsA do not influence enzyme activity or receptor binding but reduce the cytosolic amount of PTS1 in target cells, suggesting that Hsp90 and Cyps are involved in the transport of PTS1 into the cytosol of these cells.

Basal cells that represent one cell type of human bronchial airway epithelial cells (hBAECs) can be differentiated to a functional airway epithelium at air–liquid interface conditions, containing ciliated and secretory cells. By analyzing the effect of PT on the differentiated cell layer by fluorescence microscopy, it became evident that PTS1 was selectively detected in secretory (CC10 or MUC5B positive) cells[41], but not in ciliated cells (β-IV-tubulin positive) (Fig. 5b). Moreover, CsA but not Rad or FK506 reduced the amount of PTS1 detected by fluorescence microscopy in this functional airway epithelium (Fig. 6). Noteworthy, the PTS1-antibody preferentially recognizes PTS1 that is not bound to the B-oligomer, which is most likely located in the cytosol. Rad, CsA or FK506 alone had no adverse effects on morphology of the airway epithelium or tight junctions (Supplemental Fig. 9a). However, VER and BFA revealed strong adverse effects on the airway epithelium showing a reduced cell number for VER-treated cells and nearly no cells were detected after BFA treatment (Supplemental Fig. 9b).

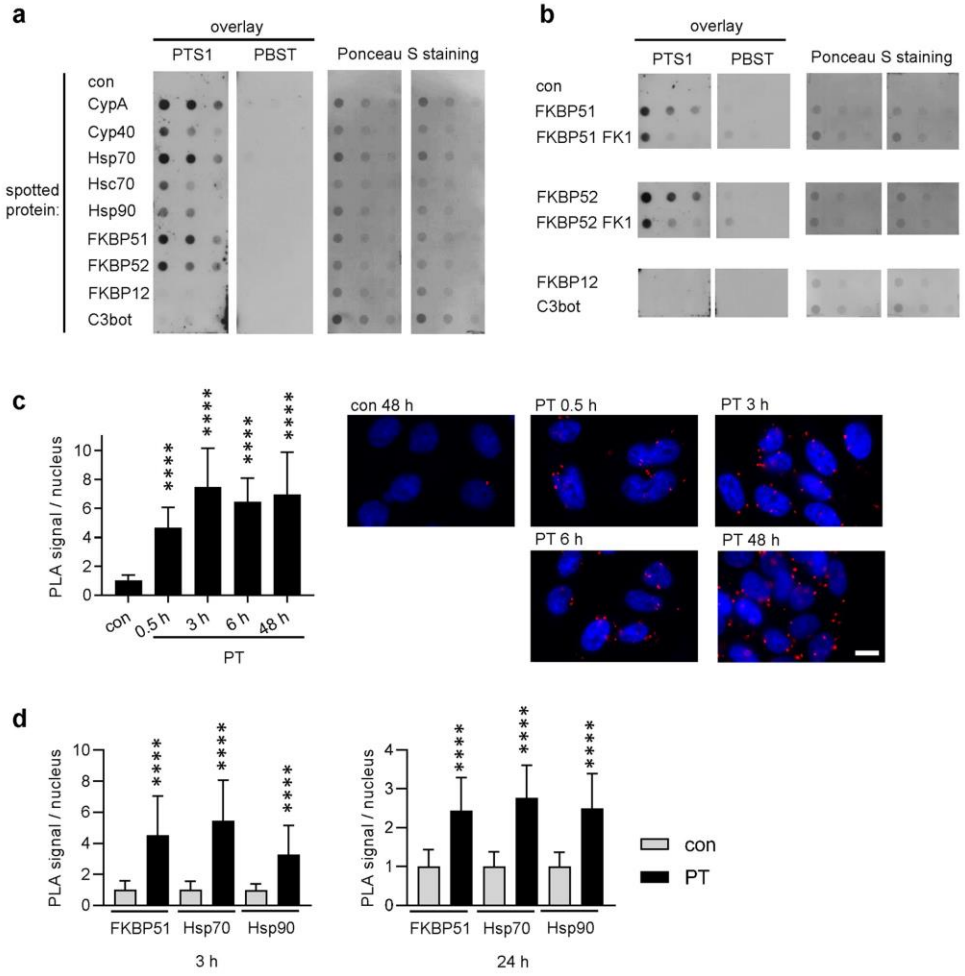

Figure 4. (**a**) PTS1 interacts with chaperones and PPIases in vitro. Purified chaperones/PPIases were spotted two times onto a nitrocellulose membrane in decreasing concentrations (1 µg, 0.5 µg, 0.25 µg). PBS and C3 toxin from *C. botulinum* were used as negative controls. Membrane was cut and overlay with His-PTS1 (200 ng/ml) or PBST was performed. After extensive washing, bound PTS1 was detected with a specific antibody. PTS1- and PBST-overlayed membranes were detected on the same X-ray film and images were cropped for display purposes only. Comparable amounts of spotted protein were confirmed by Ponceau S-staining. (**b**) PTS1 binds to the isolated PPIase domains of FKBP51/52. FKBP51/52 and their FK1 fragments i.e. isolated PPIase domains were spotted onto a nitrocellulose membrane. The experiment was further conducted as described in A. All signals were detected on the same X-ray film and images were cropped for display purposes only. (**c**) Cyp40 interacts with PTS1 in cells. CHO-K1 cells were incubated on ice with PT (5 µg/ml) for 30 min to enable binding or left untreated for control. After washing, the cells were further incubated for 0.5 h, 3 h, 6 h and 48 h at 37 °C. Cells were fixed and fluorescence-based PLA assay was performed according to the manufacturer's manual. PLA signals represent one protein interaction event of PTS1 and Cyp40 and were counted from fluorescence pictures (n = 10 pictures per condition, mean ± SD) with ImageJ. Values were normalized to the mean of the control samples. Significance was tested by one-way ANOVA with Dunnett's multiple comparisons test and refers to untreated control samples (****p < 0.0001). One representative image is shown for each condition (blue = nucleus, red = PLA signal). Scale bar = 10 µm. (**d**) FKBP51, Hsp70 and Hsp90 interact with PTS1 in cells. CHO-K1 cells were treated with PT (3 µg/ml) for 3 h (left) or 24 h (right) at 37 °C. Then, cells were fixed, and fluorescence-based PLA assay was performed according to the manufacturer's manual. PLA signals were counted from fluorescence pictures (n = 20 images per condition from at least 2 independent experiments, mean ± SD) with ImageJ. Values were normalized to the mean of the control samples. Significance was tested by Mann–Whitney test and refers to the respective untreated controls (****p < 0.0001).

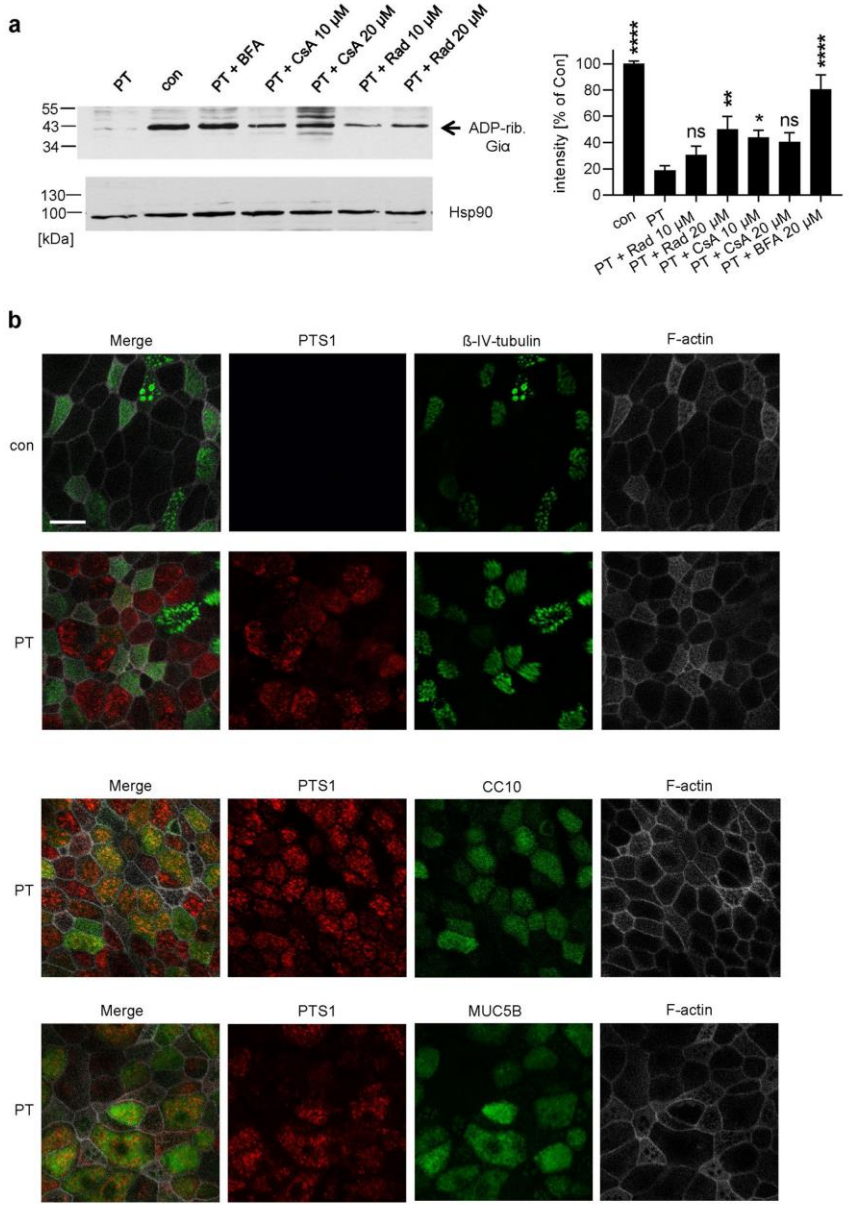

Figure 5. (**a**) Rad and CsA inhibit ADP-ribosylation of Giα in PT-treated basal cells. Basal cells were pre-incubated with Rad, CsA or BFA (20 µM) for 45 min or left untreated for control (con). Subsequently, 10 ng/ml PT was added for 4 h and the ADP-ribosylation status of Giα was determined as described before. A representative Western blot result is shown. Comparable protein loading was confirmed by Ponceau S (not shown) and Hsp90 staining. Western blot signals were quantified and normalized to protein loading (n = 8 independent experiments, mean ± SEM). Significance was tested by one-way ANOVA with Dunnett's multiple comparisons test and refers to samples treated with PT only (****$p < 0.0001$, **$p < 0.01$, *$p < 0.05$, *ns* not significant). For uncropped blots see Supplemental Fig. S13. (**b**) PTS1 is detected in secretory (CC10+, MUC5B+) cells but not in ciliated (β-IV-tubulin+) cells. hBAECs were incubated with PT (20 µg/ml) from the apical side for at least 72 h or left untreated for control. Cells were fixed with 4% PFA. For permeabilization and quenching of autofluorescence, cells were treated with 0.2% saponin. F-actin was stained with phalloidin-FITC. PTS1, β-IV-tubulin, CC10 and Muc5B were stained with specific primary and fluorescence-labeled secondary antibodies, respectively. Pictures were taken with an inverted confocal microscope. Scale bar = 20 µm.

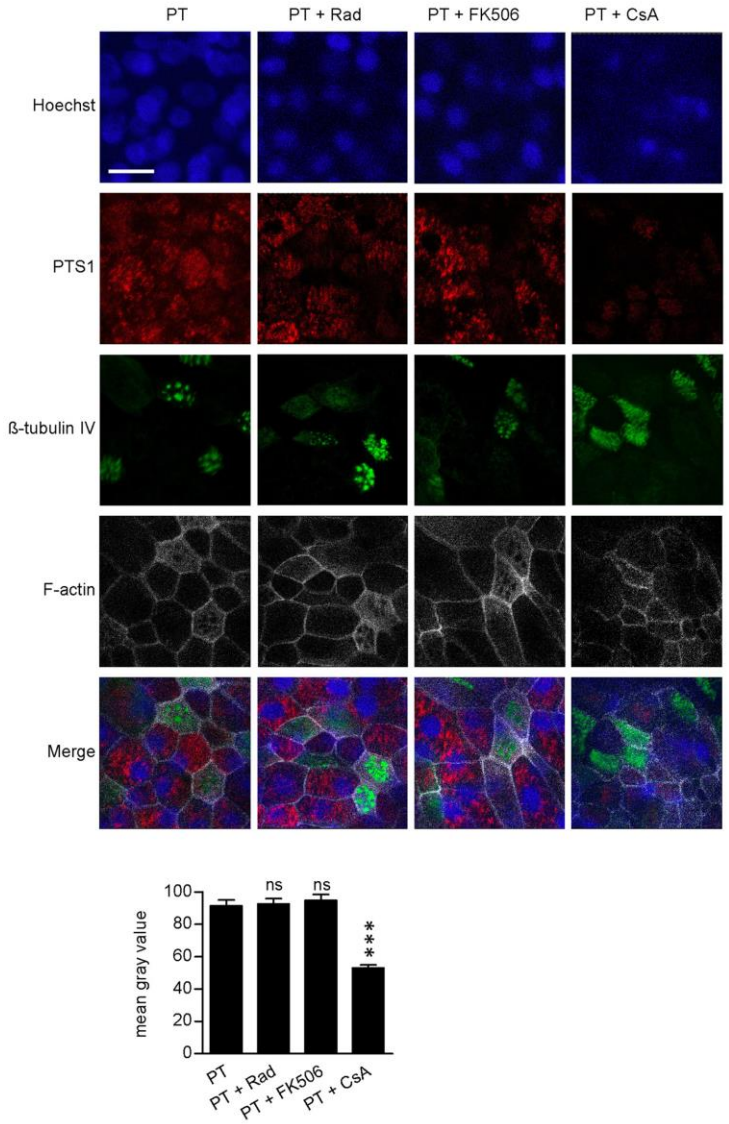

Figure 6. Effect of Rad, FK506 and CsA on uptake of PTS1 into hBAECs. hBAECs were pre-treated with respective inhibitors (20 µM) and then incubated with PT (20 µg/ml) from the apical side for 72 h. Cells were fixed with 4% PFA. For permeabilization and quenching of autofluorescence, cells were treated with 0.2% saponin. F-actin was stained with phalloidin-FITC. PTS1 and β-IV-tubulin were stained with specific primary and respective fluorescence-labeled secondary antibodies. Pictures were taken with a Cell Observer inverse microscope (Zeiss, Germany). Mean Gray Value Intensity was measured and plotted for PTS1 (after background subtraction) in PT and PT + inhibitor treated cultures. Values are given as mean ± SEM (n = 60 cells/condition). Significance was tested by Kruskal–Wallis test and refers to samples treated with only PT (***$p < 0.001$, *ns* not significant). Scale bar = 20 µm.

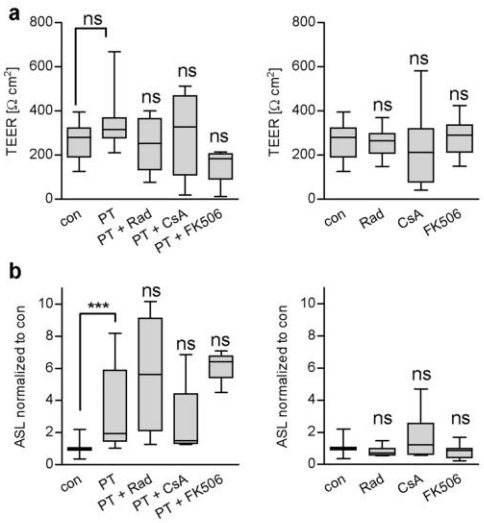

Figure 7. PT does not impair barrier function but increased apical surface liquid. (**a**) hBAECs were pre-incubated with Rad, CsA or FK506 (20 µM) for 30 min or left untreated. Then 20 µg/ml PT was added for 72 h or cells were left untreated. Transepithelial electrical resistance (TEER) was measured using CellZScope from NanoAnalytics. (**b**) hBAECs were treated as described in A. After 72 h the apical surface liquid was determined. Values were obtained from at least two independent experiments ($n \geq 4$). Significance was tested by Kruskal–Wallis test and refers to samples treated with only PT or as indicated (***$p < 0.001$, *ns* not significant).

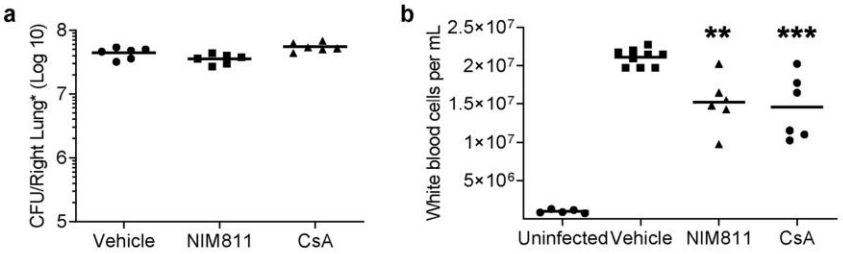

Figure 8. Cyclophilin inhibition reduces *B. pertussis* induced leukocytosis. Following aerosol infection 7-day old C57BL/6 pups were treated daily with vehicle, CsA (25 mg/kg) or NIM811 (25 mg/kg). No differences were determined in bacterial burden (**a**) however significant reduction in leukocytosis was noted in drug treated animals versus vehicle control (**b**). Each data point represents one animal. Significance was determined by one-way ANOVA with Dunnett's multiple comparisons test (***$p < 0.001$, **$p < 0.01$ vs. vehicle). Bars represent mean values.

Next, effects of PT on functional aspects of the human bronchial airway epithelium were investigated. PT showed no significant effect on trans-epithelial electrical resistance (TEER) of the human bronchial airway epithelium (Fig. 7a). However, PT significantly increased the apical surface liquid (ASL) of the functional human airway epithelium compared to untreated controls (Fig. 7b). This effect was not impaired by the chaperone inhibitors suggesting that other mechanisms might play a role that do not require PTS1 activity in the cytosol such as binding of the B-pentamer to the cell surface. Chaperone/PPIase inhibitors alone led to no significant effects on ASL or TEER values of treated samples compared to control (Fig. 7, right panels).

Cyp inhibitors reduce leukocytosis in an infant model of pertussis disease. Finally, effects of CsA and its non-immunosuppressive derivative NIM811[42] were investigated in an infant mouse model of pertussis. This model has recently been established and recapitulates several hallmarks of severe disease observed in humans such as leukocytosis and death, which are both PT-dependent[8]. Here, 7-day old mice were infected

with a PT-producing wild type strain of *B. pertussis* via aerosol and then treated intranasally with either CsA or NIM811 or vehicle. Treatment with CsA or NIM811 had no effect on the colony forming units detected from lung homogenates (Fig. 8). However, PT-induced leukocytosis was significantly reduced by CsA or NIM811 treatment in infant mice implicating a protective effect upon Cyp inhibition for the first time in vivo.

Discussion

Pertussis disease is a reemerging public health crisis for which there is currently no effective treatment. The current standard of care, treatment with macrolide antibiotics is only associated with improved symptoms when administered during the catarrhal stage of disease[43]. This is challenging as it is before the onset of the characteristic "whooping" cough. *B. pertussis* mediates disease through its ADP-ribosylating toxin (ADP-RT) PT. The ability of ADP-RTs to translocate their enzyme subunits to target cell cytosols has been the subject of much research (for review see[44,45]). We have shown other membrane translocating ADP-RTs, such as *Corynebacterium diphtheriae* diphtheria toxin, *C. botulinum* C2 toxin, *C. perfringens* iota toxin, and *C. difficile* CDT, require the chaperone activity of heat shock proteins Hsp90 and Hsp70, Cyps as well as PPIases from the FKBP family to transfer their enzymatic subunits from vesicular compartments to the cytosol of target cells[37,40,46–53]. Identifying commonalities in these toxins mechanisms of action may allow for the development of treatments which function for across diverse bacterial species.

Our previous work identified Cyp inhibitors as potent inhibitors of PT intoxication of mammalian cells[29]. Previously, we determined that Cyp isoforms CypA and Cyp40 interact with PTS1 in vitro and are required for uptake of PTS1 into the cytosol. This study revealed host Hsp90, Hsp70, Cyps and FKBPs are required for uptake of PTS1 into the cytosol. A direct and specific interaction of PTS1 with Hsp90, Hsp70, CypA, Cyp40, FKBP51 and FKBP52 was detected in vitro and interaction with FKBPs was partly mediated by the PPIase domain of these proteins. Human bronchial derived airway epithelial cells differentiated under air–liquid interface conditions allowed us to identify secretory cells as targets for PTS1 intoxication. Further, pharmacological inhibitors of Cyps protected against leukocytosis in an in vivo murine model of infant pertussis disease demonstrating the clinical potential of these molecules.

ADP-ribosylation of GTP-binding regulatory protein Giα by PT[1,2] induces distinct morphological changes in CHO-K1 cells in a sensitive and reproducible manner[35]. This phenomenon is the basis of routine assays to determine monoclonal antibody function and to measure antitoxin responses[54,55]. Here, we utilized this CHO-K1 assay and pharmacological inhibitors of heat shock proteins, Cyps and FKBPs to show PT interactions with Hsp90, Hsp70, FKBP and Cyps are required for PT-intoxication of CHO-K1 cells. Further, we determined inhibition of these host molecules prevents ADP-ribosylation of Giα protein and intracellular cAMP accumulation of CHO-K1 by preventing uptake of PT into the cytosol, not by inhibiting PT enzymatic activity. Immobilization of the studied host chaperones and folding helper proteins on a nitrocellulose membrane and incubation with PTS1 identified Hsp90, Hsp70 and Hsc70, CypA, Cyp40, FKBP51 and FKBP52 as binding partners of PTS1 in a specific and concentration-dependent manner. Interestingly, Hsp90 requirement for translocation of PTS1 from the ER into the cytosol was shown in a previous study. In this study, PTS1 was expressed directly in the ER of transfected CHO cells and it was demonstrated that Hsp90-inhibition in these cells prevented translocation of PTS1 from the ER to the cytosol[56]. The effect of CsA, FK506 and VER on translocation of PTS1 from the ER to the cytosol was not investigated in such an isolated manner and therefore we cannot fully exclude an inhibiting effect of CsA, FK506 or VER on endocytosis or retrograde transport to the ER. Nevertheless, assistance of Cyps, FKBPs and Hsp70 during translocation into the cytosol as demonstrated for Hsp90 is conceivable.

Cyp40, FKBP51 and FKBP52 contain three TPR domains through which they bind to Hsp90[32,57] forming a Hsp90–multichaperone complex[30,31]. The Hsp90–multichaperone complex facilitates the stabilization, folding and activation of more than 200 mammalian proteins including steroid hormone receptors[30,58–60]. For folding and activation of steroid hormone receptors, activity of chaperones is required in a concerted and sequenced manner[30]. First, Hsp70 binds the unfolded protein and transfers it to an Hsp90 dimer. Subsequent binding of FKBPs or Cyps through TPR domains influences Hsp90 activity, in particular its ability to bind and hydrolyze ATP. ATP hydrolysis leads to conformational changes in Hsp90, which are transferred onto the unfolded protein resulting in a native folded protein. Since the same composition of cellular chaperones is required for the cytosolic delivery of ADP-RTs including PT it is conceivable that also in this case the chaperones act in a concerted manner.

Recently, it has been shown that cholera toxin requires Hsc/Hsp70 but not Cyps in addition to Hsp90 for its cellular uptake[61]. However, interaction of Hsc/Hsp70 and Hsp90 with CTA1, the enzyme domain of cholera toxin, occurs independently since both chaperones can bind simultaneously to CTA1, and binding occurs in the absence of the adapter protein Hop. This suggests an alternative interaction mechanism between cholera toxin and Hsp90/Hsc/Hsp70 that differs from the described Hsp90–multichaperone machinery.

We showed that interaction between Cyp40 and PTS1 was detected after 48 h after PT incubation. This suggests that Cyp40 not only facilitates the uptake of PTS1 into the cytosol but is required to stabilize PTS1 in an active conformation. A comparable mechanism is described for the cholera toxin, which also harbors ADP-ribosyltransferase activity and belongs to the group of long trip toxins. Hsp90 facilitates translocation of CTA1 to the cytosol, refolds CTA1 into an active conformation in an ATP-dependent manner and continues to bind to refolded CTA1[62,63]. The finding that CTA1 and PTS1 require the assistance of chaperones even after translocation and refolding might be due to the fact that both enzyme subunits are thermally unstable. This means that unfolding of CTA1 and PTS1 occurs at 37 °C after dissociation from the B-subunit. Therefore, releasing of toxin subunits from chaperones after translocation/refolding could again result in unfolding. Recently, two Hsp90 binding motifs in CTA1, which both are necessary for efficient translocation of CTA1 into the cytosol were identified[56]. One of these binding motifs was also identified in other ER-translocating ADP-ribosylating toxins including PT and Hsp90 requirement for PT uptake into the cytosol was demonstrated confirming and

supporting the findings in the present study. Interestingly, the identified Hsp90-binding motif was absent in ADP-ribosylating toxins that translocate from endosomes suggesting an interaction mechanism distinct to some extent between short trip and long trip ADP-ribosylating toxins.

B. pertussis colonizes its host through attachment to the ciliated cells of the airways. It is known that PT can bind to various sialic acid-containing glycoproteins and various receptors have been found[11,13]. However, so far it is not clear which cell types are the target for PT in humans. Human bronchial airway epithelial basal cells differentiated in air–liquid interface conditions recapitulate the characteristics of the airway epithelial barrier. These epithelial cells differentiate into pseudostratified, polarized cells including ciliated and goblet (secretory) cells. From this, we determined that CC10 or MUC5B positive secretory cells, and not β-IV-tubulin positive ciliated cells were the target of PTS1 intoxication. It was determined that pharmacological inhibition of Cyps, but not Hsp90 or FKBP reduced detectable cytosolic PTS1 in these cells. Moreover, PT had no effect on the trans-epithelial resistance but increases the ASL of the differentiated human airway epithelium. These data suggest that PT does not impact gross epithelial barrier integrity but rather affects vectorial ion or fluid transport. The ASL shields the mucosal surface of lung epithelia and forms the first line of defense against airborne noxae and pathogens. A major task of lung epithelial cells is therefore to tightly regulate the ASL volume to maintain appropriate lung function and to ensure mucociliary clearance. ASL volume homeostasis is regulated by balancing water secretion and resorption. Secretion is driven by apical chloride channels (e.g. CFTR), whereas the epithelial Na^+ channel (ENaC) mediates resorption. Hence, our observation that PT disturbs ASL homeostasis might reflect an impact on vectorial ion transport, either activating apical chloride channels or inhibiting ENaC. It has been demonstrated that PT intoxication results in increased intracellular cAMP levels, and CFTR is activated by intracellular cAMP[64]. Yet, future studies, including Ussing chamber measurements, will be required to decipher the impact of PT intoxication on transepithelial ion/water transport in more detail.

Results from another previous study in mice showed an upregulation of the epithelial anion exchanger pendrin in the lung after infection with *B. pertussis*[65]. Pendrin knockout mice showed reduced lung inflammatory pathology but even higher bacterial loads during infection suggesting a role of pendrin in the pathology. Pendrin exports bicarbonate to the ASL and thereby increases pH, which possibly contributes to promoting the inflammatory pathology. These results indicate that manipulation of ASL parameters like volume or pH might be mediated by PT and play a role for the pathology and course of disease.

The mouse model of pertussis disease recapitulates the age-dependent nature of severe pertussis illness. Infant mice succumb to lethal infection at doses tolerated by adult mice. Leukocytosis, the rapid increase in vascular leukocytes, correlates with disease severity and lethality and is PT-mediated[10,66]. Infant mice, like humans, show robust increases in circulating leukocytes following infection. Here, we showed that inhibition of Cyp activity by CsA, a licensed drug with well-known pharmacokinetics and safety profiles[67,68], and its non-immunosuppressive derivative NIM811[42] led to significantly decreased leukocytosis upon infection with PT-producing *B. pertussis* strains. To our knowledge, this is the first time that Cyps were pharmacologically targeted to successfully prevent cytotoxic effects of a bacterial AB-type toxin in an in vivo model. Together with our detailed mechanistic studies in CHO-K1 cells and in vitro differentiated human airway epithelial model, these results provide a promising basis for the development of novel therapeutic strategies to prevent severe symptoms like leukocytosis caused by PT during *B. pertussis* infection.

Methods

Protein expression and purification. Recombinant proteins were expressed and purified as described before: Hsp70, Hsc70[37], Hsp90[51], FKBP12, FKBP51, FKBP52[52], CypA, Cyp40[40], FK1 domains of FKBP51 and FKBP52[53], C3bot[69], PTS1 and Giα[70].

Protein–protein interaction studies via dot blot system. Purified recombinant chaperones, PPIases and PPIase fragments were vacuum aspirated onto a nitrocellulose membrane as serial dilution starting with 1 µg/ml using the dot blot system (Bio-Rad, Feldkirchen, Germany). Recombinant C3 toxin from *C. botulinum* (C3bot) was chosen as a random protein to exclude unspecific protein–protein interactions. Successful transfer was confirmed by Ponceau S staining. Membrane was blocked with 5% skim milk powder in PBS-Tween (PBST) and then cut and probed with PTS1 (Aviva Systems, San Diego, California, USA) or for control with PBST. After extensive washing, both membranes were incubated with anti-PTS1 antibody (Santa Cruz, Heidelberg, Germany) to detect bound PTS1 using HRP-coupled secondary antibody (Santa Cruz) in combination with ECL (enhanced chemiluminescence, Millipore, Merck, Darmstadt, Germany) system. Signals for both membranes were detected on the same X-ray film. Pictures were cropped for display purposes only.

Cell culture and intoxication experiments. Cell culture materials were obtained from Gibco unless indicated otherwise. Chinese hamster ovary cells strain K1 (CHO-K1, from DSMZ, Braunschweig, Germany) were cultivated in DMEM and HAM's F12 containing 5% heat-inactivated fetal calf serum (Invitrogen, Thermo Fisher Scientific, Waltham, Massachusetts, USA), 1 mM sodium-pyruvate and Penicillin–Streptomycin (Pen-Strep) (1:100) (Thermo Fisher Scientific). Cells were grown at 37 °C and 5% CO_2 as described before[29]. Cells were trypsinized and reseeded every two to three days for at most 15–20 times. For intoxication experiments[29,46,48], cells were seeded in culture dishes and the specific pharmacological inhibitors radicicol (inhibitor of ATP-binding site of Hsp90, Sigma-Aldrich, Merck, Darmstadt, Germany), cyclosporine A (inhibitor of Cyp activity, Sigma-Aldrich, Merck), FK506 (inhibitor of FKBP activity, Sigma-Aldrich, Merck), VER (inhibitor of ATP-binding site of Hsp70, Hsc70 and Grp78, Tocris Bioscience, Wiesbaden-Nordenstadt, Germany), HA9 (inhibitor of the substrate binding domain of Hsp70)[37] and brefeldin A (disrupts Golgi apparatus, Sigma-Aldrich, Merck) were added for 30 min. Then, PT (Sigma-Aldrich, Merck) was added either for 1 h with subsequent removal and

further incubation for 18 h at 37 °C or PT was added for 18 h. Morphology of cells was documented by using a Zeiss Axiovert 40CFL microscope with a Jenoptik ProgRes C10 CCD camera. At least 3 images per treatment were taken and analyzed and the experiment was repeated independently at least 3 times. To quantify toxin-induced effects on CHO-K1 cells total number of cells per picture was manually counted using ImageJ (National Institutes of Health, Bethesda). Untreated control cells were set as 100% and values of other samples were calculated accordingly. Materials for cell culture experiments were obtained from TPP Techno Plastic Products (Trasadingen, Schweiz).

Primary human bronchial airway epithelial cell culture. Frozen primary human bronchial airway epithelial cells (hBAECs, Epithelix, Geneva, Switzerland) were obtained at passage 1. Of all cell types that are obtained from a human airway epithelium, only the basal cells survive. Basal cells were proliferated in growth medium (Promocell, Heidelberg, Germany) supplemented with Penicillin–Streptomycin (PenStrep, Thermo Fisher Scientific) until reaching 80% confluence in a T75 flask. Growth medium was replaced every two days. Cells were detached using DetachKIT (Promocell). 3.5×10^4 cells were seeded onto a transwell filter (Corning Costar 3470; Corning, Wiesbaden, Germany) pre-coated with collagen solution (StemCell Technologies, Cologne, Germany). Cells were maintained with 200 µl growth medium in the apical and 600 µl of growth medium in the basolateral compartment. To obtain a fully differentiated epithelium containing secretory and ciliated cells, apical medium was removed after 72 h and basolateral medium was switched to differentiation medium. Differentiation medium was a 50:50 mixture of DMEM-H without glutamine and pyruvate and LHC basal (both from Thermo Fisher Scientific) supplemented with supplement pack (Promocell), PenStrep and different trace elements as described in detail before[71]. Cells were grown until day 25 day with the basolateral medium being changed every three days. From day 14 onwards, cells were washed on the apical side every three days for 30 min with Dulbecco's phosphate buffered solution (DPBS, Biochrom, Berlin, Germany) to remove accumulated mucus. hBAECs cultures from 2–3 different donors were used for each experiment.

Sequential ADP-ribosylation of Giα in lysates from toxin-treated cells. CHO-K1 cells or human basal cells were pre-incubated with respective inhibitors and then intoxicated with PT for given incubation periods. Cells were lysed by freezing in ADP-ribosylation buffer (0.1 mM Tris–HCl (pH 7.6), 20 mM DTT and 0.1 µM ATP) or plus protease inhibitor complete (Roche, Basel, Switzerland) as described earlier[17,29,70], followed by incubation with PTS1 (170 ng (of the commercially obtained PTS1) or 50 nM (of the recombinantly expressed rPTxS1)) and biotin-labeled NAD^+ (10 µM or 1 µM, Trevigen, Gaithersburg, Maryland, USA) for 40–60 min at room temperature for in vitro ADP-ribosylation of Giα, which had not yet been ADP-ribosylated by PT during the previous incubation. Samples were subjected to SDS-PAGE, blotted and ADP-ribosylated, i.e. biotin-labeled, Giα detected with streptavidin-peroxidase (Strep-POD, Sigma-Aldrich, Merck) using the ECL system. Comparable amounts of protein were confirmed by Ponceau-S-staining. Densitometric quantification of Western blot signals was measured using Adobe Photoshop CS6 and values were normalized on the amount of loaded protein.

iGIST bioassay. The iGIST bioassay was performed as previously described[38]. In brief, HEK293 cells that have been stably transfected with Giα-coupled somatostatin receptor 2 (SSTR2) GPCR were seeded as 60,000 cells/well into 96-well plates with light-tight walls in DMEM/F-12 (1:1) medium (Gibco), supplemented with fetal calf serum (10%) and Pen-Strep (1%) 1 day prior to the experiment. Cells were pre-incubated with inhibitors (5 µM) or matched solvents (DMSO or ethanol) for 30 min and then challenged with PT (500 ng/ml) or matched buffer SolC (both in 50% glycerol, 50 mM TRIS, 10 mM glycine, 0.5 M NaCl, pH 7.5) for 3 h. After addition of the inducing medium containing the luminescent GloSensor cAMP reagent (Promega, Walldorf, Germany), baseline luminescence was recorded for 15 min at the Orion Microplate Luminometer (Berthold Detection Systems). To activate the adenylate cyclase, forskolin (Sigma-Aldrich, Merck) was added and at the same time octreotide (Bachem, Bubendorf, Switzerland) was applied to stimulate the Giα-coupled SSTR2 GPCR. After spiking, luminescence was measured for 1 h.

In vitro enzyme activity of PTS1. Recombinant Giα (0.5 µM) was incubated for 30 min with 10 µM Rad, CsA, 20 µM FK506 or VER at room temperature. As a control Giα was incubated with buffer (50 nM sodium phosphate buffer, pH 7) only. After 30 min rPTxS1[70] (50 nM) was added together with biotin-labeled NAD^+ (1 µM, Trevigen) and incubated for 40 min at room temperature. Samples were subjected to SDS-PAGE and blotted onto a nitrocellulose membrane. ADP-ribosylated, i.e. biotin-labeled, Giα was detected with Strep-POD. Comparable amounts of protein were confirmed by Ponceau-S-staining.

Toxin binding assay. CHO-K1 cells were pre-incubated with 10 µM Rad, CsA, FK506 or 30 µM VER. The assay was performed as previously described[29,46]. Cells were cooled down to 4 °C for 15 min to prevent endocytosis. 500 ng/ml PT were added, and cells were incubated for 30 min at 4 °C. Subsequently, culture medium was removed, and cells were washed with PBS to remove unbound PT. Then cells were scraped with boiling SDS-sample buffer and heated for 10 min at 95 °C. SDS-PAGE and Western Blotting was performed. To detect cell-bound PT an antibody against the S1 subunit of PT and a peroxidase-coupled secondary antibody were used.

Immunofluorescence. Fluorescence microscopy was performed as described earlier[29,46]. Cells were fixed after intoxication experiments with 4% paraformaldehyde (PFA), permeabilized with Triton-X 100 (0.4% in PBS), treated with glycine (100 nM in PBS) and blocked with 5% skim milk powder or 10% normal goat serum

(Jackson ImmunoResearch, West Grove, Pennsylvania, USA) and 1% BSA in PBST for 1 h at 37 °C. Samples were incubated with anti-PTS1 antibody (Santa Cruz, 1:50 diluted in 10% NGS and 1% BSA in PBST) for 1 h at 37 °C. After washing, fluorescence-labeled secondary antibody anti-mouse 568 (goat) (Invitrogen) was added (1:750 diluted in 10% NGS and 1% BSA in PBST) for 1 h at 37 °C. Nuclei were stained with Hoechst and F-actin with phalloidin-FITC (Sigma-Aldrich, Merck). Between the individual working steps, cells were washed with PBS. Fluorescence imaging was performed with the iMIC Digital Microscope (FEI Munich, Germany) using the Live Acquisition 2.6 software (FEI Munich) and processed with ImageJ 1.4.3.47 software (National Institutes of Health, Bethesda).

hBAECs grown on transwell filters were fixed for 15 min in 4% paraformaldehyde in DPBS. Cells were then permeabilized and blocked for 5 min in DPBS containing 0.2% saponin and 10% FBS (Thermo Fisher Scientific). Cells were stained with primary (1:25–50) and secondary (1:400) antibodies in DPBS, 0.2% saponin and 10% FBS. The α-β-IV rabbit monoclonal antibody (ab179509) and ZO-1 (ab99462) were purchased from Abcam (Cambridge, United Kingdom), α-club cell secretory protein rat monoclonal antibody (MAB4218) was from R&D Systems (Minneapolis, Minnesota, USA) and the α-Muc5B rabbit polyclonal antibody (HPA008246) was from Sigma-Aldrich. Fluorescently labeled secondary antibodies were obtained from Molecular Probes (Thermo Fisher Scientific). Alexa Fluor 647-Phalloidin (8940) was obtained from NEB. Images were taken on an inverted confocal microscope (Leica TCS SP5, Leica, Wetzlar, Germany) using a 63×lens (Leica HCX PL APO lambda blue 63.0×1.40 OIL UV). Images for the blue (DAPI), green (AlexaFluor 488), red (AlexaFluor 568) and far-red (AlexaFluor 647) channels were taken in sequential mode using appropriate excitation and emission settings.

Protein interaction analysis in cultured cells by Duolink using proximity ligation assay (PLA). CHO-K1 cells were incubated with PT for indicated periods of time. Cells were fixed with 4% PFA, permeabilized and blocked with 10% NGS and 1% BSA in PBST. Subsequently, cells were incubated with mouse anti-PTS1 (Santa Cruz or Abcam) and rabbit anti-Cyp40 (Thermo Fisher Scientific), rabbit anti-Hsp90 (Thermo Fisher Scientific), rabbit anti-Hsp70 (Enzo Life Sciences) or rabbit anti-FKBP51 (Santa Cruz) antibodies for 1 h at 37 °C. PLA assay was performed according to the manufacturer's protocol (Duolink using PLA technology, Sigma-Aldrich, Merck) and as described before[46,47].

Measurement of the transepithelial electrical resistance (TEER). TEER was analyzed by impedance spectrometry using the cellZscope (NanoAnalytics, Münster, Germany). For measurements, the basal electrode was overlaid by 500 µl equilibrated DMEM-H medium filters inserted and 250 µl ediuDMEM-H medium was added to the apical side of the filter. Measurements were performed immediately after positioning of apical electrodes. Data were acquired and analyzed using the software provided with the instrument (NanoAnalytics).

Measurement of apical surface liquid (ASL) volume. ASL measurements were performed using the D_2O dilution method as described previously[72]. Filters with confluent cell layers were placed in 500 µl of differentiation medium containing respective inhibitors and pre-incubated for 30 min at 37 °C. 25 µl of isotonic NaCl, containing respective inhibitors, was added to the apical compartment. Silicon sealed control filters loaded with 25 µl isotonic NaCl solution were randomly distributed throughout the plate to estimate volume changes caused by evaporation. After 72 h apical fluid volumes were collected with 25 µl D_2O containing 0.9% (w/v) NaCl for analysis. Water concentrations were measured by attenuated total reflexion mid-infrared spectroscopy on A Vertex 70 FT-IR spectrometer, equipped with a BioATRCell-II unit and a liquid nitrogen cooled MCT detector (Bruker Optics, Fällanden, Switzerland), to calculate ASL volumes. Data acquisition and processing was performed using OPUS 6.5 (Bruker Optics). Before each measurement a background spectrum of the empty ATR-unit was collected and a calibration series (0%, 15%, 25%, 40%, 50%, 65% (v/v) of isotone NaCl solution in H_2O and 0.9% NaCl solution in D_2O) was measured. Areas below absorption bands were blotted against water concentration and linear regression was calculated through data points to obtain the slope (m) and y-interception (y_0), to calculate water concentrations as described in detail before[72]. The apical volume (V_{api}) was calculated according to:

$$V_{api} = C_{H_2O} \times V_{D_2O}/(100\% - C_{H_2O})$$

with V_{D_2O} being the volume (25 µl) of D_2O in 0.9% NaCl. Changes in apical volume (ΔV_{api}) were calculated by subtracting the remaining volume from the initial volume (25 µl isotonic NaCl solution). Changes in apical volumes in experimental filters were corrected for changes in evaporation controls.

Infant mouse studies. 7-day old C57BL/6 mice were used in accordance with the University of Maryland, Baltimore Institutional Animal Care and Use Committee. A streptomycin resistant derivative of the Tohama I "wild-type" *B. pertussis* strain was grown on Bordet-Gengou (BG) agar plates supplemented with defibrinated sheep blood (10%, Lampire Biological Products, Pipersville, Pennsylvania, USA) and 200 µg/ml streptomycin (Sigma-Aldrich, Merck). All comparisons were made between littermates pre-designated as receiving vehicle or one of the inhibitors. When dividing mice into groups attempts were made to match bodyweights between groups instead of true randomization. Tails were marked with colored pens daily to distinguish experimental groups within a litter. Only litters between sized between 5 and 8 pups were used to minimize variability associated with litter size. Animals were challenged via aerosol administered by a nebulizer system (Pari Vios) for twenty minutes. Lungs were excised post-euthanasia, homogenized mechanically (Omni International, Tulsa, Oklahoma, USA) and bacterial burden determined by plating on BG agar. Animals were intranasally administered vehicle (Cremophor:Ethanol:Saline 10:1:89), CsA (25 mg/kg, Sigma-Aldrich, Merck) or NIM811 (25 mg/

kg, MedChemExpress, Monmouth, New Jersey, USA). To measure leukocytosis blood was harvested 7 days post-infection by cardiac puncture into ethylenediaminetetraacetic acid (EDTA) containing 1.7 ml tubes (Fisher Scientific) and treated with ammonium-chloride-potassium (ACK) lysis buffer to lyse red blood cells. The investigator performing the harvest then assigned the samples numbers unrelated to their group. White blood cells were then counted using a hemocytometer by an investigator blind to sample identifications. Inhibitor treated mice were compared to vehicle treated animals by ANOVA with Dunnett's multiple comparisons test using GraphPad Prism. Studies were performed in both male and female mice, but exact numbers of each gender could not be determined at time of infection (7-days-old).

Ethics statement. Animals were used in accordance with the University of Maryland Institutional Animal Care and Use Committee protocol 0417005 (University of Maryland, Baltimore, MD) following approval by the Office of Animal Welfare Assurance. Animals were euthanized by CO_2 asphyxiation followed by cervical dislocation and thoracotomy. All methods were performed in accordance with the relevant guidelines and regulations. The study was carried out in compliance with the ARRIVE guidelines.

Received: 3 August 2020; Accepted: 16 February 2021
Published online: 08 March 2021

References

1. Kilgore, P. E., Salim, A. M., Zervos, M. J. & Schmitt, H.-J. Pertussis: Microbiology, disease, treatment, and prevention. *Clin. Microbiol. Rev.* **29**, 449–486 (2016).
2. Mattoo, S. & Cherry, J. D. Molecular pathogenesis, epidemiology, and clinical manifestations of respiratory infections due to *Bordetella pertussis* and other *Bordetella* subspecies. *Clin. Microbiol. Rev.* **18**, 326–382 (2005).
3. Carbonetti, N. H. Pertussis leukocytosis: Mechanisms, clinical relevance and treatment. *Pathog. Dis.* **74**, ftw087 (2016).
4. Heininger, U., Klich, K., Stehr, K. & Cherry, J. D. Clinical findings in *Bordetella pertussis* infections: results of a prospective multicenter surveillance study. *Pediatrics* **100**, E10 (1997).
5. Publication, W. H. O. Pertussis vaccines: WHO position paper—recommendations. *Vaccine* **29**, 2355–2356 (2011).
6. Domenech de Cellès, M., Magpantay, F. M. G., King, A. A. & Rohani, P. The pertussis enigma: Reconciling epidemiology, immunology and evolution. *Proc. Biol. Sci.* **283**, 20152309 (2016).
7. Carbonetti, N. H. Contribution of pertussis toxin to the pathogenesis of pertussis disease. *Pathog. Dis.* **73**, ftv73 (2015).
8. Scanlon, K. M., Snyder, Y. G., Skerry, C. & Carbonetti, N. H. Fatal pertussis in the neonatal mouse model is associated with pertussis toxin-mediated pathology beyond the airways. *Infect. Immun.* **85**, e00355–17 (2017).
9. Pittman, M. The concept of pertussis as a toxin-mediated disease. *Pediatr. Infect. Dis.* **3**, 467–486 (1984).
10. Scanlon, K., Skerry, C. & Carbonetti, N. Association of pertussis toxin with severe pertussis disease. *Toxins* **11**, 373 (2019).
11. Stein, P. E. *et al.* The crystal structure of pertussis toxin. *Struct. Lond. Engl.* **1993**(2), 45–57 (1994).
12. Tamura, M. *et al.* Subunit structure of islet-activating protein, pertussis toxin, in conformity with the A–B model. *Biochemistry* **21**, 5516–5522 (1982).
13. Locht, C., Coutte, L. & Mielcarek, N. The ins and outs of pertussis toxin. *FEBS J.* **278**, 4668–4682 (2011).
14. Witvliet, M. H., Burns, D. L., Brennan, M. J., Poolman, J. T. & Manclark, C. R. Binding of pertussis toxin to eucaryotic cells and glycoproteins. *Infect. Immun.* **57**, 3324–3330 (1989).
15. Lippincott-Schwartz, J., Yuan, L. C., Bonifacino, J. S. & Klausner, R. D. Rapid redistribution of Golgi proteins into the ER in cells treated with brefeldin A: Evidence for membrane cycling from Golgi to ER. *Cell* **56**, 801–813 (1989).
16. Plaut, R. D. & Carbonetti, N. H. Retrograde transport of pertussis toxin in the mammalian cell. *Cell Microbiol.* **10**, 1130–1139 (2008).
17. Xu, Y. & Barbieri, J. T. Pertussis toxin-mediated ADP-ribosylation of target proteins in Chinese hamster ovary cells involves a vesicle trafficking mechanism. *Infect. Immun.* **63**, 825–832 (1995).
18. Hazes, B., Boodhoo, A., Cockle, S. A. & Read, R. J. Crystal structure of the pertussis toxin-ATP complex: A molecular sensor. *J. Mol. Biol.* **258**, 661–671 (1996).
19. Plaut, R. D., Scanlon, K. M., Taylor, M., Teter, K. & Carbonetti, N. H. Intracellular disassembly and activity of pertussis toxin require interaction with ATP. *Pathog. Dis.* **74**, ftw065 (2016).
20. Murrell-Lagnado, R. D. & Frick, M. P2X4 and lysosome fusion. *Curr. Opin. Pharmacol.* **47**, 126–132 (2019).
21. Banerjee, T. *et al.* Thermal unfolding of the pertussis toxin S1 subunit facilitates toxin translocation to the cytosol by the mechanism of endoplasmic reticulum-associated degradation. *Infect. Immun.* **84**, 3388–3398 (2016).
22. Pande, A. H., Moe, D., Jamnadas, M., Tatulian, S. A. & Teter, K. The pertussis toxin S1 subunit is a thermally unstable protein susceptible to degradation by the 20S proteasome. *Biochemistry* **45**, 13734–13740 (2006).
23. Worthington, Z. E. V. & Carbonetti, N. H. Evading the proteasome: Absence of lysine residues contributes to pertussis toxin activity by evasion of proteasome degradation. *Infect. Immun.* **75**, 2946–2953 (2007).
24. Bokoch, G. M., Katada, T., Northup, J. K., Hewlett, E. L. & Gilman, A. G. Identification of the predominant substrate for ADP-ribosylation by islet activating protein. *J. Biol. Chem.* **258**, 2072–2075 (1983).
25. Katada, T. & Ui, M. Direct modification of the membrane adenylate cyclase system by islet-activating protein due to ADP-ribosylation of a membrane protein. *Proc. Natl. Acad. Sci. U.S.A.* **79**, 3129–3133 (1982).
26. Kirimanjeswara, G. S., Agosto, L. M., Kennett, M. J., Bjornstad, O. N. & Harvill, E. T. Pertussis toxin inhibits neutrophil recruitment to delay antibody-mediated clearance of *Bordetella pertussis*. *J. Clin. Investig.* **115**, 3594–3601 (2005).
27. Spangrude, G. J., Sacchi, F., Hill, H. R., Van Epps, D. E. & Daynes, R. A. Inhibition of lymphocyte and neutrophil chemotaxis by pertussis toxin. *J. Immunol. Baltim. Md* **1950**(135), 4135–4143 (1985).
28. Andreasen, C. & Carbonetti, N. H. Pertussis toxin inhibits early chemokine production to delay neutrophil recruitment in response to *Bordetella pertussis* respiratory tract infection in mice. *Infect. Immun.* **76**, 5139–5148 (2008).
29. Ernst, K. *et al.* Pharmacological cyclophilin inhibitors prevent intoxication of mammalian cells with bordetella pertussis toxin. *Toxins* **10**, 181 (2018).
30. Li, J. & Buchner, J. Structure, function and regulation of the hsp90 machinery. *Biomed. J.* **36**, 106–117 (2013).
31. Pratt, W. B. & Toft, D. O. Regulation of signaling protein function and trafficking by the hsp90/hsp70-based chaperone machinery. *Exp. Biol. Med. Maywood NJ* **228**, 111–133 (2003).
32. Schiene-Fischer, C. Multidomain peptidyl prolyl cis/trans isomerases. *Biochim. Biophys. Acta* https://doi.org/10.1016/j.bbagen.2014.11.012 (2014).

33. Porter, G. A. & Beutner, G. Cyclophilin D, somehow a master regulator of mitochondrial function. *Biomolecules* **8**, 176 (2018).
34. Gestal, M. C., Johnson, H. M. & Harvill, E. T. Immunomodulation as a novel strategy for prevention and treatment of *Bordetella* spp. infections. *Front. Immunol.* **10**, 2869 (2019).
35. Hewlett, E. L., Sauer, K. T., Myers, G. A., Cowell, J. L. & Guerrant, R. L. Induction of a novel morphological response in Chinese hamster ovary cells by pertussis toxin. *Infect. Immun.* **40**, 1198–1203 (1983).
36. el Bayâ, A., Linnemann, R., von Olleschik-Elbheim, L., Robenek, H. & Schmidt, M. A. Endocytosis and retrograde transport of pertussis toxin to the Golgi complex as a prerequisite for cellular intoxication. *Eur. J. Cell Biol.* **73**, 40–48 (1997).
37. Ernst, K. *et al.* A novel Hsp70 inhibitor prevents cell intoxication with the actin ADP-ribosylating *Clostridium perfringens* iota toxin. *Sci. Rep.* **6**, 20301 (2016).
38. Paramonov, V. M., Sahlgren, C., Rivero-Müller, A. & Pulliainen, A. T. iGIST-A kinetic bioassay for pertussis toxin based on its effect on inhibitory GPCR signaling. *ACS Sens.* **5**, 3438–3448 (2020).
39. Dmochewitz, L. *et al.* Role of CypA and Hsp90 in membrane translocation mediated by anthrax protective antigen. *Cell Microbiol.* **13**, 359–373 (2011).
40. Ernst, K. *et al.* Cyclophilin-facilitated membrane translocation as pharmacological target to prevent intoxication of mammalian cells by binary clostridial actin ADP-ribosylated toxins. *J. Mol. Biol.* **427**, 1224–1238 (2015).
41. Okuda, K. *et al.* Localization of secretory mucins MUC5AC and MUC5B in normal/healthy human airways. *Am. J. Respir. Crit. Care Med.* **199**, 715–727 (2019).
42. Rosenwirth, B. *et al.* Inhibition of human immunodeficiency virus type 1 replication by SDZ NIM 811, a nonimmunosuppressive cyclosporine analog. *Antimicrob. Agents Chemother.* **38**, 1763–1772 (1994).
43. Altunaiji, S., Kukuruzovic, R., Curtis, N. & Massie, J. Antibiotics for whooping cough (pertussis). *Cochrane Database Syst. Rev.* https://doi.org/10.1002/14651858.CD004404.pub3 (2007).
44. Barth, H. & Ernst, K. Chaperones and ADP-ribosylating bacterial toxins. In *Microbial Toxins* (eds Gopalakrishnakone, P. *et al.*) 1–22 (Springer, Dordrecht, 2016). https://doi.org/10.1007/978-94-007-6725-6_7-1.
45. Ernst, K., Schnell, L. & Barth, H. Host cell chaperones Hsp70/Hsp90 and peptidyl-prolyl cis/trans isomerases are required for the membrane translocation of bacterial ADP-ribosylating toxins. *Curr. Top. Microbiol. Immunol.* **406**, 163–198 (2017).
46. Ernst, K. *et al.* Hsp70 facilitates trans-membrane transport of bacterial ADP-ribosylating toxins into the cytosol of mammalian cells. *Sci. Rep.* **7**, 2724 (2017).
47. Ernst, K., Kling, C., Landenberger, M. & Barth, H. Combined pharmacological inhibition of cyclophilins, FK506-binding proteins, Hsp90, and Hsp70 protects cells from *Clostridium botulinum* C2 toxin. *Front. Pharmacol.* **9**, 1287 (2018).
48. Haug, G. *et al.* The host cell chaperone Hsp90 is essential for translocation of the binary *Clostridium botulinum* C2 toxin into the cytosol. *J. Biol. Chem.* **278**, 32266–32274 (2003).
49. Haug, G., Aktories, K. & Barth, H. The host cell chaperone Hsp90 is necessary for cytotoxic action of the binary iota-like toxins. *Infect. Immun.* **72**, 3066–3068 (2004).
50. Kaiser, E., Pust, S., Kroll, C. & Barth, H. Cyclophilin A facilitates translocation of the Clostridium botulinum C2 toxin across membranes of acidified endosomes into the cytosol of mammalian cells. *Cell Microbiol.* **11**, 780–795 (2009).
51. Kaiser, E. *et al.* Membrane translocation of binary actin-ADP-ribosylating toxins from *Clostridium difficile* and *Clostridium perfringens* is facilitated by cyclophilin A and Hsp90. *Infect. Immun.* **79**, 3913–3921 (2011).
52. Kaiser, E. *et al.* FK506-binding protein 51 interacts with *Clostridium botulinum* C2 toxin and FK506 inhibits membrane translocation of the toxin in mammalian cells. *Cell Microbiol.* **14**, 1193–1205 (2012).
53. Schuster, M. *et al.* The Hsp90 machinery facilitates the transport of diphtheria toxin into human cells. *Sci. Rep.* **7**, 613 (2017).
54. Dalby, T., Sørensen, C., Petersen, J. W. & Krogfelt, K. A. Pertussis serology: Assessment of IgG anti-PT ELISA for replacement of the CHO cell assay. *APMIS Acta Pathol. Microbiol. Immunol. Scand.* **118**, 968–972 (2010).
55. Markey, K., Asokanathan, C. & Feavers, I. Assays for determining pertussis toxin activity in acellular pertussis vaccines. *Toxins* **11**, 417 (2019).
56. Kellner, A., Taylor, M., Banerjee, T., Britt, C. B. T. & Teter, K. A binding motif for Hsp90 in the A chains of ADP-ribosylating toxins that move from the endoplasmic reticulum to the cytosol. *Cell Microbiol.* https://doi.org/10.1111/cmi.13074 (2019).
57. Ratajczak, T. & Carrello, A. Cyclophilin 40 (CyP-40), mapping of its hsp90 binding domain and evidence that FKBP52 competes with CyP-40 for hsp90 binding. *J. Biol. Chem.* **271**, 2961–2965 (1996).
58. McClellan, A. J. *et al.* Diverse cellular functions of the Hsp90 molecular chaperone uncovered using systems approaches. *Cell* **131**, 121–135 (2007).
59. Millson, S. H. *et al.* A two-hybrid screen of the yeast proteome for Hsp90 interactors uncovers a novel Hsp90 chaperone requirement in the activity of a stress-activated mitogen-activated protein kinase, Slt2p (Mpk1p). *Eukaryot. Cell* **4**, 849–860 (2005).
60. Zhao, R. *et al.* Navigating the chaperone network: an integrative map of physical and genetic interactions mediated by the hsp90 chaperone. *Cell* **120**, 715–727 (2005).
61. Burress, H., Kellner, A., Guyette, J., Tatulian, S. A. & Teter, K. HSC70 and HSP90 chaperones perform complementary roles in translocation of the cholera toxin A1 subunit from the endoplasmic reticulum to the cytosol. *J. Biol. Chem.* https://doi.org/10.1074/jbc.RA119.008568 (2019).
62. Burress, H., Taylor, M., Banerjee, T., Tatulian, S. A. & Teter, K. Co- and post-translocation roles for HSP90 in cholera intoxication. *J. Biol. Chem.* **289**, 33644–33654 (2014).
63. Taylor, M. *et al.* Hsp90 is required for transfer of the cholera toxin A1 subunit from the endoplasmic reticulum to the cytosol. *J. Biol. Chem.* **285**, 31261–31267 (2010).
64. Csanády, L., Vergani, P. & Gadsby, D. C. Structure, gating, and regulation of the CFTR anion channel. *Physiol. Rev.* **99**, 707–738 (2018).
65. Scanlon, K. M. *et al.* Epithelial anion transporter pendrin contributes to inflammatory lung pathology in mouse models of *Bordetella pertussis* infection. *Infect. Immun.* **82**, 4212–4221 (2014).
66. Carbonetti, N. H. *Bordetella pertussis*: New concepts in pathogenesis and treatment. *Curr. Opin. Infect. Dis.* **29**, 287–294 (2016).
67. Borel, J. F., Feurer, C., Gubler, H. U. & Stähelin, H. Biological effects of cyclosporin A: A new antilymphocytic agent. *Agents Actions* **6**, 468–475 (1976).
68. Liu, J. *et al.* Calcineurin is a common target of cyclophilin-cyclosporin A and FKBP-FK506 complexes. *Cell* **66**, 807–815 (1991).
69. Fahrer, J. *et al.* Selective and specific internalization of clostridial C3 ADP-ribosyltransferases into macrophages and monocytes. *Cell Microbiol.* **12**, 233–247 (2010).
70. Ashok, Y. *et al.* Discovery of compounds inhibiting the ADP-ribosyltransferase activity of pertussis toxin. *ACS Infect. Dis.* **6**, 588–602 (2020).
71. Fulcher, M. L., Gabriel, S., Burns, K. A., Yankaskas, J. R. & Randell, S. H. Well-differentiated human airway epithelial cell cultures. in *Human Cell Culture Protocols* 183–206 (Humana Press, Totowa, 2005). https://doi.org/10.1385/1-59259-861-7:183.
72. Neubauer, D. *et al.* Deuterium oxide dilution: a novel method to study apical water layers and transepithelial water transport. *Anal. Chem.* **85**, 4247–4250 (2013).

Acknowledgements
This work was supported by the Deutsche Forschungsgemeinschaft [DFG, German Research Foundation, Grant BA2087/2-2 to H.B. and project number 251293561-SFB 1149, Project A05 (H.B. and M.F.)] and the Medical Faculty Ulm (Baustein 3.2 to K.E.). This project is supported by the European Social Fund and by the Ministry of Science, Research and the Arts Baden-Württemberg (fellowship to K.E.). C.K. is supported by a PhD fellowship by Cusanuswerk. V.W. and C.K. are fellows of the International Graduate School in Molecular Medicine Ulm (IGradU) and N.E. and R.L. were supported by the "Promotionsprogramm Experimentelle Medizin" of the Medical Faculty Ulm. Cordelia Schiene-Fischer is thanked for providing Cyp, FKBP and Hsp/c70 proteins, Johannes Buchner for providing Hsp90 protein, and Felix Hausch for FKBP FK1 fragments.

Author contributions
K.E. designed the study, supervised and conducted experiments and wrote the manuscript. A.K.M., C.K., V.W., N.E., A.A., M.S., R.L. and J.W. conducted experiments. M.S. and A.P. purified recombinant PTxS1 and Giα. C.S. and N.H.C. designed and conducted experiments and wrote parts of the manuscript. M.F. designed experiments and wrote parts of the manuscript. H.B. designed and supervised the study and worked on the manuscript.

Funding
Open Access funding enabled and organized by Projekt DEAL.

Competing interests
The authors declare no competing interests.

Additional information
Supplementary Information The online version contains supplementary material available at https://doi.org/10.1038/s41598-021-84817-2.

Correspondence and requests for materials should be addressed to K.E. or H.B.

Reprints and permissions information is available at www.nature.com/reprints.

Publisher's note Springer Nature remains neutral with regard to jurisdictional claims in published maps and institutional affiliations.

Open Access This article is licensed under a Creative Commons Attribution 4.0 International License, which permits use, sharing, adaptation, distribution and reproduction in any medium or format, as long as you give appropriate credit to the original author(s) and the source, provide a link to the Creative Commons licence, and indicate if changes were made. The images or other third party material in this article are included in the article's Creative Commons licence, unless indicated otherwise in a credit line to the material. If material is not included in the article's Creative Commons licence and your intended use is not permitted by statutory regulation or exceeds the permitted use, you will need to obtain permission directly from the copyright holder. To view a copy of this licence, visit http://creativecommons.org/licenses/by/4.0/.

© The Author(s) 2021

2.2 Human Peptides α-Defensin-1 and -5 Inhibit Pertussis Toxin

Toxins (2021) 13 (7), 480. https://doi.org/10.3390/toxins13070480

Carolin Kling, Arto T. Pulliainen, Holger Barth and Katharina Ernst[#]

[#]corresponding author

The reuse of the present article in my dissertation is permitted by the Creative Commons Attribution 4.0 International License (CC BY 4.0) (https://creativecommons.org/licenses/by/4.0/).

2.2.1 Own contributions

- Data and Figures of **Figure 1a-d** (Human α-defensin-1 and -5 inhibit enzyme activity of PTS1)
- Data and Figures of **Figure 2a-d** (Effect of human α-defensin-1 and -5 on the ADP-ribosylation status of Gαi in PT-treated cells.)
- Data and Figures of **Figure 3a-c** (Human α-defensin-1 and -5 inhibit PT-mediated effects on cAMP signaling)
- Preparation of parts of the manuscript and revision

2.2.2 Summary of Results

The present publication identified the human peptides α-defensin-1 and -5, but not β-defensin-1 as two novel inhibitors of PT and characterized their protective effect.

First, the effect of α-defensin-1 and -5 on enzyme activity of PTS1 was investigated *in vitro*. Different conditions were tested, where Gαi or PTS1 was pre-incubated with the respective defensin for 30 min at 37°C before adding the remaining components, including biotin-labeled NAD^+, to the enzyme reaction. With both conditions of pre-incubation, but also to a slightly lesser extent without pre-incubation of any components, α-defensin-1 and -5, but not β-defensin-1 showed a clear reduction of ADP-ribosylated Gαi. This indicates a direct inhibition of PTS1 activity by α-defensin-1 and -5. The inhibitory effect was also shown to be concentration-dependent and more pronounced for α-defensin-1 than for α-defensin-5.

Next, the effect of the defensins on the intoxication of cells with the holotoxin PT was investigated. CHO-K1 cells were incubated with PT and the defensins after pre-incubation of both components or directly without a pre-incubation. After 4h, cells were lysed and Gαi, that has not been ADP-

ribosylated during intoxication, was sequentially ADP-ribosylated and therefore labeled for detection in an *in vitro* reaction. Both α-defensin-1 and -5 reduced the amount of ADP-ribosylated Gαi in cells treated with PT with or without pre-incubation of PT with the defensin, indicating an inhibition of PT intoxication by the α-defensins. The effect was specific, as β-defensin-1 did not show any inhibition. For α-defensin-5 a concentration-dependency could be clearly shown, but also α-defensin-1 showed this tendency. Cell viability was not reduced by the defensins under the same conditions, as shown in a cell viability assay.

The consequence of ADP-ribosylation of Gαi is its lack of inhibition of the AC, resulting in disturbed cAMP signaling. This downstream effect of PT was investigated with the iGIST bioassay (see Figure 5). Both α-defensin-1 and -5 showed a clear reduction of the PT-induced increase of cAMP levels after activation of the AC and SSTR2 with forskolin and octreotide. This effect did not trace back to effects of the defensins on the iGIST sensor cells as shown in a control experiment, where iGIST sensor cells were incubated only with the defensins without addition of PT. Maximal levels of cAMP were also reached, when the cells were treated with forskolin but not octreotide, independent of the presence of PT.

Taken together, the present publication demonstrated that the human peptides α-defensin-1 and -5 inhibit enzyme activity of PTS1 and protect cells from intoxication with PT.

2.2.3 Discussion

Pertussis is a serious infectious disease that still causes thousands of deaths annually, despite available vaccination. PT is associated with severe and lethal cases of pertussis in young infants, the most vulnerable group for the disease (reviewed in Scanlon et al., 2019). Thus, there is an urgent need of finding novel pharmacological inhibitors against pertussis, and PT can serve as a meaningful target for future pharmacological inhibitors.

Prompted by the findings, that human α-defensin-1 and -5 inhibit several other AB-type toxins, such as LF, TcdA, TcdB and CDT (see Table 2), their effect on PT was investigated in this thesis. For many AB-type toxins, human defensins showed an inhibition of the enzymatic activity of the toxin (Kim et al., 2005, 2006). In this thesis, it was shown, that α-defensin-1 and -5 inhibit enzyme activity of PTS1 as well. Moreover, it was also shown, that both α-defensins protect cells from intoxication by PT, as the amount of ADP-ribosylated Gαi and the increase in cAMP levels within intoxicated cells was reduced.

These findings were specific to α-defensin-1 and -5, as β-defensin-1 did not show any inhibition of PTS1 or PT. All three defensins have their cationic nature in common, and they all carry six cysteines, forming three intramolecular disulfide bonds (Cederlund et al., 2011). This results in a predominant β-sheet structure. These features alone seem to be insufficient for inhibition of PTS1 and PT, as β-defensin-1, carrying these features, had no effect on the toxin. The difference between human α- and β-defensins, besides their site of expression, is the distribution of the cysteines, and thus their disulfide bonds, as well as their molecular weight (Cederlund et al., 2011). α-Defensins are lacking the N-terminal α-helix, characteristic for β-defensins, and are therefore shorter than β-defensins (Kudryashova et al., 2017). For the inhibition of other toxins, structural elements of α-defensins could be correlated to their anti-toxin activity (Kudryashova et al., 2017). For example, the integrity of the three disulfide bonds of the α-defensins were crucial for toxin inactivation of LF, TcdB, and CDCs (Giesemann et al., 2008; Kim et al., 2005; Lehrer et al., 2009; Wei et al., 2009). Also hydrophobicity correlated with anti-toxin activity, since, for example, mutations in hydrophobic residues, led to the most detrimental effects on α-defensin-1 in its ability to inhibit LF (Wei et al., 2010). Cationicity and particularly the arginine content of defensins also seems to be an important factor for their activity against toxins. Human α-defensins have high arginine contents, such as 13.3% for α-defensin-1 or 18.8% for α-defensin-5, whereas β-defensin-1 only has 2.8% arginine residues (Kudryashova et al., 2017). This is in line with the broad anti-toxin activity of α-defensins, compared to β-defensin-1. Remarkably, β-defensin-3, containing 16% arginines showed activity against different toxins (Wei et al., 2009). Other factors, like the invariant glycine residue, stereo-specificity or the conserved salt bridges of the α-defensins did only correlate slightly with their ability to inhibit toxins (Kudryashova et al., 2017). The exact molecular structure of the defensins, responsible for inhibition of PT has not been elucidated yet. However, the structural differences of α- and β-defensins might explain their distinct ability to inhibit PT and PTS1.

In this publication, α-defensin-1 and -5 were demonstrated to inhibit enzyme activity of PTS1. Hence, it can be assumed, that this inhibition of PTS1 activity is the main mechanism of inhibition of the α-defensins, responsible for the protection of cells from PT. However, the prevention of PT from binding to cells or uptake of PTS1 into the cytosol by α-defensin-1 or -5 could not be excluded yet. There is one hint, suggesting, that further mechanisms of inhibition might play a role in inhibition of PT by α-defensin-1 and -5. α-defensin-1 showed a stronger inhibition of enzyme activity of PTS1 than α-defensin-5, while, with the same concentrations, showing a weaker

inhibition of the effects of the holotoxin PT on cells compared to α-defensin-5. Therefore, other additional mechanisms of inhibition are also conceivable to play a role in preventing effects of PT. These differential mechanisms of action were studied in the following publication.

toxins

MDPI

Article

Human Peptides α-Defensin-1 and -5 Inhibit Pertussis Toxin

Carolin Kling [1], Arto T. Pulliainen [2], Holger Barth [1] and Katharina Ernst [1,*]

[1] Institute of Pharmacology and Toxicology, Ulm University Medical Center, 89081 Ulm, Germany; carolin.kling@uni-ulm.de (C.K.); holger.barth@uni-ulm.de (H.B.)
[2] Institute of Biomedicine, Research Unit for Infection and Immunity, University of Turku, FI-20520 Turku, Finland; arto.pulliainen@utu.fi
* Correspondence: katharina.ernst@uni-ulm.de

Abstract: *Bordetella pertussis* causes the severe childhood disease whooping cough, by releasing several toxins, including pertussis toxin (PT) as a major virulence factor. PT is an AB_5-type toxin, and consists of the enzymatic A-subunit PTS1 and five B-subunits, which facilitate binding to cells and transport of PTS1 into the cytosol. PTS1 ADP-ribosylates α-subunits of inhibitory G-proteins (Gαi) in the cytosol, which leads to disturbed cAMP signaling. Since PT is crucial for causing severe courses of disease, our aim is to identify new inhibitors against PT, to provide starting points for novel therapeutic approaches. Here, we investigated the effect of human antimicrobial peptides of the defensin family on PT. We demonstrated that PTS1 enzyme activity in vitro was inhibited by α-defensin-1 and -5, but not β-defensin-1. The amount of ADP-ribosylated Gαi was significantly reduced in PT-treated cells, in the presence of α-defensin-1 and -5. Moreover, both α-defensins decreased PT-mediated effects on cAMP signaling in the living cell-based interference in the Gαi-mediated signal transduction (iGIST) assay. Taken together, we identified the human peptides α-defensin-1 and -5 as inhibitors of PT activity, suggesting that these human peptides bear potential for developing novel therapeutic strategies against whooping cough.

Keywords: pertussis toxin; defensins; ADP-ribosylating toxin; bacterial AB-type toxin; human peptide; antimicrobial peptide; toxin inhibitor

Key Contribution: Human antimicrobial peptides α-defensin-1 and -5, but not ß-defensin-1, inhibit the enzyme activity of pertussis toxin (PT). The treatment of cells with PT in the presence of α-defensin-1 or -5 results in decreased amounts of ADP-ribosylated Gαi, which is the substrate of PT. Moreover, the PT-mediated effects on cAMP signaling in living cells were reduced by α-defensin-1 and -5.

check for updates

Citation: Kling, C.; Pulliainen, A.T.; Barth, H.; Ernst, K. Human Peptides α-Defensin-1 and -5 Inhibit Pertussis Toxin. *Toxins* **2021**, *13*, 480. https://doi.org/10.3390/toxins13070480

Received: 14 June 2021
Accepted: 9 July 2021
Published: 11 July 2021

Publisher's Note: MDPI stays neutral with regard to jurisdictional claims in published maps and institutional affiliations.

Copyright: © 2021 by the authors. Licensee MDPI, Basel, Switzerland. This article is an open access article distributed under the terms and conditions of the Creative Commons Attribution (CC BY) license (https://creativecommons.org/licenses/by/4.0/).

1. Introduction

As an AB_5 protein toxin, *Bordetella (B.) pertussis* toxin (PT) consists of an enzyme subunit, the A-protomer PTS1, and five B-subunits forming a holotoxin with a pyramid-like structure, which is secreted by the bacteria [1–3]. The B-pentamer facilitates binding to the cell surface via sialoglycoproteins that are present on most cell types [1,4–6]. After internalization by endocytosis, PT follows a retrograde intracellular transport through the Golgi to the endoplasmic reticulum (ER) [7]. This retrograde transport is inhibited by brefeldin A (BFA), which disrupts vesicle transport between the ER and Golgi apparatus [7,8]. In the ER, the binding of ATP to the toxin causes destabilization of the interaction between PTS1 and the B-pentamer, which results in the release of PTS1 from the holotoxin [9–11]. The released PTS1 is thermally unstable, leading to its unfolding under physiological conditions [12–14]. Thereby, it is detected by the ER-associated degradation (ERAD) pathway, and transported from the ER to the cytosol. A lack of lysine residues protects PTS1 from ubiquitination, and thus from proteasomal degradation [15]. The molecular mechanism underlying the membrane transport of PTS1 into the cytosol of the target cells is not well understood. We

have recently shown that cellular protein folding helper enzymes play a role in the uptake of PTS1 into the host-cell cytosol [16,17].

In the cytosol, PTS1 covalently transfers an ADP-ribose moiety from its co-substrate NAD^+ onto inhibitory α-subunit G-proteins (Gαi) of G-protein-coupled receptors (GPCRs) [18,19]. ADP-ribosylation inactivates Gαi, which results in disturbed cAMP signaling, because Gαi no longer functions as a negative regulator of adenylate cyclase (AC). The consequences of disturbed GPCR and cAMP signaling are multifaceted, and depend on the cell type. In the early stages of infection, PT inhibits the recruitment of neutrophils, monocytes, and lymphocytes to the lung, and leads to a reduction in pro-inflammatory chemokines and cytokines, as well as to increased bacterial burden in a mouse model [20–22].

PT is an important virulence factor for causing the disease whooping cough, which is characterized by long-lasting (ca. 10 weeks) paroxysmal coughing. Patients often suffer from secondary complications, such as vomiting and pneumothorax. In severe cases, pneumonia, encephalopathy, seizures, or apnea occur, which can be life-threatening, especially in newborns and young infants [23]. In 2014, the WHO estimated the number of pertussis cases in children <5 years of age at >24.1 million, with 160,700 deaths worldwide [24]. Despite a high vaccination rate in western countries (e.g., ca. 93% vaccination coverage of children starting school in Germany in 2017; ca. 85% vaccination coverage of infants worldwide in 2019 [25,26]), increasing case numbers have been recorded, reaching an all-time high since introducing vaccination in the 1950s. Therapeutic options to treat pertussis are very limited. Antibiotic therapy eliminates *B. pertussis* bacteria, which is important because it prevents transmission by droplet infection. However, antibiotic treatment has no relieving effect on pertussis symptoms, except if treatment is started up to two weeks after infection, which rarely occurs because, in most cases, the diagnosis is made later [23]. It was demonstrated that PT causes severe and long-lasting inflammation of the airways in a mouse model [27]. *B. pertussis* strains not expressing PT did not cause leukocytosis, which is a hallmark of severe pertussis, or death. These results clearly indicate a pivotal role of PT in causing severe courses of disease, which makes it an attractive target for the development of novel pharmacological strategies [28–30].

Here, the effect of human antimicrobial peptides of the defensin family on PT was investigated in vitro and in living cells. Defensins are small, cysteine-rich cationic peptides, and they play an important role in innate immunity, because they inactivate bacterial pathogens [31–33]. However, it was discovered that some defensins additionally neutralize bacterial protein toxins, such as *Clostridioides difficile* toxins or diphtheria toxin [31,34–36]. In the present study, we show that α-defensin-1 and -5 inhibited the enzyme activity of PT in vitro, in a concentration-dependent manner. Moreover, when the cells were treated with PT in the presence of α-defensin-1 or -5, the amount of ADP-ribosylated Gαi was reduced, compared to the cells treated with PT only. An inhibitory effect of α-defensin-1 and -5 was also shown on the PT-mediated effects on cAMP signaling in a living cell-based assay. Notably, the structurally related ß-defensin-1 exhibited no inhibition in the same experiments, suggesting a specific inhibitory mechanism of α-defensin-1 and -5 on PT.

2. Results

2.1. Human α-Defensin-1 and -5 Inhibit the Enzyme Activity of PTS1 In Vitro

Prompted by previous findings that defensins inhibited the enzyme activity of ADP-ribosylating toxins such as diphtheria toxin [31], we investigated whether defensins interfere with the enzyme activity of PTS1. Therefore, recombinant PTS1 was incubated with Gαi, in the presence of its biotin-labeled co-substrate NAD^+. PTS1 transfers the ADP-ribose moiety, and thereby the biotin-label, onto its specific substrate Gαi. ADP-ribosylated, i.e., biotin-labeled Gαi, was detected by Western blot. The results in Figure 1 show that α-defensin-1 and -5, but not ß-defensin-1, inhibit the enzyme activity of PTS1 in vitro. The inhibitory effect was comparable when either Gαi (Figure 1a) or PTS1 (Figure 1b) were pre-incubated with the defensins in a reaction tube. Without pre-incubation, inhibition by

α-defensin-1 and -5 was still observed, but to a slightly lesser extent (Figure 1b). Moreover, a concentration dependency of the inhibitory effect of α-defensin-1 and -5 was observed. Concentrations of 6 µM or higher of α-defensin-1 or -5 showed a significant inhibitory effect on PTS1 enzyme activity (Figure 1c,d).

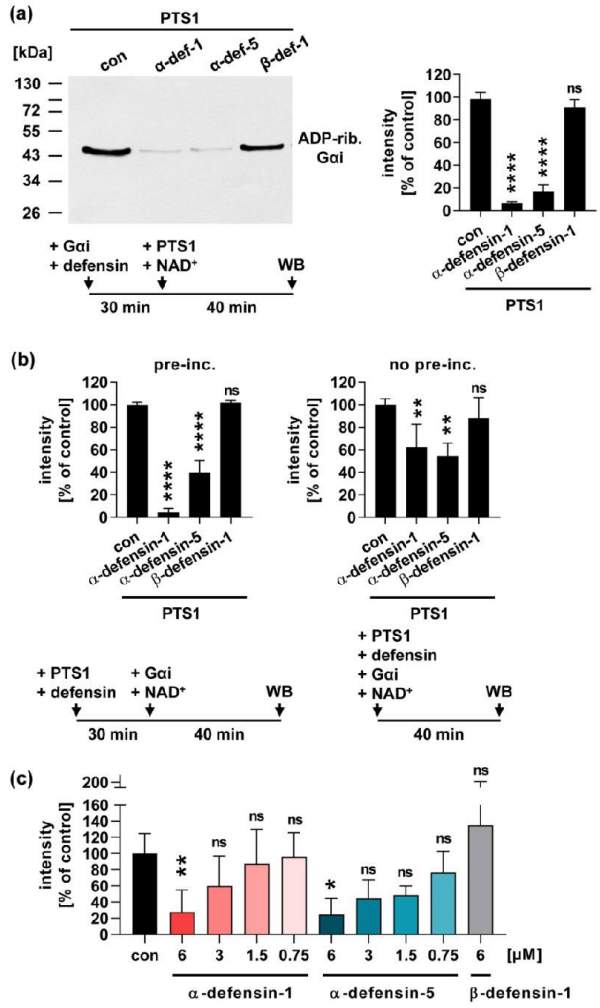

Figure 1. *Cont.*

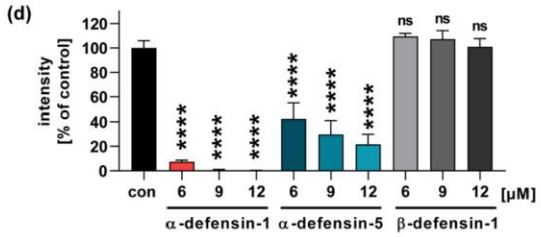

Figure 1. Human α-defensin-1 and -5 inhibit enzyme activity of PTS1. (**a**) Recombinant Gαi was pre-incubated with 6 µM α-defensin-1, α-defensin-5 or ß-defensin-1, or with the respective amount of solvent (H_2O) for 30 min at 37 °C. PTS1 (50 nM) and biotin-labeled NAD^+ were added for 40 min at RT. Biotin-labeled, i.e., ADP-ribosylated Gαi, was detected via Western blot. One representative Western blot result is shown, and the bar graph shows quantified Western blot signals from three independent experiments. Values are given as percent of control, mean ± SEM (n = 6 from three independent experiments). (**b**) PTS1 (50 nM) was pre-incubated with 6 µM α-defensin-1, α-defensin-5 or ß-defensin-1, or with the respective amount of solvent (H_2O) for 30 min at 37 °C. Gαi and biotin-labeled NAD^+ were added for 40 min at RT. Biotin-labeled, i.e., ADP-ribosylated Gαi was detected via Western blot. Bar graph shows quantified Western blot signals from three independent experiments. Values are given as percent of control, mean ± SD (n = 3 from three independent experiments). (**c**) PTS1 (50 nM) was pre-incubated with decreasing amounts of α-defensin-1 or α-defensin-5, 6 µM ß-defensin-1, or with the respective amount of solvent (H_2O) for 30 min at 37 °C. Gαi and biotin-labeled NAD^+ were added for 40 min at RT. Biotin-labeled, i.e., ADP-ribosylated Gαi, was detected via Western blot. Bar graph shows quantified Western blot signals from at least four independent experiments. Values are given as percent of control, mean ± SEM (n = at least four from at least four independent experiments). (**d**) PTS1 (50 nM) was pre-incubated with increasing amounts of α-defensin-1, α-defensin-5 or ß-defensin-1, or with the respective amount of solvent (H_2O) and then samples were processed as described in (c). (**a–d**) Significance was tested using one-way ANOVA followed by Dunnett's multiple comparison test and refers to respective untreated controls (* $p \leq 0.1$, ** $p \leq 0.01$, **** $p \leq 0.0001$, *ns* not significant). WB = Western blot.

2.2. In the Presence of α-Defensin-1 and -5 Less Gαi Is ADP-Ribosylated in PT-Treated Cells

After demonstrating a significant and specific inhibition of PTS1 enzyme activity by α-defensin-1 and -5, we tested whether the defensins also impair intoxication of CHO-K1 cells with the PT holotoxin. PT and the defensins were either added simultaneously to the cells (Figure 2a), or after pre-incubation in a reaction tube (Figure 2b). After 4 h, the ADP-ribosylation status of Gαi was determined in the lysates of treated cells, by sequential ADP-ribosylation. Therefore, recombinant PTS1 and biotin-NAD^+ were added to the lysates. This allows ADP-ribosylation, and thereby biotin-labeling of Gαi that was not modified during the treatment of the living cells. Thus, the untreated control cells result in a strong signal of biotin-labeled Gαi, and the signal of PT-treated cells is significantly reduced (Figure 2). The samples treated with PT in the presence of α-defensin-1 and -5 resulted in increased signals compared to the samples treated with PT only. This indicates that the cells were protected from intoxication with PT. The inhibition by α-defensin-1 and -5 was comparable with or without the pre-incubation of PT with the defensins. A concentration-dependent inhibition was clearly observed for α-defensin-5, and a trend was revealed for the inhibition by α-defensin-1 (Figure 2c). Again, ß-defensin-1 did not protect the cells from intoxication with PT (Figure 2a and b). Notably, all three defensins did not reduce the cell viability on their own, under the same experimental conditions (Figure 2d).

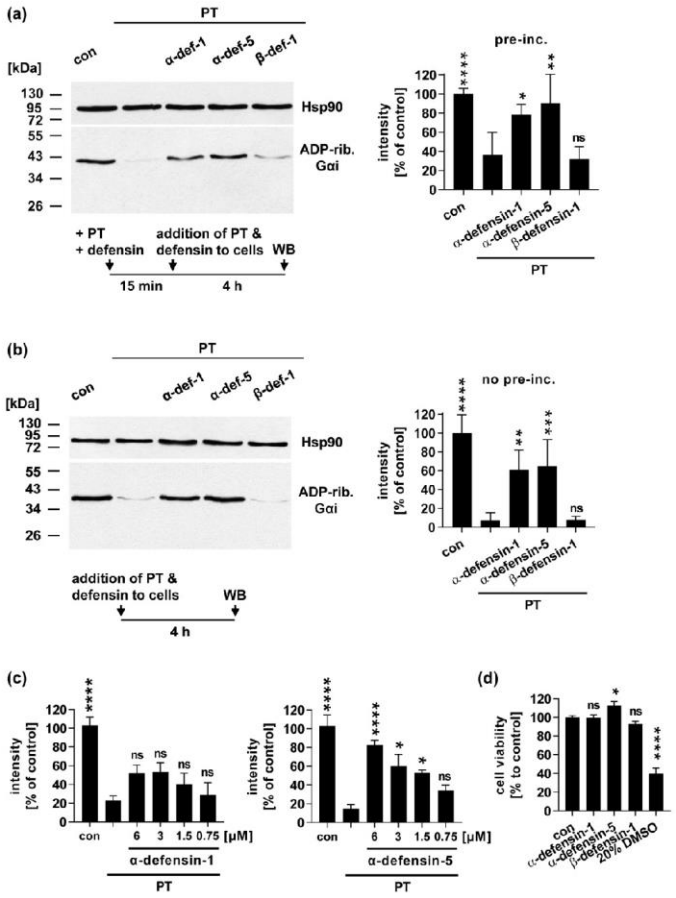

Figure 2. Effect of human α-defensin-1 and -5 on the ADP-ribosylation status of Gαi in PT-treated cells. (**a**) PT (10 ng/mL) was pre-incubated with 6 μM α-defensin-1, α-defensin-5 or ß-defensin-1, or with the respective amount of solvent (H_2O) for 15 min at room temperature and then added to CHO-K1 cells for 4 h at 37°C. For further control, cells were left untreated. Cells were lysed and Gαi, which has not been ADP-ribosylated in the cells during intoxication, was ADP-ribosylated and thus biotin-labeled by incubation with PTS1 in the presence of biotin-labeled NAD^+. Biotin-labeled Gαi was detected via Western blot. Comparable protein loading was confirmed with Ponceau-S- (not shown) and Hsp90-staining. One representative Western blot is shown, and bar graphs show quantified Western blot signals from three independent experiments. Values are given as percent of untreated control, normalized to Hsp90, mean ± SD (n = 3 from three independent experiments); (**b**) PT (10 ng/mL) and 6 μM α-defensin-1, α-defensin-5 or ß-defensin-1, or the respective amount of solvent (H_2O) were added to cells at the same time. Subsequently, the experiment was performed as described in (a); (**c**) CHO-K1 cells were treated at the same time with PT (10 ng/mL) and decreasing concentrations of α-defensin-1 or α-defensin-5 (as indicated) for 4 h at 37 °C. ADP-ribosylation status was determined as described in (a). Bar graphs show quantified Western blot signals from four independent experiments. Values are given as percent of untreated control, normalized to Hsp90, mean ± SEM (n = 4 from four independent experiments); (**d**) CHO-K1 cells were treated with 6 μM α-defensin-1, α-defensin-5 or ß-defensin-1, or with the respective amount of solvent (H_2O) or 20% DMSO as a positive cell viability decreasing control for 4 h at 37 °C. Cell viability was measured by MTS assay. Absorbance values are given as percent of untreated control, mean ± SEM (n = 12 from four independent experiments). Significance was tested using one-way ANOVA followed by Dunnett's multiple comparison test and refers to controls treated with PT only (**a**–**c**) or untreated controls (**d**) (* $p \leq 0.1$, ** $p \leq 0.01$, *** $p \leq 0.001$, **** $p \leq 0.0001$, *ns* not significant). WB = Western blot.

2.3. α-Defensin-1 and -5 Inhibit the PT-Mediated Effects on cAMP Signaling in Cells

A consequence of PT-mediated Gαi-ADP-ribosylation is its inactivation, which leads to disturbed cAMP signaling, because Gαi can no longer efficiently inhibit the adenylate cyclase. The iGIST bioassay has been developed to measure the effect of PT on Gαi signaling in cells [37]. The method is based on HEK293 cells that ectopically express the Gαi-coupled GPCR somatostatin receptor 2 (SSTR2), together with a luminescent cAMP probe (iGIST sensor cells). Experimentally, these cells are treated with forskolin, to directly activate the adenylate cyclase, and additionally with octreotide to activate the SSTR2. This only leads to a moderate increase in cAMP in the control samples, because Gαi inhibits the adenylate cyclase due to SSTR2 stimulation (Figure 3a, grey curve). When the cells were treated with PT prior to stimulation with forskolin and octreotide, cAMP levels significantly increased, because inhibition of the adenylate cyclase by Gαi was decreased due to its ADP-ribosylation by PT (Figure 3a, red curve). When the cells were treated with forskolin, but not octreotide, maximal levels of cAMP were reached in the presence and absence of PT (Figure 3c). The treatment of the cells with PT that had been pre-incubated with α-defensin-1 and -5, resulted in an inhibited increase in intracellular cAMP, suggesting that the defensins also impaired PT activity in this bioassay (Figure 3a and b). Notably, ß-defensin-1 did not inhibit the PT-mediated cAMP increase, and in the absence of PT, the defensins had no significant effect on cAMP levels compared to the control samples (Figure 3b, right graph).

Taken all together, we demonstrated that human α-defensin-1 and -5, but not ß-defensin-1, inhibit the enzyme activity of PTS1 in vitro, and impair the consequences of PT in living cells, as analyzed by the ADP-ribosylation of Gαi, as well as by measuring the PT-mediated cAMP increase in stimulated HEK sensor cells using the iGIST bioassay. The results suggest a potential role for human defensins as inhibitors against PT during *B. pertussis* infection.

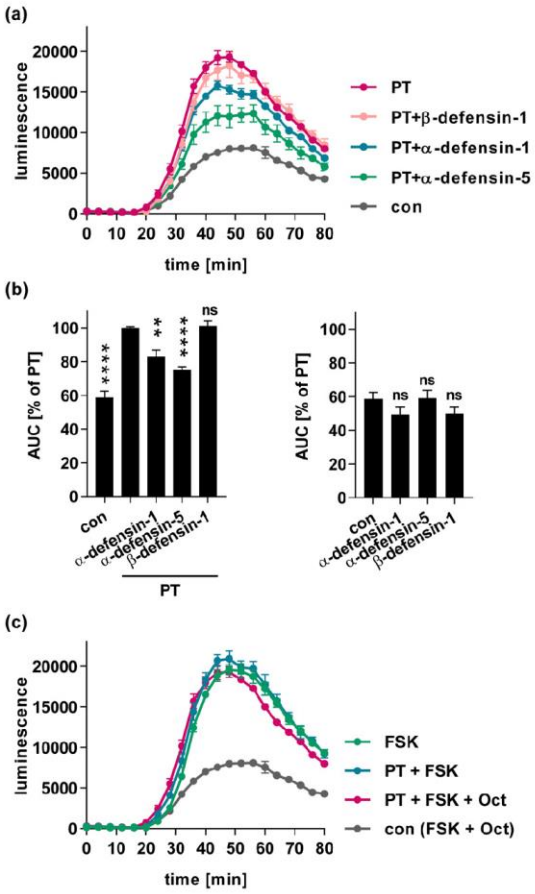

Figure 3. Human α-defensin-1 and -5 inhibit PT-mediated effects on cAMP signaling. PT (100 ng/mL) was pre-incubated with 12 µM α-defensin-1, α-defensin-5 or ß-defensin-1, or with the respective amount of solvent (H_2O) for 15 min at room temperature and then added to iGIST sensor cells for 5 h at 37°C. For further control, cells were treated only with the solvent of PT. Then, inducing medium containing the luciferase substrate for the luminescent biosensor for cAMP was added. After 15 minutes of baseline measurement, cells were spiked with forskolin to activate adenylate cyclase and octreotide acetate to activate Gαi-coupled SSTR2 GPCR. Luminescence was recorded for further 60 minutes. (**a**) cAMP kinetic curves from one representative experiment are shown as mean ± SD (n = 3 from one experiment), con = cells treated only with forskolin (FSK) plus octreotide (Oct). (**b**) Bar graphs show baseline-subtracted area under the curve (AUC) from at least three independent experiments. Values are given as percent of PT-only-treated samples, mean ± SEM (n = at least nine from at least three independent experiments). Values for control samples are identical in both graphs. Results are shown in two separate graphs for better clarity. Significance was tested using one-way ANOVA followed by Dunnett's multiple comparison test and refers to samples treated with PT only (left graph) or untreated controls (right graph) (** $p \leq 0.01$,**** $p \leq 0.0001$, *ns* not significant). (**c**) For control, iGIST sensor cells were treated only with FSK or with PT plus FSK in the absence of Oct to measure the maximal cAMP response in this assay. Values for control samples and samples treated with PT plus FSK and Oct are identical to values in (**a**).

3. Discussion

B. pertussis produces several virulence factors that contribute to the development of the disease, including the AB_5-type toxin PT [38]. PT is essential for causing the disease, since *B. pertussis* strains that do not express PT only elicit weak symptoms [28]. The precise role of PT and other virulence factors, as well as their interplay for *B. pertussis* pathogenesis, is not fully understood. It was demonstrated that PT causes severe and long-lasting inflammation of the airways in a mouse model [27]. *B. pertussis* strains not expressing PT did not cause leukocytosis or death. These results clearly indicate a pivotal role of PT in causing severe courses of disease, which makes it an attractive target for the development of novel pharmacological strategies [28–30].

Here, we demonstrated that the human antimicrobial peptides α-defensin-1 and -5 inhibit the enzyme activity of PT. Moreover, we showed that less Gαi was ADP-ribosylated in the cells treated with PT, and the PT-mediated cAMP increase in the sensor cells was reduced in the presence of α-defensin-1 and -5. Interestingly, these effects were not observed with ß-defensin-1, suggesting that the inhibition of PT by α-defensin-1 and -5 is more specific and not just based on the cationic nature of defensins. Human defensins can be subdivided into α- and ß-defensins based on their molecular weight, and the distribution of cysteines and disulfide bonds [33]. The positive charge of defensins plays an important role in their antimicrobial activity, because this enables the defensins to interact with the negatively charged phospholipids of microbial membranes. Defensins then cause disruption of the membrane, and thereby facilitate the killing of bacteria [33]. So far, it is not fully understood which characteristics and structural elements of defensins are crucial for their anti-toxin activity. Intramolecular disulfide bonds, hydrophobicity, and high arginine content seem to be essential, and dimerization as well as cationicity were important for anti-toxin activity [32]. Interestingly, the arginine content of α-defensin-1 (13.3%) and α-defensin-5 (18.8%) is higher than in ß-defensin-1 (2.7%) [32,39]. Moreover, α-defensin-1 and -5 share a very similar three-dimensional structure that differs from the ß-defensin-1 structure [32,40]. Although the anti-toxin activity cannot be pinpointed to one structural element, these differences between the defensins might be the reason why α-defensin-1 and -5, but not ß-defensin-1, inhibit PT and other toxins.

Interestingly, it has been reported that, additionally to their antimicrobial activity, human defensins also exhibit anti-toxin activity [32,40]. Both α-defensin-1 and -5 inhibit the *C. difficile* toxins TcdA, TcdB, and CDT. For TcdA and TcdB, the underlying mechanism of inhibition is the aggregation of the toxins by the defensins [34–36]. For CDT, it was shown that pore formation by the B-component of the toxin is impaired by α-defensin-1 and -5 [34,35]. A comparable mechanism was observed for the *Clostridium perfringens* iota toxin that is closely related to CDT [41]. Notably, no inhibition of the *C. difficile* toxins or iota toxin was detected for ß-defensin-1 [34,35,41]. Human α-defensin-1 also inhibited the enzyme activity of the *Bacillus anthracis* lethal toxin, a metalloprotease, as well as of the diphtheria toxin and *Pseudomonas* exotoxin ETA, which are both ADP-ribosyltransferases, similarly to PT [31,42]. The active site, in particular the NAD^+ binding pocket, is structurally conserved among ADP-ribosylating toxins. Thus, the inhibition of ADP-ribosyltransferase activity by α-defensin-1 and -5 might be a common mechanism for this group of toxins. However, further inhibitory mechanisms of defensins against bacterial toxins have been identified, which might also play an additional role for the inhibition of PT by α-defensin-1 and -5. It was shown that the thermally unstable effector domains of MARTX from *V. cholerae* and *Aeromonas hydrophilia*, which display an auto-processing protease and actin crosslinking activity, were inhibited by α-defensin-1 [39]. This inhibition was due to local unfolding, which increased the thermal melting and precipitation, and exposed additional regions for proteolysis [39]. Since the enzyme subunit of PT is also known to be thermally unstable, which is a necessary requisite for its transport from the ER to the cytosol [14], increased unfolding, mediated by the defensins, might be an additional inhibitory mechanism. Up to now, a common mechanism of the inhibition of bacterial toxins has not been identified, and

it is not known which is the common characteristic of the small peptides that is essential for inhibition.

Further, α-defensin-1 is expressed in neutrophils and stored in granules. Upon pro-inflammatory or bacterial stimuli, it is released by degranulation [43]. In the early stages of infection, PT suppresses the recruitment of neutrophils. Later, neutrophils are recruited to the infection site again, but are inhibited by another toxin of *B. pertussis*, the adenylate cyclase toxin (ACT) [44]. Also, α-defensin-5 is found in Paneth cells in the crypts of the small intestine [45], raising the question of its physiological role during the *B. pertussis* infection that is located in the respiratory tract. However, human defensins bear the potential to serve as starting points for the development of novel therapeutic strategies against the severe symptoms of whooping cough, which are associated with PT activity [28,30].

4. Materials and Methods

4.1. Compounds and Reagents

Recombinant Gαi and recombinant PTS1 were expressed and purified as described earlier [46]. The used peptides α-defensin-1 and -5 as well as β-defensin-1 were purchased from PeptaNova (Sandhausen, Germany). *Bordetella pertussis* toxin (PT) was purchased from Sigma-Aldrich, Merck (Darmstadt, Germany).

4.2. In vitro Enzyme Activity of PTS1

Recombinant Gαi (0.5 µM) was incubated with recombinant PTS1 (50 nM = 1.17 µg/mL) and biotin-labeled NAD^+ (1 µM; R&D Systems, Abingdon, United Kingdom) in a 50 nM sodium phosphate buffer (pH 7.0) in the presence of the respective defensin or H_2O (solvent of defensins) as a control for 40 min at room temperature. Subsequently, samples were subjected to SDS-PAGE and Western blotting with streptavidin–peroxidase (Strep–POD, Sigma-Aldrich, Merck, Darmstadt, Germany) for detection of biotin-labeled and thus ADP-ribosylated Gαi. Densitometric quantification of signals was performed using ImageJ software (NIH). Ponceau-S-staining was used to control equal loading of samples.

4.3. Cell Lines

All materials for cell culture were purchased from Gibco unless indicated otherwise. Chinese hamster ovary cells strain K1 (CHO-K1, DSMZ, Braunschweig, Germany) were cultivated in DMEM and HAM's F12 (1:1) supplemented with 5% heat-inactivated fetal calf serum (Invitrogen, Thermo Fisher Scientific, Waltham, MA, USA), 1 mM sodium pyruvate and penicillin–streptomycin (1:100) (Thermo Fisher Scientific, Waltham, MA, USA). HEK293 cells (HEK-Gs/SSTR2_HA), ectopically expressing Gαi-coupled somatostatin receptor 2 (SSTR2) GPCR as well as a luminescence cAMP probe (GloSensor-22F, Promega, Mannheim, Germany) [37], were cultivated in DMEM/F12 (containing glutamine and sodium pyruvate) supplemented with 10% heat-inactivated fetal calf serum (Invitrogen) and penicillin–streptomycin (1:100) (Thermo Fisher Scientific). Cells were grown under humidified conditions at 37 °C with 5% CO_2, and trypsinized and reseeded every two to three days for at most 25 times. For intoxication experiments, cells were seeded in culture dishes one or two days before and treated in FCS-free media with PT and the respective compounds.

4.4. Sequential ADP-Ribosylation of Gαi in Lysates from Toxin-Treated Cells

CHO-K1 cells were seeded into 24-well plates and treated with PT (10 ng/mL = 0.095 nM) and defensin or H_2O as a control in FCS-free medium for 4 h. Then, cells were washed to remove unbound protein and frozen for cell lysis. As described earlier [47], ADP-ribosylation buffer (0.1 mM Tris-HCL (pH 7.6), 20 mM DTT, 0.1 µM ATP and protease inhibitor complete (Roche)) was added and cell lysates were transferred into reaction tubes. For sequential ADP-ribosylation of Gαi in vitro, which had not been modified by PT in the cells during intoxication, recombinant PTS1 (50 nM) and biotin-labeled NAD^+ (1 µM; R&D Systems) were added and incubated for 40 min at room temperature. Subsequently, samples

were subjected to SDS-PAGE and Western blot analysis with streptavidin–peroxidase (Strep-POD, Sigma-Aldrich) for detection of biotin-labeled and thus sequentially ADP-ribosylated Gαi. Densitometric quantification of signals was performed using ImageJ software (NIH). Hsp90 (primary antibody from Santa Cruz Biotechnology, Dallas, TX, USA) signals were detected as a loading control.

4.5. Cell Viability Assay

CHO-K1 cells were seeded in 96-well plates and treated with defensin or H_2O as a control in FCS-free medium for 4 h. As a positive control, DMSO (20%) was added to the cells to cause cell death. Cell viability was determined by Cell Titer 96® Aqueous One Solution cell proliferation assay (MTS assay, Promega), which was added to the cells and incubated for 60 min at 37 °C. Absorbance was measured at 490 nm via a plate reader.

4.6. iGIST Bioassay

The iGIST bioassay was performed as previously described [37]. HEK293 cells ectopically expressing Gαi-coupled somatostatin receptor 2 (SSTR2) GPCR as well as a luminescence cAMP probe (GloSensor-22F, Promega) were seeded in 96-well plates with white walls and a translucent bottom (View-Plate 96, Perkin Elmer). PT (100 ng/mL) or matched buffer SolC (50% glycerol, 50 mM Tris, 10 mM glycine, 0.5 M NaCl, pH 7.5) and defensins (12 µM) or H_2O as a control were pre-incubated in FCS-free medium for 15 min and then added to the cells for 5 h. Subsequently, medium was removed and 45 µL inducing medium (comprised of 2% GloSensor reagent (Promega), 400 µM of the phosphodiesterase inhibitor IBMX (Sigma) in DMEM/F12 medium and CO_2-independent medium (4v of DMEM/F12 per 5v CO_2-independent medium), supplemented with 0.1% (w/v) bovine serum albumin) was added and equilibrated for 45 min at room temperature in the dark. With the Orion microplate luminometer (Berthold Detection Systems) baseline luminescence was recorded for 15 min. Then cells were spiked with forskolin (10 µM, Merck Sigma, Darmstadt, Germany) to activate adenylate cyclase and octreotide acetate (20 nM, Bachem, Bubendorf, Switzerland) to activate the Gαi-coupled SSTR2 GPCR in 25 mM HEPES buffer (pH 7.4). Luminescence, corresponding to cAMP levels in the cells was measured for another 60 min. For quantification of kinetic curves, the baseline-subtracted area under the curve (AUC) was calculated by GraphPad Prism software employing the trapezoidal rule.

Author Contributions: K.E.: conceptualization, formal analysis, writing—original draft preparation, visualization, supervision, project administration, funding acquisition. C.K.: formal analysis, investigation, visualization. A.T.P.: resources, methodology. H.B.: resources, writing—review and editing. All authors have read and agreed to the published version of the manuscript.

Funding: This work was supported by the Deutsche Forschungsgemeinschaft (DFG, German Research Foundation)—project number 316249678-SFB 1279 (A07, funding to K.E.; C02, funding to H.B.). K.E. is a fellow of the Margarete von Wrangell Habilitation program supported by the European Social Fund and Ministry of Science, Research and Art Baden-Wurttemberg. C.K. is supported by a PhD fellowship by Cusanuswerk and is a fellow of the International Graduate School in Molecular Medicine Ulm (IGradU).

Institutional Review Board Statement: Not applicable.

Informed Consent Statement: Not applicable.

Data Availability Statement: The datasets generated and/or analyzed during the current study are either included in the study and/or available from the corresponding author on reasonable request.

Acknowledgments: Anna Anastasia is thanked for her excellent technical assistance.

Conflicts of Interest: The authors declare no conflict of interest.

References

1. Stein, P.E.; Boodhoo, A.; Armstrong, G.D.; Cockle, S.A.; Klein, M.H.; Read, R. The crystal structure of pertussis toxin. *Structure* **1994**, *2*, 45–57. [CrossRef]
2. Tamura, M.; Nogimori, K.; Murai, S.; Yajima, M.; Ito, K.; Katada, T.; Ui, M.; Ishii, S. Subunit structure of islet-activating protein, pertussis toxin, in conformity with the A-B model. *Biochemistry* **1982**, *21*, 5516–5522. [CrossRef] [PubMed]
3. Weiss, A.A.; Johnson, F.D.; Burns, D.L. Molecular characterization of an operon required for pertussis toxin secretion. *Proc. Natl. Acad. Sci. USA* **1993**, *90*, 2970–2974. [CrossRef]
4. Armstrong, G.D.; Howard, L.A.; Peppler, M.S. Use of glycosyltransferases to restore pertussis toxin receptor activity to asialoagalactofetuin. *J. Biol. Chem.* **1988**, *263*, 8677–8684. [CrossRef]
5. Hausman, S.Z.; Burns, D.L. Binding of pertussis toxin to lipid vesicles containing glycolipids. *Infect. Immun.* **1993**, *61*, 335–337. [CrossRef] [PubMed]
6. Witvliet, M.H.; Burns, D.L.; Brennan, M.J.; Poolman, J.T.; Manclark, C.R. Binding of pertussis toxin to eucaryotic cells and glycoproteins. *Infect. Immun.* **1989**, *57*, 3324–3330. [CrossRef]
7. El Bayâ, A.; Linnemann, R.; Von Olleschik-Elbheim, L.; Robenek, H.; Schmidt, M.A. Endocytosis and retrograde transport of pertussis toxin to the Golgi complex as a prerequisite for cellular intoxication. *Eur. J. Cell Biol.* **1997**, *73*, 40–48.
8. Lippincott-Schwartz, J.; Yuan, L.C.; Bonifacino, J.S.; Klausner, R.D. Rapid Redistribution of Golgi Proteins into the ER in Cells Treated with Brefeldin A: Evidence for Membrane Cycling from Golgi to ER. *Cell* **1989**, *56*, 801–813. [CrossRef]
9. Burns, D.L.; Manclark, C.R. Adenine nucleotides promote dissociation of pertussis toxin subunits. *J. Biol. Chem.* **1986**, *261*, 4324–4327. [CrossRef]
10. Hazes, B.; Boodhoo, A.; Cockle, S.A.; Read, R. Crystal Structure of the Pertussis Toxin–ATP Complex: A Molecular Sensor. *J. Mol. Biol.* **1996**, *258*, 661–671. [CrossRef] [PubMed]
11. Plaut, R.; Scanlon, K.M.; Taylor, M.; Teter, K.; Carbonetti, N.H. Intracellular disassembly and activity of pertussis toxin require interaction with ATP. *Pathog. Dis.* **2016**, *74*, 74. [CrossRef]
12. Banerjee, T.; Cilenti, L.; Taylor, M.; Showman, A.; Tatulian, S.A.; Teter, K. Thermal Unfolding of the Pertussis Toxin S1 Subunit Facilitates Toxin Translocation to the Cytosol by the Mechanism of Endoplasmic Reticulum-Associated Degradation. *Infect. Immun.* **2016**, *84*, 3388–3398. [CrossRef] [PubMed]
13. Hazes, B.; Read, R. Accumulating Evidence Suggests That Several AB-Toxins Subvert the Endoplasmic Reticulum-Associated Protein Degradation Pathway To Enter Target Cells. *Biochemistry* **1997**, *36*, 11051–11054. [CrossRef] [PubMed]
14. Pande, A.H.; Moe, D.; Jamnadas, M.; Tatulian, S.A.; Teter, K. The Pertussis Toxin S1 Subunit Is a Thermally Unstable Protein Susceptible to Degradation by the 20S Proteasome†. *Biochemistry* **2006**, *45*, 13734–13740. [CrossRef] [PubMed]
15. Worthington, Z.E.V.; Carbonetti, N.H. Evading the Proteasome: Absence of Lysine Residues Contributes to Pertussis Toxin Activity by Evasion of Proteasome Degradation. *Infect. Immun.* **2007**, *75*, 2946–2953. [CrossRef]
16. Ernst, K.; Eberhardt, N.; Mittler, A.-K.; Sonnabend, M.; Anastasia, A.; Freisinger, S.; Schiene-Fischer, C.; Malešević, M.; Barth, H. Pharmacological Cyclophilin Inhibitors Prevent Intoxication of Mammalian Cells with Bordetella pertussis Toxin. *Toxins* **2018**, *10*, 181. [CrossRef]
17. Ernst, K.; Mittler, A.-K.; Winkelmann, V.; Kling, C.; Eberhardt, N.; Anastasia, A.; Sonnabend, M.; Lochbaum, R.; Wirsching, J.; Sakari, M.; et al. Pharmacological targeting of host chaperones protects from pertussis toxin in vitro and in vivo. *Sci. Rep.* **2021**, *11*, 1–17. [CrossRef]
18. Bokoch, G.M.; Katada, T.; Northup, J.K.; Hewlett, E.L.; Gilman, A.G. Identification of the predominant substrate for ADP-ribosylation by islet activating protein. *J. Biol. Chem.* **1983**, *258*, 2072–2075. [CrossRef]
19. Katada, T.; Ui, M. Direct modification of the membrane adenylate cyclase system by islet-activating protein due to ADP-ribosylation of a membrane protein. *Proc. Natl. Acad. Sci. USA* **1982**, *79*, 3129–3133. [CrossRef]
20. Andreasen, C.; Carbonetti, N.H. Pertussis Toxin Inhibits Early Chemokine Production to Delay Neutrophil Recruitment in Response to Bordetella pertussis Respiratory Tract Infection in Mice. *Infect. Immun.* **2008**, *76*, 5139–5148. [CrossRef]
21. Kirimanjeswara, G.S.; Agosto, L.M.; Kennett, M.J.; Bjornstad, O.N.; Harvill, E.T. Pertussis toxin inhibits neutrophil recruitment to delay antibody-mediated clearance of Bordetella pertussis. *J. Clin. Investig.* **2005**, *115*, 3594–3601. [CrossRef]
22. Spangrude, G.J.; Sacchi, F.; Hill, H.R.; Van Epps, D.E.; Daynes, R.A. Inhibition of lymphocyte and neutrophil chemotaxis by pertussis toxin. *J. Immunol.* **1985**, *135*, 4135–4143.
23. Mattoo, S.; Cherry, J.D. Molecular Pathogenesis, Epidemiology, and Clinical Manifestations of Respiratory Infections Due to Bordetella pertussis and Other Bordetella Subspecies. *Clin. Microbiol. Rev.* **2005**, *18*, 326–382. [CrossRef] [PubMed]
24. Yeung, K.H.T.; Duclos, P.; Nelson, E.A.S.; Hutubessy, R.C.W. An update of the global burden of pertussis in children younger than 5 years: A modelling study. *Lancet Infect. Dis.* **2017**, *17*, 974–980. [CrossRef]
25. Robert-Koch-Institut. Impfquoten bei der Schuleingangsuntersuchung in Deutschland 2017. *Epid Bull* **2019**, *18*, 147–153. [CrossRef]
26. WHO. Immunization Coverage. Available online: https://www.who.int/news-room/fact-sheets/detail/immunization-coverage (accessed on 7 June 2021).
27. Connelly, C.E.; Sun, Y.; Carbonetti, N.H. Pertussis Toxin Exacerbates and Prolongs Airway Inflammatory Responses during Bordetella pertussis Infection. *Infect. Immun.* **2012**, *80*, 4317–4332. [CrossRef] [PubMed]

28. Carbonetti, N.H. Contribution of pertussis toxin to the pathogenesis of pertussis disease: Graphical Abstract Figure. *Pathog. Dis.* **2015**, *73*, ftv073. [CrossRef]
29. Pittman, M. The concept of pertussis as a toxin-mediated disease. *Pediatr. Infect. Dis. J.* **1984**, *3*, 467–486. [CrossRef]
30. Scanlon, K.; Skerry, C.; Carbonetti, N. Association of Pertussis Toxin with Severe Pertussis Disease. *Toxins* **2019**, *11*, 373. [CrossRef]
31. Kim, C.; Slavinskaya, Z.; Merrill, A.R.; Kaufmann, S.H.E. Human α-defensins neutralize toxins of the mono-ADP-ribosyltransferase family. *Biochem. J.* **2006**, *399*, 225–229. [CrossRef]
32. Kudryashova, E.; Seveau, S.M.; Kudryashov, D.S. Targeting and inactivation of bacterial toxins by human defensins. *Biol. Chem.* **2017**, *398*, 1069–1085. [CrossRef]
33. Cederlund, A.; Gudmundsson, G.H.; Agerberth, B. Antimicrobial peptides important in innate immunity. *FEBS J.* **2011**, *278*, 3942–3951. [CrossRef] [PubMed]
34. Fischer, S.; Ückert, A.; Landenberger, M.; Papatheodorou, P.; Hoffmann-Richter, C.; Mittler, A.; Ziener, U.; Hägele, M.; Schwan, C.; Müller, M.; et al. Human peptide α-defensin-1 interferes withClostridioides difficiletoxins TcdA, TcdB, and CDT. *FASEB J.* **2020**, *34*, 6244–6261. [CrossRef]
35. Korbmacher, M.; Fischer, S.; Landenberger, M.; Papatheodorou, P.; Aktories, K.; Barth, H. Human α-Defensin-5 Efficiently Neutralizes Clostridioides difficile Toxins TcdA, TcdB, and CDT. *Front. Pharmacol.* **2020**, *11*, 1204. [CrossRef] [PubMed]
36. Giesemann, T.; Guttenberg, G.; Aktories, K. Human α-Defensins Inhibit Clostridium difficile Toxin B. *Gastroenterology* **2008**, *134*, 2049–2058. [CrossRef] [PubMed]
37. Paramonov, V.M.; Sahlgren, C.; Rivero-Müller, A.; Pulliainen, A.T. iGIST—A Kinetic Bioassay for Pertussis Toxin Based on Its Effect on Inhibitory GPCR Signaling. *ACS Sens.* **2020**, *5*, 3438–3448. [CrossRef]
38. Kilgore, P.E.; Salim, A.M.; Zervos, M.J.; Schmitt, H.-J. Pertussis: Microbiology, Disease, Treatment, and Prevention. *Clin. Microbiol. Rev.* **2016**, *29*, 449–486. [CrossRef]
39. Kudryashova, E.; Quintyn, R.; Seveau, S.; Lu, W.; Wysocki, V.; Kudryashov, D.S. Human Defensins Facilitate Local Unfolding of Thermodynamically Unstable Regions of Bacterial Protein Toxins. *Immunity* **2014**, *41*, 709–721. [CrossRef]
40. Kim, C.; Kaufmann, S.H. Defensin: A multifunctional molecule lives up to its versatile name. *Trends Microbiol.* **2006**, *14*, 428–431. [CrossRef]
41. Fischer, S.; Popoff, M.R.; Barth, H. Human alpha-defensin-1 protects cells from intoxication with Clostridium perfringens iota toxin. *Pathog. Dis.* **2018**, *76*, 76. [CrossRef] [PubMed]
42. Kim, C.; Gajendran, N.; Mittrücker, H.-W.; Weiwad, M.; Song, Y.-H.; Hurwitz, R.; Wilmanns, M.; Fischer, G.; Kaufmann, S.H.E. Human -defensins neutralize anthrax lethal toxin and protect against its fatal consequences. *Proc. Natl. Acad. Sci. USA* **2005**, *102*, 4830–4835. [CrossRef]
43. Sengeløv, H.; Follin, P.; Kjeldsen, L.; Lollike, K.; Dahlgren, C.; Borregaard, N.; Sengeløv, H.; Follin, P.; Kjeldsen, L.; Lollike, K.; et al. Mobilization of granules and secretory vesicles during in vivo exudation of human neutrophils. *J. Immunol.* **1995**, *154*, 4157–4165. [PubMed]
44. Eby, J.C.; Hoffman, C.; Gonyar, L.A.; Hewlett, E.L. Review of the neutrophil response toBordetella pertussisinfection. *Pathog. Dis.* **2015**, *73*, ftv081. [CrossRef] [PubMed]
45. Jones, D.; Bevins, C. Paneth cells of the human small intestine express an antimicrobial peptide gene. *J. Biol. Chem.* **1992**, *267*, 23216–23225. [CrossRef]
46. Ashok, Y.; Miettinen, M.; de Oliveira, D.K.H.; Tamirat, M.Z.; Näreoja, K.; Tiwari, A.; Hottiger, M.O.; Johnson, M.S.; Lehtiö, L.; Pulliainen, A.T. Discovery of Compounds Inhibiting the ADP-Ribosyltransferase Activity of Pertussis Toxin. *ACS Infect. Dis.* **2020**, *6*, 588–602. [CrossRef]
47. Xu, Y.; Barbieri, J.T. Pertussis toxin-mediated ADP-ribosylation of target proteins in Chinese hamster ovary cells involves a vesicle trafficking mechanism. *Infect. Immun.* **1995**, *63*, 825–832. [CrossRef] [PubMed]

2.3 Inhibition of Pertussis Toxin by Human α-Defensins-1 and -5: Differential Mechanisms of Action

International Journal of Molecular Sciences (2023) 24 (13), 10557.
https://doi.org/10.3390/ijms241310557

Carolin Kling, Anja Sommer, Yasser Almeida-Hernandez, Armando Rodríguez, Julio A. Pérez-Erviti, Rajendra Bhadane, Ludger Ständker, Sebastian Wiese, Holger Barth, Mario Pupo-Meriño, Arto T. Pulliainen, Elsa Sanchez-Garcia and Katharina Ernst[#]

[#]corresponding author

The reuse of the present article in my dissertation is permitted by the Creative Commons Attribution 4.0 International License (CC BY 4.0) (https://creativecommons.org/licenses/by/4.0/).

2.3.1 Own contributions

- Data and Figures of **Figure 1a-c** and **Figure 1e** (Effect of defensins on ADP-ribosylation status of Gαi in PT-treated cells and enzyme activity of PTS1 *in vitro*)
- Data and Figures of **Figure 2a-f** (Effect of defensins on binding of PT to cells)
- Data and Figures of **Figure 3** (Effect of defensins on PT signals in cells)
- Data and Figures of **Figure 4a-c** (Uptake of defensins into cells)
- Data and Figures of **Figure 5a-d** (Interaction of defensins with PTS1 in cells)
- Data and Figures of **Figure 7a** (Interaction of α-defensin-1 with PTS1 and Gαi *in vitro*)
- Preparation of the main part of the manuscript and revision

2.3.2 Summary of Results

After identifying α-defensin-1 and -5 as inhibitors of PT and PTS1 enzyme activity in the previous publication, the present publication further investigates the underlying mechanism of inhibition in more detail.

First, the protective effect of α-defensin-1 and -5, previously shown on CHO-K1 and HEK293 cells, was now demonstrated in the lung adenocarcinoma cell line A549, a pathophysiologically more relevant cell line. In the PT-intoxicated A549 cells, less Gαi was ADP-ribosylated in the presence of α-defensin-1 or -5 but not β-defensin-1. Additionally, other defensins of the same

family were investigated. It was shown that α-defensin-2, -3, and -4 also protected cells from PT intoxication, whereas α-defensin-6, and β-defensin-2 had no effect on the ADP-ribosylation status of Gαi in PT-intoxicated cells. To investigate the relevance of the characteristic disulfide bonds of α-defensin-1 and -5, the cysteine residues in their amino acid sequence were replaced by serine residues, thus resulting in linearized forms of the peptides. The linearized peptides did not show an inhibitory effect on PT intoxication even with higher concentrations, demonstrating the importance of the tertiary structure of α-defensin-1 and -5 for inhibition of PT. Furthermore, the linearized forms of α-defensin-1 and -5 did not inhibit enzyme activity of PTS1 in an *in vitro* assay. Their native forms, however, demonstrated a clear reduction of ADP-ribosylated Gαi. As seen in the previous publication, α-defensin-1 exhibited a stronger inhibition of PTS1 enzyme activity than α-defensin-5.

Next, the underlying mechanism of inhibition was further investigated, by examining the binding of fluorescently labeled PT to A549 and CHO-K1 cells in a flow cytometry experiment. In the presence of α-defensin-1 a reduction of PT-binding could only been shown with pre-incubation of PT with the defensin. In contrast, α-defensin-5 strongly reduced PT bound to cells in both cell lines with and without pre-incubation. The same results were obtained with an alternative approach by fluorescence microscopy in CHO-K1 cells. Moreover, neither α-defensin-1 nor -5 reduced the amount of PT bound to cells, when they were added after PT had already bound. As a result of reduced binding of PT to the cell surface, less PT should be found inside the cells. With fluorescence microscopy, it was shown, that α-defensin-5 strongly reduced the intensity of PT signals in cells after incubation for 4 h, whereas α-defensin-1 showed only a slight reduction.

So far, the results indicated that α-defensin-5 mainly inhibits PT intoxication by preventing PT from entering cells and α-defensin-1 rather inhibits PTS1 enzyme activity (Figure 6). For α-defensin-1 to effectively inhibit PTS1 activity intracellularly, it has to reach the cytosol. To test this hypothesis, different cell lines were incubated with α-defensin-1 and -5 for 4 h, then cells were fixed and the defensins were stained with specific antibodies. By omitting the permeabilization step, necessary for the antibodies to reach intracellular targets, it could be distinguished between intracellular and extracellular signals of the defensins. This way, it could be shown, that α-defensin-1 is taken up into different cell lines. The signal of α-defensin-5 in the cells was much weaker and did not differ as much with or without permeabilization. In line with the hypothesis

(Figure 6), α-defensin-1, but not α-defensin-5 was detected in close proximity to PTS1 in A549 and CHO-K1 cells, as investigated by the proximity ligation assay (PLA).

Computational modeling revealed specific interaction sites for α-defensin-1 with PTS1 and vice versa, as opposed to α-defensin-5. By using PPI-Detect, a model for the prediction of protein-protein interactions, α-defensin-1 obtained higher interaction scores with PTS1 than α-defensin-5. Simulations of the complexes of α-defensin-1 and -5 with PTS1 displayed different binding modes with different residues of PTS1. α-Defensin-1 bound PTS1 at the cleft between α-helices h3 and h5, the binding site of the substrate Gαi. In contrast, α-defensin-5 did not present conserved interactions with specific residues of PTS1, neither did PTS1 target specific regions of α-defensin-5.

Finally, in a dot blot assay, a direct binding of α-defensin-1 to PTS1, but not PT was detected *in vitro*. Interestingly, the binding of α-defensin-1 exhibited an even more pronounced affinity towards the substrate Gαi. Therefore, the effect of α-defensin-1 on NADase activity of PTS1 was examined in the absence of Gαi. It was shown, that α-defensin-1 had no significant impact on NADase activity of PTS1 independently of Gαi. This is in line with the results, that α-defensin-1 does not occlude the NAD^+ binding site of PTS1, but the binding site of Gαi.

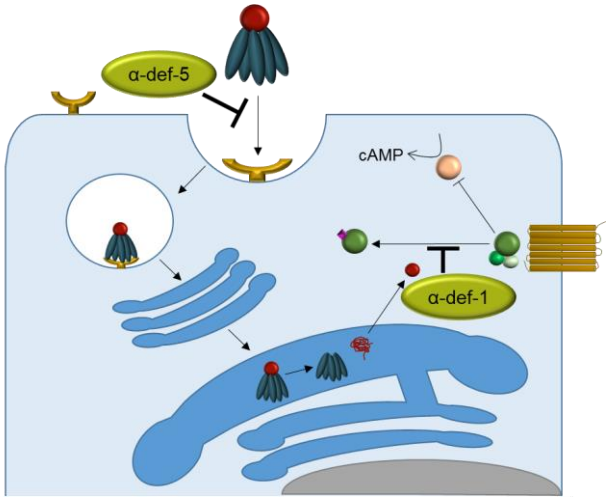

Figure 6: Differential Mechanisms of Action of α-Defensin-1 and -5 for Inhibition of PT
α-Defensin-1 affects PT mainly by inhibition of enzyme activity of PTS1, and thus protects Gαi from ADP-ribosylation. α-Defensin-5 affects PT mainly by inhibiting binding of PT to the cell surface and thus preventing uptake of PT into the cell.

Taken together, both α-defensin-1 and -5 protect cells from PT but use differential mechanisms of inhibition. While α-defensin-1 enters cells and mainly impairs the ADP-ribosylation step of Gαi by PTS1, α-defensin-5 mainly impairs uptake of PT into the cell (Figure 6).

2.3.3 Discussion

In the previous publication, α-defensin-1 and -5 were identified as inhibitors of PT and PTS1 enzyme activity. The present publication represents an extension of the results by demonstrating the defensins' protective effect on the human lung adenocarcinoma cell line A549, and more precisely characterizing their underlying molecular mechanism of inhibition.

Since α-defensin-1 and -5 have been demonstrated to inhibit other AB-type toxins in different ways, several mechanisms of inhibition are conceivable for their inhibition of PT. Similar to the effect on PTS1, α-defensin-1 showed inhibition on enzyme activity of other A-subunits of toxins, such as LF, DT and ETA (Kim et al., 2005, 2006). Similar to its role in preventing the uptake of PT into cells, α-defensin-5 has been shown to neutralize TcdA extracellularly by the formation of inactive TcdA-defensin aggregates, and CDT by impairing the binding and transport component (Korbmacher et al., 2020). In contrast, enzyme activity of TcdA or CDT was not inhibited by α-defensin-5. However, α-defensin-1 has not only shown inhibition of the enzyme subunit of AB-type toxins, but also inhibition of the binding and transport subunit B: α-defensin-1 impaired pore formation of the B-component of CDT, interacted with the B-component of *C. perfringens* iota toxin, and inhibited binding of TcdA and TcdB to cells (Fischer et al., 2018, 2020). Another reported mechanism of inhibition is the inhibition of enzyme activity of MARTX by α-defensin-1, and, to a lesser extent, by α-defensin-5 by local unfolding of MARTX effector domains, leading to thermal unfolding, increased susceptibility to proteolysis and precipitation (Kudryashova et al., 2014). Thermal unfolding of PTS1 is also a conceivable mechanism of inhibition, since PTS1 is thermally unstable, which is a prerequisite for its translocation from the ER to the cytosol (Pande et al., 2006). This could be investigated in the future, for example by differential scanning fluorimetry (DSF), where the changes in protein tertiary structure can be monitored by the increase in fluorescence of a dye that interacts with hydrophobic residues, exposed upon denaturation. This assay has shown for example, that α-defensin-1 potentiates thermal unfolding of TcdB, and CDCs, amongst others (Kudryashova et al., 2014).

Understanding the mechanism of inhibition in detail is an important requirement for optimization of the peptide sequence of α-defensin-1 and -5 for future application. *In silico* modeling revealed the interaction regions of α-defensin-1 with PTS1, which allows to identify the peptide sequences in α-defensin-1 with the highest inhibitory potential against PT. In future steps, the α-defensins could be optimized concerning their activity, solubility and stability by altering or shortening the peptide sequence or adding chemical modifications. This could be done based on computational modeling results, or also in an alanine scanning approach. Here, amino acid residues are exchanged systematically one by one by an alanine residue. The resulting peptides could then be tested, which would reveal the importance of the different amino acid residues or even create optimized modified versions of the peptide. For clinical application, the distribution, tolerability, and bioavailability of the peptides should be tested first in animal models, and optimized, e.g., by improving the formulation. As peptides have been recognized as a promising group of therapeutics over the last decades, many studies already dealt with their optimization. As an example, the HIV-1 (human immunodeficiency virus) inhibitor peptide T20 was successfully translated from *in vitro* application into the clinics and then further optimized in potency, stability and higher barrier for resistance development (Schütz et al., 2020). This improvement was achieved using an artificial peptide strategy, where a non-native protein sequence was designed, based on the universal artificial peptide template of 5HRu (Zhu et al., 2015). Moreover, novel delivery systems for peptides are investigated, including biocompatible porous silicon and aerosolization for improved parenteral peptide delivery (Kovalainen et al., 2015).

Current challenges of applying host defense antimicrobial peptides, such as defensins, in clinical use are their susceptibility to proteolysis, their low activity in physiological conditions and their high cost of production (Pachón-Ibáñez et al., 2017). Development of derivatives, analogs and mimetics, as well as improvement of production processes may overcome these issues. Human α-defensin-5 has already been examined as a prophylactic or therapeutic treatment in the mouse model of lethal HSV-2 (Herpes simplex virus 2) and showed an increased survival rate and decreased pathology score (A. Wang et al., 2013). Treatment with the α-defensin-5 derivative E21R-HD5, which has been enhanced for anti-HSV-2 activity by a single arginine substitution, displayed about a 1.5-fold-higher survival rate than with the parental α-defensin-5 (A. Wang et al., 2013). E21R-HD5 has been demonstrated later to have increased ability to penetrate cell

membranes (C. Wang et al., 2015). These current advances show the potential of human α-defensins and prospective optimized derivatives to be employed as therapeutics in the future.

Taken together, this thesis identified and characterized new approaches to inhibit PT. The investigated compounds were the small molecule inhibitors of cellular chaperones Rad, FK506, VER and CsA, and the human peptides α-defensin-1 and -5. The inhibitors exerted different molecular mechanisms of action within the intoxication process of PT. While α-defensin-5 prevented uptake of PT into cells, the chaperone inhibitors Rad, FK506, VER and CsA prevented the uptake of PTS1 to the cytosol and α-defensin-1 prevented the final enzymatic ADP-ribosylation of Gαi by PTS1. These different modes of inhibition might complement each other in a therapeutic context. Additionally to antibiotics, which eliminate the toxin-producing bacteria, α-defensin-5 could neutralize unbound toxin. PT that still enters the cells could be prevented from reaching its cytosolic target by chaperone inhibitors, and PTS1 that still enters the cytosol could be prevented from its cytotoxic effect by α-defensin-1. Certainly, extensive research is still required before the investigated inhibitors or their derivatives can be clinically used and alleviate pertussis symptoms of patients. However, this thesis forms a stepping stone for the optimization and development of novel therapeutic strategies against the life-threatening disease pertussis.

International Journal of *Molecular Sciences*

MDPI

Article

Inhibition of Pertussis Toxin by Human α-Defensins-1 and -5: Differential Mechanisms of Action

Carolin Kling [1], Anja Sommer [1], Yasser Almeida-Hernandez [2], Armando Rodríguez [3,4], Julio A. Perez-Erviti [2], Rajendra Bhadane [5], Ludger Ständker [3], Sebastian Wiese [4], Holger Barth [1], Mario Pupo-Meriño [6], Arto T. Pulliainen [5], Elsa Sánchez-García [2] and Katharina Ernst [1,*]

[1] Institute of Experimental and Clinical Pharmacology, Toxicology and Pharmacology of Natural Products, Ulm University Medical Center, 89081 Ulm, Germany
[2] Computational Bioengineering, Fakultät Bio- und Chemieingenieurwesen, Technische Universität Dortmund, 44227 Dortmund, Germany
[3] Core Facility Functional Peptidomics, Faculty of Medicine, Ulm University, 89081 Ulm, Germany
[4] Core Unit Mass Spectrometry and Proteomics, Faculty of Medicine, Ulm University, 89081 Ulm, Germany
[5] Institute of Biomedicine, University of Turku, FI-20520 Turku, Finland; arto.pulliainen@utu.fi (A.T.P.)
[6] Departamento de Bioinformática, Centro de Matemática Computacional, Universidad de las Ciencias Informáticas (UCI), Havana 19370, Cuba
* Correspondence: katharina.ernst@uni-ulm.de

Abstract: Whooping cough is a severe childhood disease, caused by the bacterium *Bordetella pertussis*, which releases pertussis toxin (PT) as a major virulence factor. Previously, we identified the human antimicrobial peptides α-defensin-1 and -5 as inhibitors of PT and demonstrated their capacity to inhibit the activity of the PT enzyme subunit PTS1. Here, the underlying mechanism of toxin inhibition was investigated in more detail, which is essential for developing the therapeutic potential of these peptides. Flow cytometry and immunocytochemistry revealed that α-defensin-5 strongly reduced PT binding to, and uptake into cells, whereas α-defensin-1 caused only a mild reduction. Conversely, α-defensin-1, but not α-defensin-5 was taken up into different cell lines and interacted with PTS1 inside cells, based on proximity ligation assay. In-silico modeling revealed specific interaction interfaces for α-defensin-1 with PTS1 and vice versa, unlike α-defensin-5. Dot blot experiments showed that α-defensin-1 binds to PTS1 and even stronger to its substrate protein Gαi in vitro. NADase activity of PTS1 in vitro was not inhibited by α-defensin-1 in the absence of Gαi. Taken together, these results suggest that α-defensin-1 inhibits PT mainly by inhibiting enzyme activity of PTS1, whereas α-defensin-5 mainly inhibits cellular uptake of PT. These findings will pave the way for optimization of α-defensins as novel therapeutics against whooping cough.

Keywords: pertussis toxin; defensins; bacterial AB-type toxin; human peptide; antimicrobial peptide; toxin inhibitor; mechanism of inhibition

check for updates

Citation: Kling, C.; Sommer, A.; Almeida-Hernandez, Y.; Rodríguez, A.; Perez-Erviti, J.A.; Bhadane, R.; Ständker, L.; Wiese, S.; Barth, H.; Pupo-Meriño, M.; et al. Inhibition of Pertussis Toxin by Human α-Defensins-1 and -5: Differential Mechanisms of Action. *Int. J. Mol. Sci.* **2023**, *24*, 10557. https://doi.org/10.3390/ijms241310557

Academic Editor: Axel T. Neffe

Received: 9 June 2023
Revised: 16 June 2023
Accepted: 16 June 2023
Published: 23 June 2023

Copyright: © 2023 by the authors. Licensee MDPI, Basel, Switzerland. This article is an open access article distributed under the terms and conditions of the Creative Commons Attribution (CC BY) license (https://creativecommons.org/licenses/by/4.0/).

1. Introduction

Bordetella (B.) pertussis toxin (PT) is an AB_5 protein toxin consisting of an enzyme subunit, the A-protomer PTS1, and a pentameric B-subunit, which together form a holotoxin with a pyramid-like structure that is secreted by the bacteria [1–3]. The B-pentamer allows binding to the cell surface via sialoglycoproteins present on most cell types [4,5]. Following internalization by endocytosis, PT undergoes retrograde intracellular transport through the Golgi to the endoplasmic reticulum (ER) [6,7]. In the ER, ATP binding to the toxin causes destabilization of the interaction between PTS1 and the B-pentamer, leading to the release of PTS1 from the holotoxin [8–11]. The released PTS1 is thermally unstable and therefore detected by the ER-associated degradation (ERAD) pathway, which transports it from the ER to the cytosol [11,12]. PTS1 lacks lysine residues, which protects it from ubiquitination and proteasomal degradation [13]. Furthermore, host cell chaperones and protein folding helper enzymes are required for the uptake of PTS1 into the host cell cytosol [14–18].

Cytosolic PTS1 covalently transfers an ADP-ribose moiety from its co-substrate NAD^+ onto the α-subunit of inhibitory G-proteins (Gαi), which are associated with G-protein-coupled receptors (GPCRs) [19,20]. ADP-ribosylation inactivates Gαi, resulting in disturbed cAMP signaling, as Gαi is no longer able to inhibit the adenylate cyclase (AC). The consequences of disturbed GPCR and cAMP signaling are varied and depend on the cell type (for review see also [21]). For example, PT was first referred to as 'islet-activating protein' because it stimulates insulin secretion [20,22]. Moreover, in the early stages of infection, PT inhibits the recruitment of neutrophils, monocytes, and lymphocytes to the lung, leading to a decrease in pro-inflammatory chemokines and cytokines, as well as an increased bacterial burden in a mouse model [23–25]. PT also reduces the surface expression of adhesion molecules and integrins (leukocyte function antigen-1, LFA-1; L-selectin) resulting in disturbed trafficking of lymphocytes and therefore trapping of lymphocytes in the vasculature [26,27].

PT is a significant virulence factor responsible for the symptoms of whooping cough, a disease characterized by a prolonged (about ten weeks) and uncontrollable cough [28,29]. Patients often experience secondary complications, including vomiting and pneumothorax. Severe cases can lead to pneumonia, encephalopathy, seizures, or apnea, which can be life-threatening, particularly in newborns and young infants [30]. According to the World Health Organization (WHO), in 2014, over 24.1 million cases of pertussis in children under five years old resulted in 160,700 deaths worldwide [31,32]. Pertussis is re-emerging despite available vaccination and high vaccination coverage in Western countries. Case numbers are at an all-time high since vaccine introduction in the 1950s [31,33]. Although antibiotic therapy eliminates *B. pertussis* bacteria, it does not relieve pertussis symptoms, except when administered within two weeks of infection, which rarely occurs due to late diagnosis [28]. Studies have demonstrated that PT causes prolonged and severe inflammation of the airways in a mouse model [34]. In fact, strains of *B. pertussis* not expressing PT did not cause severe symptoms such as leukocytosis or death, indicating the crucial role of PT especially in severe cases [21]. As a result, PT represents an attractive target for the development of novel therapeutic strategies.

Recently, we identified the human antimicrobial peptides α-defensin-1 and α-defensin-5, also known as human neutrophil peptide 1 (HNP1) and human defensin-5 (HD5), respectively, as inhibitors of PT [35]. Defensins are small, cationic, and cysteine-rich peptides with a crucial role in innate immunity by inactivating bacterial pathogens [36]. α-Defensin-1 and α-defensin-5 but not the structurally related ß-defensin-1 protected cells from PT-intoxication and from PT-mediated effects on intracellular cAMP signaling. We showed that α-defensin-1 and -5 inhibited the enzyme activity of PTS1 in vitro [35]. In the present study, the underlying inhibitory mechanism of α-defensin-1 and -5 on the mode of action and uptake mechanism of PT was characterized in detail to elucidate innate immune defense mechanisms against PT as well as to provide a starting point for novel therapeutic strategies against PT-mediated symptoms of whooping cough.

2. Results

2.1. Human α-Defensin-1 and -5 Inhibit ADP-Ribosylation of Gαi in PT-Treated Cells and Enzyme Activity of PTS1 In Vitro

As we previously demonstrated the inhibitory effects of α-defensin-1 and -5 on CHO-K1 and HEK293 cells [35], we now confirmed this finding in the lung adenocarcinoma cell line A549, which is a more relevant cell line regarding the pathophysiology of infection and PT secretion. A549 cells were treated with PT for 4 h, either after pre-incubation of PT with the defensin (Figure 1a) or direct administration (Figure 1b). Afterwards, the ADP-ribosylation status of Gαi in the cell lysate was determined by sequential ADP-ribosylation: Gαi, which has not been ADP-ribosylated in cells during intoxication was biotin-labeled by incubation with PTS1 and biotin-NAD^+. Thus, samples from PT-treated cells show a weaker signal in the Western blot than samples from untreated cells (con). In the presence of α-defensin-1 or -5, the PT-mediated ADP-ribosylation of Gαi in A549 cells was inhibited, whereas β-defensin-1 had no effect (Figure 1a,b).

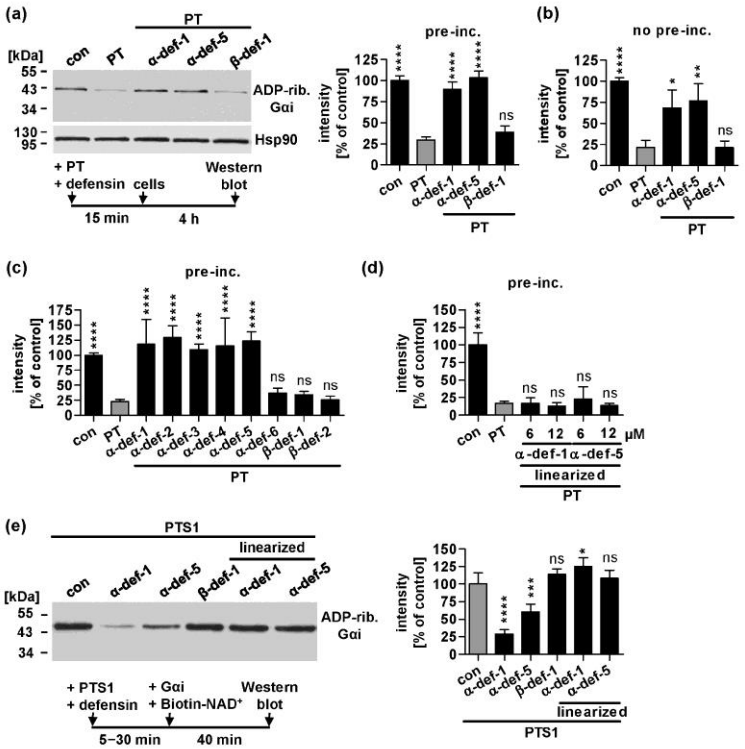

Figure 1. Effect of defensins on ADP-ribosylation status of Gαi in PT-treated cells and enzyme activity of PTS1 in vitro (**a**) PT (50 ng/mL) was pre-incubated with defensin (12 µM) or with the respective amount of solvent (H_2O) for 15 min at room temperature and then added to A549 cells for 4 h at 37 °C. Cells were left untreated for a further control (con). Subsequently, cells were lysed, and Gαi, which has not been ADP-ribosylated in cells during intoxication was ADP-ribosylated and therefore biotin-labeled by incubation with PTS1 and biotin-labeled NAD^+. Biotin-labeled Gαi was detected via Western blot. Hsp90 was detected as a control of equal protein loading. The bar graph shows quantified Western blot signals from four independent experiments. Values are given as percent of untreated control, normalized to Hsp90, mean ± SEM (n = 4 from four independent experiments) (**b**) PT (50 ng/mL) and defensin (12 µM) or the respective amount of solvent (H_2O) were added directly to A549 cells and incubated for 4 h at 37 °C. Subsequently, the experiment was performed as described in (**a**). (**c**,**d**) PT (10 ng/mL) was pre-incubated with defensins (6 µM (**c**) or as indicated (**d**)) for 15 min at room temperature and added to CHO-K1 cells and incubated for 4 h at 37 °C. Subsequently, the experiment was performed as described in (**a**). (**c**) Values in bar graphs are given as percent of untreated control, normalized to Hsp90, mean ± SEM (n ≥ 4 from at least four independent experiments). (**d**) Values in bar graphs are given as percent of untreated control, normalized to Hsp90, mean ± SD (n = 3 from three independent experiments). (**e**) PTS1 (50 nM) was pre-incubated with 6 µM defensin or the respective amount of solvent (H_2O) for 5–30 min at 37 °C. Gαi and biotin-labeled NAD^+ were added for 40 min at room temperature. ADP-ribosylated and therefore biotin-labeled Gαi was detected via Western blot. The bar graph shows quantified Western blot signals from at least three independent experiments. Values are given as percent of control, mean ± SEM (n ≥ 6 from at least four independent experiments. (**a**–**e**) Significance was tested using one-way ANOVA followed by Dunnett's multiple comparison test and refers to controls treated with PT only ((**a**–**d**), grey bars) or untreated controls ((**e**), grey bars) (* $p \leq 0.1$, ** $p \leq 0.01$, *** $p \leq 0.001$ **** $p \leq 0.0001$, ns not significant).

In addition, other defensins of the same family were investigated in this assay, and α-defensin-2, -3 and -4 exhibited the same inhibitory effect as α-defensin-1 and -5 (Figure 1c). In contrast, α-defensin-6, along with β-defensin-1 and -2, had no effect on the PT-induced ADP-ribosylation of Gαi. Moreover, the common characteristic disulfide bonds of human α-defensins were disrupted by replacing cysteine residues with serine residues in their amino acid sequence. These thereby linearized peptides α-defensin-1 and -5, lacking disulfide bonds, were unable to reduce the levels of ADP-ribosylated Gαi in PT-treated cells, even in higher concentrations (Figure 1d). This demonstrates the importance of the tertiary structure of α-defensin-1 and -5 to inhibit PT.

The enzyme activity of PTS1 was assessed separately by pre-incubating PTS1 with the respective defensins and then adding Gαi and biotin-NAD^+ to the in vitro reaction (Figure 1e). ADP-ribosylated and thus biotin-labeled Gαi was detected by Western blot, and a reduction in the signal indicates inhibition of PTS1 activity. The linearized α-defensin-1 and -5 did not exhibit inhibitory activity against PTS1, whereas their native forms demonstrated a clear reduction in ADP-ribosylated Gαi. Notably, α-defensin-1 exhibits a stronger inhibition of PTS1 enzyme activity than α-defensin-5.

2.2. *α-Defensin-5 Reduces the Amount of Cell-Bound PT Stronger Than α-Defensin-1*

Prompted by these findings, we further investigated the mechanism of inhibition of α-defensin-1 and -5. When cells are incubated with PT on ice, the toxin can only bind to the cell surface but is not taken up into the cells. We analyzed bound PT on A549 and CHO-K1 cells by flow cytometry (Figure 2a–d). In both A549 and CHO-K1 cells, α-defensin-1 only inhibited binding of PT to the cell surface when it was pre-incubated with PT before adding it to the cells (Figure 2b,d). However, when this pre-incubation step was omitted, α-defensin-1 showed no inhibitory effect (Figure 2a,c). α-Defensin-5 showed a clear and strong reduction in the amount of PT bound to the cell surface, regardless of whether pre-incubation was performed or not. β-Defensin-1 and the unrelated protein BSA served as negative controls and had no effect on PT binding to cells. α-Defensin-1 and -5 alone did not reduce the auto-fluorescence of the analyzed cells (Figure 2a–d on the right). Furthermore, neither α-defensin-1 nor -5 showed a reduction in the amount of PT bound to the cell surface when they were added to the cells after PT had already bound (Figure 2e).

As an alternative approach, the amount of PT bound to the cell surface after incubation on ice in the presence of α-defensin-1 and -5 was also investigated by fluorescence microscopy, utilizing a specific antibody against PT (Figure 2f). Here, the amount of PT on the cell surface was only reduced by α-defensin-5 but not α-defensin-1, regardless of whether pre-incubation was performed or not.

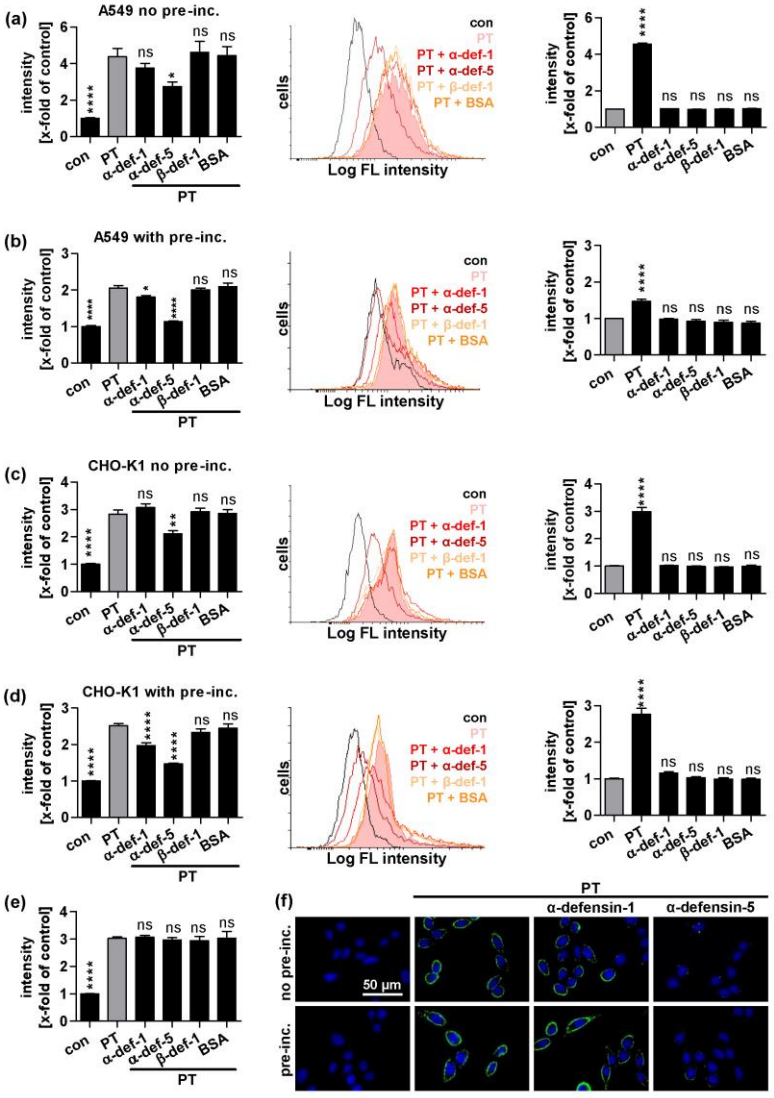

Figure 2. Effect of defensins on binding of PT to cells. PT that was 488-labeled (1 µg/mL (**a**,**b**) or 0.5 µg/mL (**c**,**d**)) was pre-incubated with defensin (12 µM) for 15 min at room temperature (**b**,**d**) or added directly (**a**,**c**) to A549 or CHO-K1 cells in suspension and incubated for 15 min on ice to enable binding of PT to the cell surface. For control, cells were left untreated (con). Cells were washed by centrifugation and binding of PT was detected by flow cytometry. Values are given as percent of control, mean ± SEM (n = 9 from three independent experiments (left) or n = at least 3 from at least one experiment (right)). Histograms show fluorescence intensity of cells in one representative experiment, respectively. (**e**) PT that was 488-labeled (0.5 µg/mL) was pre-incubated with CHO-K1 cells for 15 min on ice. Cells were washed and incubated with defensin (12 µM) for 15 min on ice. For control, cells were left untreated (con). Subsequently, the experiment was performed as described above. Values are given as percent of control, mean ± SEM (n = 8 from three independent experiments)

(**a**–**e**) Significance was tested using one-way ANOVA followed by Dunnett's multiple comparison test and refers to controls treated with PT only (left, grey bars) or untreated controls (right, grey bars) (* $p \leq 0.1$, ** $p \leq 0.01$, **** $p \leq 0.0001$, ns not significant). (**f**) PT (1 µg/mL) was pre-incubated with defensin (6 µM) for 15 min at room temperature (lower row) or added directly (upper row) to CHO-K1 cells and incubated for 40 min on ice to enable binding of PT to the cell surface. Cells were washed, fixed, permeabilized, blocked and probed with an antibody against PTS1 (green). Nuclei were stained with Hoechst (blue). Representative images of three individual experiments are shown.

2.3. Treatment with α-Defensin-5 Results in a Reduction in the Amount of PT in Cells

After observing the inhibitory effect of α-defensin-5 on PT binding to the cell surface, we proceeded to investigate the overall amount of PT in cells. Therefore, A549 cells were treated with PT at 37 °C for 4 h, and then the signal intensity of PT within the cells was analyzed (Figure 3). In the presence of α-defensin-1, the signal intensity of PT was only slightly reduced, whereas in the presence of α-defensin-5, a substantial decrease in signal intensity was observed.

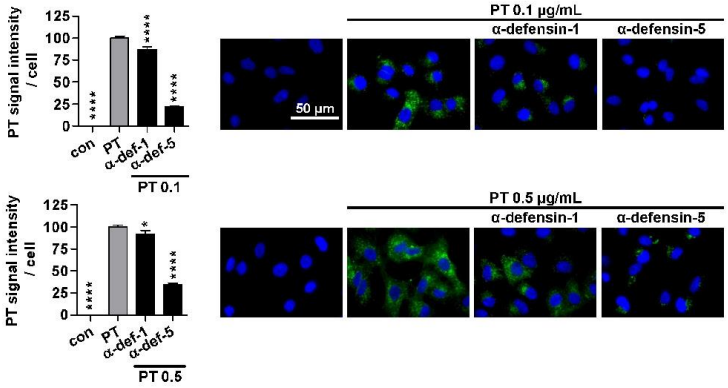

Figure 3. Effect of defensins on PT signals in cells. A549 cells were treated with PT (0.1 or 0.5 µg/mL) and defensin (6 µM) for 4 h at 37 °C. For control, cells were left untreated (con). Cells were washed, fixed, permeabilized, blocked and probed with an antibody against PT (green). Nuclei were stained with Hoechst (blue). Representative images of three independent experiments are shown. The overall intensity of the PT signal was determined with ImageJ v.1.52a. Values are baseline-corrected, normalized to cell numbers and given as mean ± SEM (n = 45 images per condition from three independent experiments). Significance was tested using one-way ANOVA followed by Dunnett's multiple comparison test and refers to samples treated only with PT (grey bars) (* $p \leq 0.1$, **** $p \leq 0.0001$, ns not significant).

2.4. α-Defensin-1 Is Internalized into Cells

Our results so far indicate that α-defensin-5 mainly inhibits PT intoxication by preventing PT from entering cells. For α-defensin-1, however, the results suggest an intracellular mechanism of PT inhibition, such as inhibiting enzyme activity of PTS1 in cells. Hence, it is plausible to consider that α-defensin-1 has to reach its target in the cytosol of the cells to interact with and inhibit PTS1. Therefore, we examined whether α-defensin-1 was taken up into cells. Different cell lines were incubated with α-defensin-1 or -5 at 37 °C for 4 h (Figure 4a,b). Then, cells were fixed and the defensins were stained with specific antibodies. Permeabilization of cells allows the antibodies to reach intracellular targets. Performing the experiment with or without permeabilization allows distinguishing the intracellular and extracellular signals of defensins (Figure 4a,b, lower row). When the cells were incubated with α-defensin-1, we observed a strong signal with permeabilization and weaker signal without permeabilization indicating a primarily intracellular signal localization (Figure 4a). Incubation with α-defensin-5 resulted in a much weaker signal, which did not differ as

much with or without permeabilization (Figure 4b). Despite the substantial uptake of α-defensin-1, it had no influence on cell viability even after incubation for 24 h (Figure 4c).

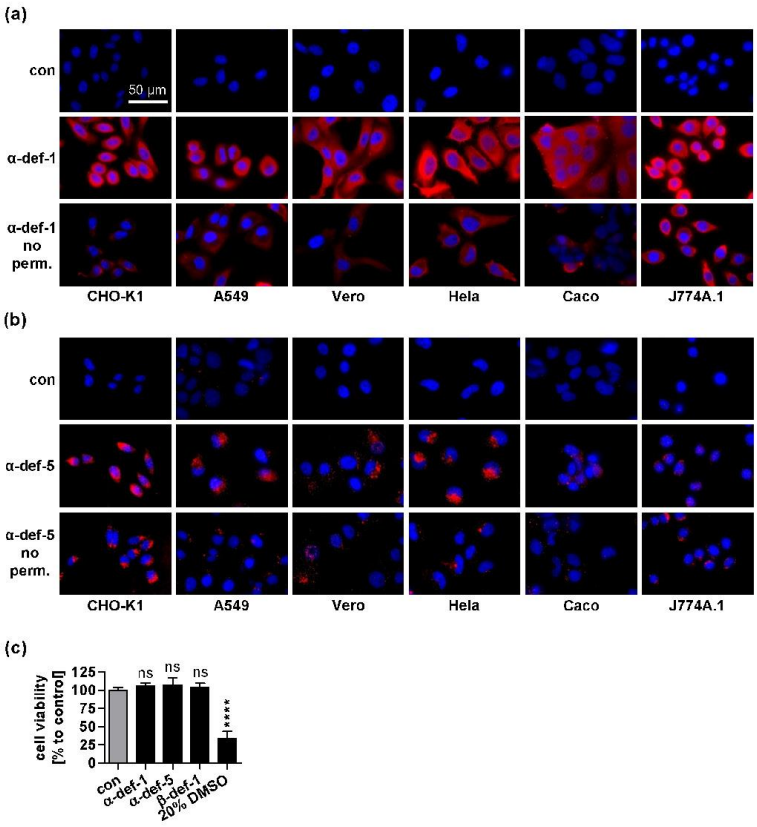

Figure 4. Uptake of defensins into cells. (**a**–**b**) Different cell lines were incubated with respective defensin (6 µM) for 4 h at 37 °C. Cells were washed, fixed and either permeabilized (upper rows) or this step was omitted (lower rows) to prevent intracellular staining with antibodies. Then, cells were blocked and probed with an antibody against α-defensin-1 (**a**) or α-defensin-5 (**b**) (both red). Nuclei were stained with Hoechst (blue). Representative images of three independent experiments are shown. (c) CHO-K1 cells were treated with defensin (6 µM) or 20 % DMSO as a positive control for decreasing cell viability for 24 h at 37 °C. Cell viability was measured by the MTS assay. Absorbance values are given as percent of untreated control, mean ± SEM (n = 9 from three independent experiments). Significance was tested using one-way ANOVA followed by Dunnett's multiple comparison test and refers to non-treated samples (grey bars) (**** $p \leq 0.0001$, ns not significant).

2.5. α-Defensin-1 but Not α-Defensin-5 Is Detected in Close Proximity to PTS1 in Cells

After demonstrating the uptake of α-defensin-1 into cells, we investigated whether it also interacts with PTS1 in cells. Therefore, the proximity ligation assay (PLA), which generates a fluorescent signal when two specific antibodies are in close proximity within fixed cells due to an internal amplification reaction was employed. A549 and CHO-K1 cells were treated with defensin and PT for 4 h at 37 °C (Figure 5). Then, cells were fixed, and the PLA was performed using antibodies against PTS1 and α-defensin-1 or -5, respectively. Even though the background PLA signals for α-defensin-1 in control cells (not treated with

PT) were significantly higher than without α-defensin-1, PLA signals in cells treated with PT and α-defensin-1 were still considerably higher (Figure 5a,c). On the other hand, PLA signals in cells treated with PT and α-defensin-5 did not surpass the background signals obtained in cells only treated with PT (Figure 5b,d). This shows that α-defensin-1 but not α-defensin-5 was detected very close to PTS1 in cells.

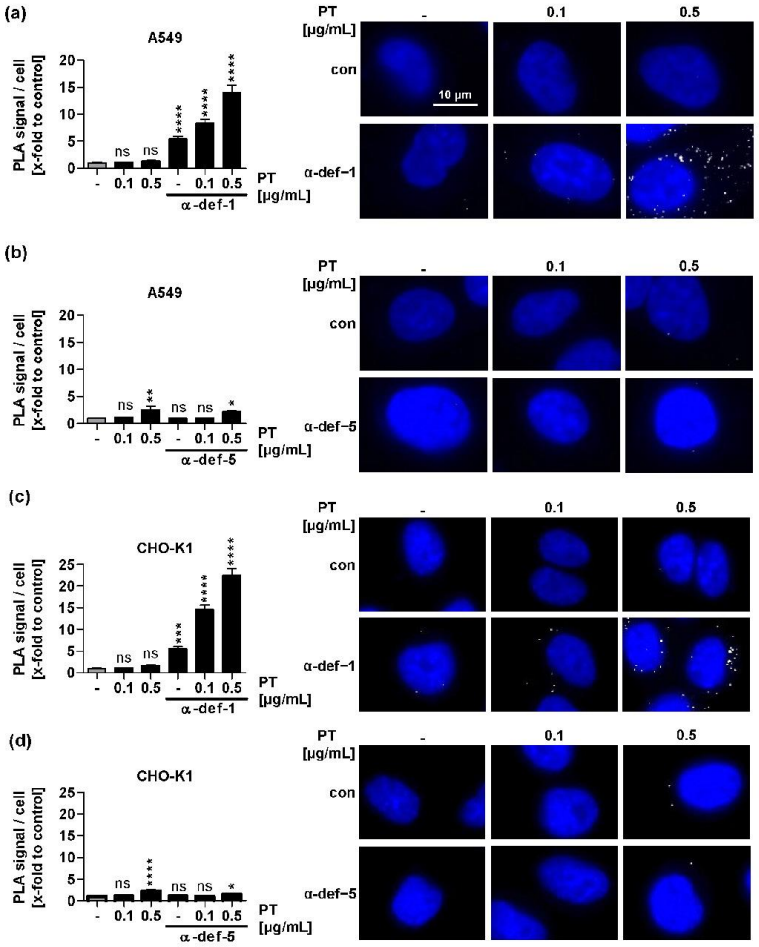

Figure 5. Interaction of defensins with PTS1 in cells. A549 (**a**,**b**) or CHO-K1 (**c**,**d**) cells were treated with PT and defensin (6 µM) for 4 h at 37 °C. After washing, cells were fixed, and the fluorescence-based PLA assay was performed according to the manufacturer's manual. Nuclei were stained with Hoechst (blue). PLA signals (white) represent protein interaction events of PTS1 and α-defensin-1 (**a**,**c**) or α-defensin-5 (**b**,**d**) and were counted from fluorescence pictures with ImageJ v.1.52a. (**a**–**d**) Graphs show quantified PLA signals per cell number. Values are given as mean ± SEM (n = 45 images per condition from three independent experiments). Significance was tested using one-way ANOVA followed by Dunnett's multiple comparison test and refers to untreated controls (grey bars) (* $p \leq 0.1$, ** $p \leq 0.01$, *** $p \leq 0.001$, **** $p \leq 0.0001$, ns not significant).

2.6. Computational Modeling of the PTS1/α-Defensin-1 and PTS1/α-Defensin-5 Binding Interface

Next, to provide mechanistic insights at the molecular level, we studied the interaction of PTS1 with α-defensin-1 and α-defensin-5. We employed different approaches to identify the binding interface of the complexes in-silico.

First, we used PPI-Detect [37], a support vector machine model for the prediction of protein–protein interactions, to map the interaction probability of different regions in the sequence of each partner. The interaction scores were relatively higher for α-defensin-1 (0.636–0.604) than for α-defensin-5 (0.577–0.548) for the top-10 pairs of sequences inside the applicability domain. This result is in line with the experimental evidence that α-defensin-1 inhibition of PTS1 is stronger than for α-defensin-5 (Figure 1e). In both cases, the best-scored interactions were located mostly in the region of residues 101–130 of PTS1. In the case of α-defensin-5, the interactions with PTS1 were wider spread with respect to α-defensin-1 (Figure 6a). For both defensins, most of the peptide's sub-sequences are involved in interactions with PTS1, except for the C-terminal region of α-defensin-1 and the N-terminal region of α-defensin-5.

Next, PTS1/α-defensin-1 and PTS1/α-defensin-5 complexes were modeled with AlphaFold Multimer (v2.2) [38] using the sequences of recombinant PTS1, α-defensin-1 and α-defensin-5 as inputs. This provided us with a structure of PTS1 based on the actual recombinant sequence used in the experiments. The models predicted the binding of both α-defensins in the region between α-helices h3 (residues 57–77) and h5 (residues 118–127) of PTS1 (Supplementary Figure S1). Furthermore, residues 118–127 of PTS1 are predicted to form a α-helix (h5), similar to the structure of the full toxin [1] and the auto-inhibited PTS1. This finding suggests that these residues might fold upon binding to a partner, unlike when PTS1 is not bound, when this region is unfolded [39].

Next, to account for the conformational flexibility of the protein and peptides and sample the conformational space of the systems, we carried out extensive molecular dynamics (MD) simulations. As a starting point for the MDs, we used the AlphaFold models with the α-defensins placed far away (40 Å) and in different orientations with respect to PTS1 (Supplementary Figure S2a). The simulation systems (PTS1/α-defensin) were allowed to move freely for 1.5 μs. Consequently, no binding sites or binding motifs were predefined. The simulation was repeated three times (replicas) for each PTS1/α-defensin system. During the first hundreds of nanoseconds of the simulations, the α-defensins diffused randomly in the solvent until binding to PTS1 was achieved. At 700 ns, both α-defensin-1 and α-defensin-5 were bound to PTS1 in all replicas (Supplementary Figure S2b, Supplementary Movies S1 and S2). Therefore, all subsequent analyses are based on the last 800 ns of each replica.

The analysis of the residues of the α-defensins and PTS1 featuring intermolecular contacts less than 4 Å away (Figure 6b,c) showed that both α-defensin-1 and α-defensin-5 display different binding modes to PTS1. In the PTS1/α-defensin-1 simulations, the interactions of α-defensin-1 with PTS1 mostly involved the PTS1 residues in α-helices h3 (residues 57–77) and h5 (residues 118–127). PTS1 residues with over 50% contact frequency with α-defensin-1 include H66 (58.0%), D70 (51.5%), L119 (55.9%), A122 (63.9%), L123 (53.4%) and Y126 (64.6%). As predicted using PPI-Detect, the residues of α-defensin-1 with more than 50% contact frequency with PTS1 are mainly located at the following regions of α-defensin-1: N-terminus (residues 1–4), β-sheet 2 (residues 16–21), the loop between β-sheet 2 and 3 (residues 22–24), and residues 25 and 28 of β-sheet 3. Conversely, α-defensin-5 interacts with several patches along the surface of PTS1: helix h4 and the C-terminal loop (100–114), the N-terminal region of segment h3 (residues 72–81), and the turn between β-sheets 8 and 9 (residues 151–154). Unlike α-defensin-1, α-defensin-5 does not display conserved interactions with specific residues of PTS1, and PTS1 does not target specific regions of α-defensin-5.

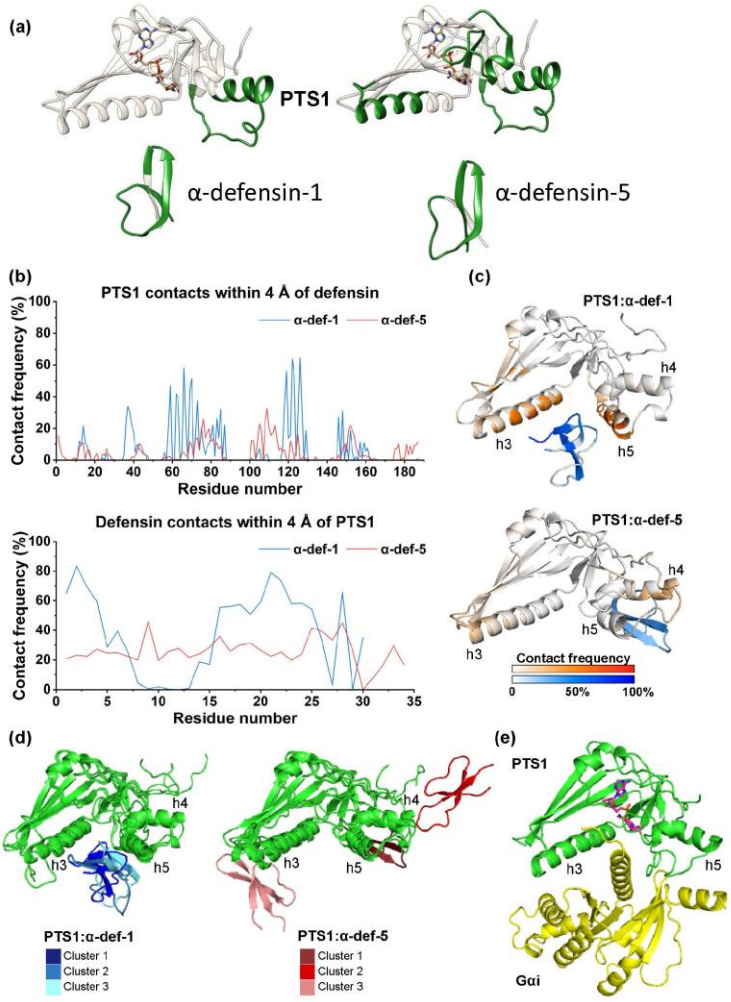

Figure 6. Computational modeling of the interaction of PTS1 with α-defensin-1 and -5 (**a**) PPI-Detect analysis of PTS1 and α-defensin-1 and -5. The stick representation shows BaAD, an NAD^+ analog [39], on PTS1 (PDB ID 7SNE). The regions in green correspond to the top-10 subsequences with the highest interaction scores (within the applicability domain of the method). (**b**) Contact frequency (expressed as the percent of simulation time per residue with contacts < 4 Å) between PTS1 and α-defensin-1 (blue) or α-defensin-5 (red) during the last 800 ns of the simulations (averaged over the last 800 ns of each replica). (**c**) 3D representation of the most populated cluster in the combined last 800 ns of the three replicas of the simulations of PTS1/α-defensin-1 (**top**) and PTS1/α-defensin-5 (**bottom**). The color scale represents the mapped contact frequency per residue of PTS1 (white to red scale) and α-defensin-1 or α-defensin-5 (white to blue scale). (**d**) 3D representations of the three most populated clusters in the combined last 800 ns of the three replicas of PTS1/α-defensin-1 (left, PTS1 in green, α-defensin-1 in shades of blue for the different clusters) and PTS1/α-defensin-5 (right, PTS1 in green, α-defensin-5 in shades of red for the different clusters). (**e**) PTS1/Gαi complex modelled by Sakari et al. [39] using AlphaFold. PTS1 is shown in green, Gαi in yellow, and NAD^+ in purple sticks.

To further clarify the binding mode between PTS1 and both defensins, we carried out root mean square deviation (RMSD) cluster analysis with 5 Å cutoff after combining the last 800 ns of the three replicas of each system. We observed no relevant changes in the secondary structure motifs of PTS1 upon binding of the defensins with respect to the starting structure of PTS1 generated by AlphaFold (Supplementary Figure S3). However, we found a different binding behavior for α-defensin-1 and α-defensin-5.

The three most populated clusters of the PTS1/α-defensin-1 simulation (Figure 6d, left) contain 50.4% of the analyzed trajectory frames. Representative structures of each cluster of α-defensin-1 bind to a cleft between helices h3 and h5, opposite to the NAD^+ binding site. In the case of PTS1/α-defensin-5, the three more populated clusters contain 41.4% of the simulation frames (Figure 6d, right). However, the representative structures of each cluster evidence interactions with different regions of PTS1, unlike the case of α-defensin-1 (Figure 6d).

The MD simulations of PTS1 with α-defensin-1/α-defensin-5 in explicit water delivered different binding modes for each defensin. α-Defensin-1 shows a clear tendency to bind PTS1 at the cleft between α-helices h3 and h5, as predicted by the AlphaFold model. Contrarily, α-defensin-5 does not have a preferred binding site at PTS1. Accordingly, the unbiased simulations allow us to discard the AlphaFold model of α-defensin-5 bound to the h3/h5 cleft of PTS1 as the preferred binding region.

The observed binding mode of α-defensin-1 to PTS1 does not occlude the NAD^+ binding site. Thus, the NAD^+ hydrolase activity of PTS1 is not expected to be affected by α-defensin-1 binding. Although no crystallographic structure of PTS1 bound to its substrate Gαi is available, the PTS1/Gαi complex was modelled by Sakari et al. [39] (Figure 6e). In this model, the N-terminus of Gαi, which contains the cysteine residue that gets ADP-ribosylated by PTS1, inserts into the PTS1 active site via the cleft between helices h3 and h5 of PTS1. This occurs in a similar manner to the preferred binding mode of α-defensin-1 observed in our simulations. This implies that α-defensin-1 could sterically block the PTS1-catalyzed Gαi ADP-ribosylation.

2.7. α-Defensin-1 Directly Binds to PTS1 and Gαi In Vitro

Prompted by the in-silico findings of specific interaction interfaces for α-defensin-1 with PTS1, we investigated the in vitro interaction of α-defensin-1 with PTS1 and its substrate Gαi by dot blot analysis. In this assay, interaction partners were spotted onto a nitrocellulose membrane, which was then incubated with α-defensin-1 or PBS-T for a control. Then, bound α-defensin-1 was detected with a specific antibody (Figure 7a). The results revealed that α-defensin-1 binds to PTS1, but surprisingly even more pronounced to Gαi. To confirm that this interaction is independent of the N-terminal 6x His-tag present in Gαi and PTS1, His-tags were enzymatically removed. The same assay was conducted with the purified proteins and a comparable result was obtained (Figure 7a, middle row). Notably, α-defensin-1 is only bound to PTS1 but not the holotoxin PT in this assay.

As we detected an interaction of α-defensin-1 with PTS1, we then analyzed whether α-defensin-1 can inhibit NADase activity of PTS1 in the absence of Gαi (Figure 7b). NAD^+ was incubated with different concentrations of PTS1 with or without α-defensin-1 and the NAD^+ consumption was measured by a fluorometric end-point assay, i.e., chemical conversion of NAD^+ into a fluorescent molecule [40]. Except for causing higher NAD^+ readings in the control wells without PTS1, α-defensin-1 had no significant impact on NADase activity of PTS1 (Figure 7b). This is in agreement with our results, obtained by computational modeling, that α-defensin-1 should not occlude the NAD^+ binding site (Figure 6d).

In conclusion, α-defensin-1 and -5 both protect human cells from PT but use different molecular mechanisms to achieve this effect. While α-defensin-1 enters cells and neutralizes PT mainly by the inhibition of its enzyme activity, α-defensin-5 primarily inhibits the uptake of PT into cells.

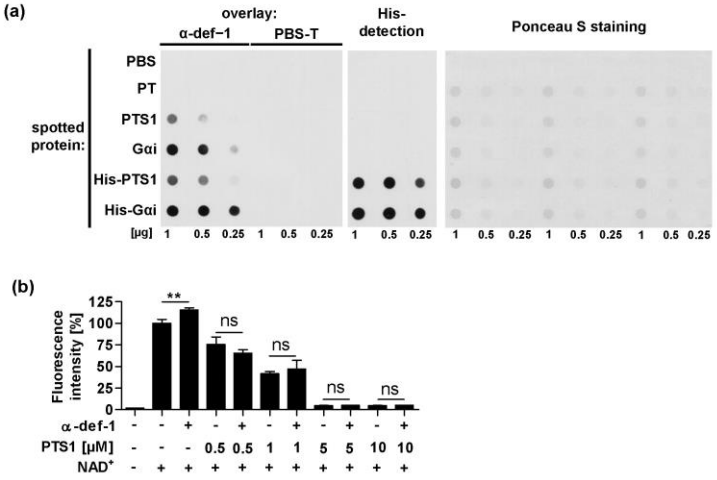

Figure 7. Interaction of α-defensin-1 with PTS1 and Gαi in vitro. (**a**) Dot blot assay. Decreasing amounts of proteins (1 µg, 0.5 µg, 0.25 µg) were spotted onto a membrane using the dot blot system. After blocking, the membrane was cut and probed with α-defensin-1 (0.4 µg/mL) or PBS-T for control. After extensive washing, bound α-defensin-1 was detected with an antibody against α-defensin-1 using the ECL system ((**left**) panel). The presence of the N-terminal 6x-His-tag was shown by an antibody against 6x-His-tag using the ECL system ((**middle**) panel). Comparable amounts of spotted protein were confirmed by Ponceau S staining ((**right**) panel). One representative blot of at least three independent experiments is shown. (**b**) NAD^+-quantitation assay. NAD^+ was incubated with PTS1 in increasing concentrations with or without α-defensin-1 in the absence of Gαi. Decrease in fluorescence is a measure of NAD^+-consuming enzymatic activity of PTS1, i.e., NAD^+ is chemically converted in the end-point assay into a fluorescent molecule. Values are given as percent of control with NAD^+ only, mean ± SD (n = 3 from one representative experiment out of three). Significance was tested using one-way ANOVA followed by Dunnett's multiple comparison test and refers to controls without α-defensin-1 (** $p \leq 0.01$, ns not significant).

3. Discussion

Pertussis is a severe disease with limited therapeutic options currently available [33,41]. Only during the early catarrhal stage of the disease, treatment with macrolide antibiotics is associated with an improvement of symptoms [42]. This presents a challenge as this stage occurs before the onset of the characteristic symptoms, such as whooping cough. Even though vaccination coverage is quite high, with ca. 81% of infants worldwide in 2021 [32], pertussis is still one of the leading causes of vaccine-preventable deaths and morbidity worldwide [43]. This precarious situation prompted us to investigate new therapeutic options against pertussis. In our approach, we directly target PT, which is a major contributor to pertussis pathology, including severe respiratory symptoms [21,29].

We demonstrated that α-defensin-1 and -5 both protect cells from intoxication with PT, though with different modes of inhibition. Uptake of PT into the cells is necessarily required for PT to reach its cellular target protein Gαi, and, therefore, to exert its mode of action. Inhibition by α-defensin-5 prevents this very first step of intoxication. In the presence of α-defensin-5, less PT was bound to the surface of cells, and less PT was taken up into cells. Contrarily, α-defensin-1 mainly inhibits the last step of PT intoxication, the enzymatic ADP-ribosylation of Gαi by PTS1. We showed that α-defensin-1 was taken up into cells, interacted with PTS1 in these cells and bound to PTS1 in-silico and in vitro. The predicted binding modes of α-defensin-1 and α-defensin-5 to PTS1 provide a rationale, at the molecular level, for the different experimental behaviors of the α-defensins 1 and 5.

The lack of a preferred binding interface in the α-defensin-5/PTS1 system, in contrast to the much favored and defined interactions of α-defensin-1 with PTS1, is in agreement with the experimental in vitro observation of α-defensin-1 as a stronger inhibitor of PTS1 with respect to α-defensin-5. These different modes of action might complement each other in a therapeutic context.

Human defensins contain six cysteine residues, which form three intramolecular disulfide bonds. Up to now, there are six different human α-defensins, which are classified based on their site of production: Human neutrophil peptides 1 to 4 (HNP 1–4 = α-defensin-1-4), found in primary granules of neutrophils, and human enteric defensins 5 and 6 (HD 5–6 = α-defensin-5-6) found in Paneth cells in the crypts of the small intestine. Notably, α-defensin-4 is found in neutrophils in substantially lower concentrations compared with α-defensin-1-3 [36], and α-defensin-1-3 only differ in their first out of 30 amino acid residues. In light of these observations and considering the lack of cellular protection from PT by α-defensin-6, we focused our investigations on α-defensin-1 and -5.

Defensins are mostly known for their antimicrobial activity. Like most antimicrobial peptides, the defensins interact and disrupt the lipid membranes of microbes, leading to their lysis [44]. In addition to their antimicrobial activity, human α-defensins inhibit several bacterial toxins with different modes of action. As an example, α-defensin-1 exhibited inhibitory effects on enzyme activity of *B. anthracis* lethal factor (LF) [45], *Diphtheria* toxin (DT) and *Pseudomonas* exotoxin A (ETA) [46]. α-Defensin-5 has been shown to neutralize *C. difficile* toxin A (TcdA) by the formation of inactive toxin–defensin aggregates and *C. difficile* transferase toxin (CDT) by influencing the binding and transport component [47]. However, α-defensin-5 had no influence on enzyme activity of TcdA or CDT. The pore formation of CDT by its B-component was impaired by α-defensin-1 and -5 [47,48], similar to the mechanism shown for *Clostridium perfringens* iota toxin [49]. Another reported mechanism of inhibition is the local unfolding of *V. cholerae* and *Aeromonas hydrophilia* MARTX effector domains, which leads to their thermal unfolding, increased susceptibility to proteolysis and precipitation, observed for α-defensin-1 and also to a lesser degree for α-defensin-5 [50]. PTS1 is also known to be thermally unstable, which is necessary for its transport from the ER to the cytosol [12], making this another conceivable inhibitory mechanism. A common mechanism of inhibition of bacterial toxins by α-defensins could not be determined so far.

Interestingly, α-defensin-1 was also shown to be a substrate for the human arginine-specific ADP-ribosyltransferase 1 (ART1) [51,52]. Consequently, we investigated whether α-defensin-1 might also be a substrate of PTS1. For this, α-defensin-1 was incubated with PTS1 for 40 min at room temperature and then analyzed by mass spectrometry. No ADP-ribosylation or any other modification of α-defensin-1 or α-defensin-5 by PTS1 was detected.

The small size of the defensins and their diverse beneficial effects make them promising candidates for drug development. Therapeutic peptides have gained significant attention over the last years, with nearly 20 new peptide-based clinical trials annually and over 60 peptide drugs already approved [53]. An advantage of their small size compared to antibodies or other proteins is their ability to bind deep into folding pockets of proteins and to reach cellular targets [53]. Furthermore, endogenous peptides, such as defensins are usually less immunogenic and therefore better tolerated by patients than foreign agents [41,53,54]. Our finding that α-defensin-1 is taken-up into all tested cell lines serves our aim of using it as a therapeutic drug reaching intracellular targets. This finding is in line with previous studies of other groups, which found that α-defensin-1 accumulates intracellularly in human cervical CaSki cells and inhibits human simplex virus, also post-entry [55] and is also taken up into bone marrow-derived macrophages [56]. While α-defensin-5, found in the intestine, does not physiologically come into contact with PT, which mainly acts in the respiratory tract, it might have therapeutic implications as an inhibitor of PT uptake into cells.

The identification of α-defensin-1 and -5 as inhibitors of PT and the characterization of their underlying mechanism of inhibition contributes to a better understanding of innate immune responses to PT. Our computational studies deliver a rationale for the mechanisms

of inhibition at the molecular level as well as an explanation for the different behaviors of α-defensin-1 with respect to α-defensin-5, based on their interactions with PTS1. Taken together, our findings will allow for the optimization of α-defensins as inhibitors of PT, paving the way for the development of novel therapeutic strategies against whooping cough.

4. Materials and Methods

4.1. Compounds and Reagents

Bordetella pertussis toxin (PT) was purchased from Sigma-Aldrich, Merck (Darmstadt, Germany). Recombinant Gαi and recombinant PTS1 were expressed and purified as described earlier (Ashok et al. [40]). The peptides α-defensin-1, -2, -3, -4, -5 and -6 and β-defensin-1 and -2 were purchased from PeptaNova (Sandhausen, Germany). Linearized α-defensin-1 and -5 (cysteine residues changed to serine residues in their amino acid sequence) were custom-made and purchased from PSL (Heidelberg, Germany). For the NADase activity assay, α-defensin-1 was purchased from ProteoGenix (Schiltigheim, France) and further refolded and purified (see Supplementary Material Figures S5 and S6).

4.2. Cell Lines

Materials for cell culture were all purchased from Gibco (Thermo Fisher Scientific, Waltham, MA, USA) unless indicated otherwise. A549 cells (human lung adenocarcinoma cells; ATCC® Manassas, VA, USA), CaCo-2 cells (human epithelial colorectal adenocarcinoma cells, HTB-37; ATCC, Manassas, VA, USA) and J774A.1 cells (murine macrophage-like cells; DSMZ, Braunschweig, Germany) were cultivated in DMEM, Vero cells (African green monkey kidney cells; DSMZ, Braunschweig, Germany) and HeLa cells (cervical carcinoma cells; DSMZ, Braunschweig, Germany) were cultivated in MEM. All media were supplemented with 10% FCS, 1 mM sodium pyruvate, 0.1 mM non-essential amino acids and 100 U/mL penicillin and 100 g/mL streptomycin. CHO-K1 cells (Chinese hamster ovary cells strain K1; DSMZ, Braunschweig, Germany) were cultivated in DMEM and HAM's F12 (1:1), supplemented with 5% FCS, 1 mM sodium pyruvate, 0.05 mM non-essential amino acids and 100 U/mL penicillin and 100 g/mL streptomycin. Cells were cultivated under humidified conditions at 37 °C with 5% CO_2 and trypsinized and reseeded every two to three days for at most 25 times. For intoxication experiments, cells were seeded in culture dishes one day before and treated in FCS-free media with PT and the respective compounds.

4.3. Sequential ADP-Ribosylation of Gαi in Lysates from Toxin-Treated Cells

Cells were seeded into 24-well plates and treated with PT and defensin or H_2O (solvent of defensins) as a control in FCS-free medium. After 4 h, cells were washed to remove unbound protein and frozen for cell lysis. ADP-ribosylation buffer (0.1 mM Tris-HCl (pH 7.6), 20 mM DTT, 0.1 µM ATP and protease inhibitor complete (Roche)) was added and cell lysates were transferred to reaction tubes. For sequential in vitro ADP-ribosylation of Gαi, which had not been modified by PT in the cells during intoxication, recombinant PTS1 (50 nM) and biotin-labeled NAD^+ (1 µM; R&D Systems, Abingdon, UK) were added and incubated for 40 min at room temperature. Then, samples were subjected to SDS-PAGE and Western blotting with streptavidin–peroxidase (Strep–POD, Sigma-Aldrich, Merck, Darmstadt, Germany) for detection of biotin-labeled and thus sequentially ADP-ribosylated Gαi. Quantification of signals was performed using ImageJ software v.1.52a (National Institutes of Health, Bethesda (NIH)). As a loading control, Hsp90 (primary antibody from Santa Cruz Biotechnology, Dallas, TX, USA) signals were detected.

4.4. In Vitro Enzyme Activity of PTS1

Recombinant PTS1 (50 nM = 1.17 µg/mL) was incubated with recombinant Gαi (0.5 µM = 20.2 µg/mL) and biotin-labeled NAD^+ (1 µM; R&D Systems) in a 50 nM sodium phosphate buffer (pH 7.0) in the presence of the respective defensin or H_2O as a control for 40 min at room temperature. After that, samples were subjected to SDS-PAGE and Western blot analysis with streptavidin-peroxidase (Strep-POD, Sigma-Aldrich, Darmstadt, Germany)

for detection of biotin-labeled and thus enzymatically modified Gαi. Quantification of signals was performed using ImageJ software v.1.52a (NIH). To control equal loading of samples, Ponceau-S-staining was used.

4.5. Flow Cytometry Binding Assay

Cells were detached from culture dishes using 25 mM EDTA in PBS and resuspended in FCS-free medium. The cells (1×10^5 in 0.2 mL per sample) were incubated with defensin and 488-labeled PT for 15 min on ice to allow binding of PT to cells but no internalization. Cells were washed twice by centrifugation to eliminate unbound 488-labeled PT. Fluorescence of cells was measured using a BD FACS Celesta™ flow cytometer (Becton, Dickinson and Company, Franklin Lakes, NJ, USA) and the BD FACSDiva™ software 8.0.1.1. DyLight488 excitation was performed with a blue laser (488 nm) and emitted fluorescence detected with a 530 nm (530/30) bandpass filter. Data analysis of gated cell populations was performed using Flowing Software v2.5.1. (Turku Centre of Biotechnology, Finland). PT was labeled with DyLight® 488 NHS Ester (Thermo Fisher Scientific, Rockford, IL, USA) according to the manufacturer's protocol and excess dye was removed with Zeba™ Spin Desalting Columns (7K MWCO, Thermo Fisher Scientific, Waltham, MA, USA).

4.6. Immunostaining and Fluorescence Microscopy

Cells were seeded in 8- or 18-well µ-slides (ibidi GmbH, Gräfelfing, Germany) and grown for one day. After respective treatments in FCS-free medium, cells were washed with PBS, fixed with 4% paraformaldehyde for 20 min, permeabilized with 0.4% (*v*/*v*) Triton X-100 in PBS for 5 min, quenched by glycine (100 mM in PBS) for 2 min and blocked with 10% NGS (Jackson ImmunoResearch, West Grove, PA, USA) and 1% BSA in PBS containing 0.1% Tween 20 (PBS-T) for 1 h at 37 °C. Subsequently, cells were incubated with primary antibodies (anti-PTS1, Santa Cruz; anti-PT, Abcam; anti-HNP and anti-α-defensin-5, Santa Cruz) and fluorescence labeled secondary antibodies in blocking solution each for 1 h at 37 °C. Nuclei were stained with Hoechst 33342 (1:10,000, Thermo Fisher Scientific, Waltham, MA, USA) for 5 min. Cells were washed with PBS-T in between individual steps. Images were obtained using an iMIC digital microscope (FEI Munich, Munich, Germany) and Live Acquisition 2.6 software (FEI Munich) and processed using ImageJ software v.1.52a (NIH).

4.7. Cell Viability Assay

CHO-K1 cells were seeded in 96-well plates and incubated with defensin or H_2O as a control for 24 h. DMSO (20%) was used as a positive control for causing cell death. Cell Titer 96® Aqueous One Solution (MTS assay, Promega, Walldorf, Germany) was then added to cells and incubated for 1 h at 37 °C to determine cell viability. Absorbance was measured at 490 nm via a microtiter plate reader.

4.8. Protein Interaction Analysis in Cells Using Proximity Ligation Assay

Cells were seeded in 18-well µ-slides (ibidi GmbH, Gräfelfing, Germany) and incubated with PT and defensin for 4 h at 37 °C. Afterwards, cells were washed with PBS, fixed with 4% PFA, permeabilized and blocked with 10% NGS and 1% BSA in PBS-T. Then, cells were incubated with rabbit anti-PT (Abcam) and mouse anti-HNP (= α-defensin-1) (Santa Cruz) or mouse anti-α-defensin-5 (Abcam) primary antibodies for 1 h at 37 °C. PLA was performed according to the manufacturer's protocol (Duolink using PLA technology, Sigma-Aldrich, Merck). In brief, cells were incubated with PLA secondary antibodies (anti-rabbit for detecting anti-PT and anti-mouse for detecting anti-defensin) having attached specific oligonucleotide sequences to each. If they get in close proximity, they can form a ring structure. By addition of ligase and polymerase, rolling circle amplification can occur. Samples were probed with fluorescence labeled oligonucleotides, complementary to the amplification product for detection of the protein interaction. PLA signals were counted from fluorescence images using ImageJ software v.1.52a (NIH).

4.9. In Silico Modeling of PTS1/Defensin Complexes

For the sequence-based predictions of interaction likelihood, the sequences of the recombinant PTS1, α-defensin-1, and α-defensin-5, were split into overlapping subsequences of 20 residues each. We used the PPI-Detect tool [37] as implemented in its web server (https://protdcal-suite.cbe.bci.tu-dortmund.de/ppi_detect/) (accessed on 12 May 2023) [57] for the predictions, considering the top-10 interacting sequence pairs inside the applicability domain (AD). The interacting sequence pairs were mapped onto the structure of PTS1 (PDB ID 7SNE [39]), α-defensin-1 (PDB ID 3GNY [58]), α-defensin-5 (PDB ID 1ZMP [59]).

PTS1/α-defensin-1 and PTS1/α-defensin-5 complexes were modeled with AlphaFold Multimer [38] using the sequences of recombinant PTS1, α-defensin-1 and α-defensin-5 as inputs. The best-scored model was then used for unbiased MD simulations where the center of masses of PTS1 and the defensins were 40 Å apart. Three different initial configurations were set for each defensin. The systems were solvated, using the TIP3P water model [60], in a cubic box with a minimum distance of 14 Å between the protein and the edge of the box. Periodic boundary conditions were applied. Na^+ and Cl^- ions were added to the box for neutralization and, in addition, to reach a concentration of 150 mM. The protein topology was set using the CHARMM36 force field [61]. The systems were minimized using a steepest descent algorithm [62] until the maximum force reached 100 kJ/mol.nm. Then, a two-step minimization, comprising a 200 ps equilibration step in the NVT ensemble, followed by 2 ns of equilibration in the NPT regime, was carried out. Protein heavy atoms were fixed during the equilibration using a 1000 kJ/mol force restraint. Finally, three replicas of 1.5 µs production MD simulations were performed without any restraints. The integration of Newton's equations of motion was performed using a leap-frog algorithm with a 2 fs time step [63]. The temperature and the pressure were maintained at 298 K and 1 bar by using the V-rescale temperature thermostat [64] and C-rescale barostat [65]. The bonds of the peptide and the osmolyte molecules were constrained by the LINCS algorithm [66]. The nonbonded Lennard–Jones interactions were cut-off at 12 Å. Electrostatic interactions were calculated using the particle mesh Ewald (PME) method [67] with a cut-off of 12 Å and a grid-spacing of 1.6 Å. All the runs were performed using the Gromacs 2022 package [68].

Trajectory frames were grouped into clusters using the Daura's et al., algorithm [69] with a RMSD cutoff of 5 Å. For each cluster, the structure with the smallest average RMSD from all other members of the cluster was selected as representative of the cluster. Contacts between PTS1 and the defensins were defined using a minimum distance cutoff of 4 Å between the atoms of both proteins. The contact frequency per residue was calculated as the number of frames where the residue is establishing contacts with the other protein divided by the total number of frames analyzed. The structures were visualized with Pymol 2.6 (PyMOL Molecular Graphics System, Version 2.6 Schrödinger, LLC).

4.10. Protein Interaction Analysis In Vitro Using Dot Blot System

Decreasing amounts of purified proteins were vacuum-aspirated onto a nitrocellulose membrane using the dot blot system (Bio-Rad, Feldkirchen, Germany) according to the manufacturer's instructions. Transfer of proteins was confirmed by Ponceau-S-staining. Then, the membrane was blocked with 5% skim milk powder in PBS-T. Membrane was cut and probed with defensin or PBS-T as a negative control for 1 h. After extensive washing (5 × 5 min), membrane was incubated with anti-HNP antibody and peroxidase-coupled anti-mouse antibody for detection of bound α-defensin-1 by using the ECL system. His-Tag was detected using anti-6x His antibody.

4.11. NADase Activity Assay

The 50 µL reactions were conducted in a flat bottom 96-well black plate (Greiner Bio-One, Polypropylene 96-well F-bottom Microplates, Fisher Scientific, Schwerte Germany) in 100 mM HEPES, 500 mM sodium chloride, 10% (*w*/*v*) glycerol, 0.5 mM TCEP (pH 7.5). The concentration of PTS1 was titrated at 0.5, 1, 5, and 10 µM while keeping the NAD^+ and α-defensin-1 concentrations constant at 10 µM and 12 µM, respectively. PTS1 was incubated

with α-defensin-1 for 15 min before addition of NAD^+ as the final reagent. The reactions were incubated for 1 h at room temperature with shaking at 300 rpm. To stop the reaction, and to convert the remaining NAD^+ to a fluorescent molecule, 20 µL of 2 M KOH and 20 µL of 20% acetophenone (Sigma, diluted with ethanol) were added, followed by incubation at room temperature for 10 min. Subsequently, 90 µL of formic acid (Fisher Scientific) was added, and the reaction mixture was further incubated for 20 min at room temperature. The fluorescence readings were recorded with the VICTOR Nivo multimode plate reader (PerkinElmer, Waltham, MA, USA), with excitation and emission wavelengths set at 355 nm (±20 nm) and 450 nm (±5 nm), respectively.

Supplementary Materials: The following supporting information can be downloaded at: https://www.mdpi.com/article/10.3390/ijms241310557/s1. Reference [70] is cited in the supplementary materials.

Author Contributions: Conceptualization, K.E.; data curation, Y.A.-H., J.A.P.-E., M.P.-M. and E.S.-G.; formal analysis, C.K., A.S., Y.A.-H., A.R., J.A.P.-E., R.B., L.S., S.W., M.P.-M. and E.S.-G.; funding acquisition, E.S.-G. and K.E.; investigation, C.K., A.S., Y.A.-H., A.R., J.A.P.-E., R.B. and M.P.-M.; methodology, C.K., Y.A.-H. and E.S.-G.; project administration, K.E.; resources, H.B., A.T.P. and E.S.-G.; supervision, E.S.-G. and K.E.; visualization, C.K., Y.A.-H., J.A.P.-E. and E.S.-G.; writing—original draft, C.K., Y.A.-H., E.S.-G., A.T.P. and K.E.; writing—review and editing, Y.A.-H., A.R., J.A.P.-E., L.S., S.W., H.B.,C.K., A.T.P., E.S.-G. and K.E. All authors have read and agreed to the published version of the manuscript.

Funding: This work was supported by the Deutsche Forschungsgemeinschaft (DFG, German Research Foundation)—project number 316249678-SFB1279 (A07, funding to K.E.; A06, funding to E.S.G.; C02, funding to H.B.; Z01, funding to A.R., L.S., S.W.). K.E. is a fellow of the Margarete von Wrangell Habilitation program supported by the European Social Fund and Ministry of Science, Research and Art Baden-Württemberg. C.K. is supported by a Ph.D. fellowship by Cusanuswerk and is a fellow of the International Graduate School in Molecular Medicine Ulm (IGradU). E.S.G. was funded by the Deutsche Forschungsgemeinschaft (DFG, German Research Foundation) under Germany's Excellence Strategy—EXC 2033—390677874—RESOLV. E.S.-G. acknowledges the DFG for major instrumentation granted under the DFG–Projektnummer 436586093. L.S. acknowledges funding by the DAAD/German Ministry for Foreign Affairs via the program Global Health and Pandemic Prevention Centers (project 57592717-GLACIER).

Institutional Review Board Statement: Not applicable.

Informed Consent Statement: Not applicable.

Data Availability Statement: The datasets generated during and/or analyzed during the current study are available from the corresponding author on reasonable request.

Acknowledgments: Merve Karacan and Carolin Weiss are thanked for their excellent technical assistance in the purification and analysis of α-defensin-1.

Conflicts of Interest: The authors declare no conflict of interest.

References

1. Stein, P.E.; Boodhoo, A.; Armstrong, G.D.; Cockle, S.A.; Klein, M.H.; Read, R.J. The Crystal Structure of Pertussis Toxin. *Structure* **1994**, *2*, 45–57. [PubMed]
2. Tamura, M.; Nogimori, K.; Murai, S.; Yajima, M.; Ito, K.; Katada, T.; Ui, M.; Ishii, S. Subunit Structure of Islet-Activating Protein, Pertussis Toxin, in Conformity with the A-B Model. *Biochemistry* **1982**, *21*, 5516–5522. [CrossRef] [PubMed]
3. Weiss, A.A.; Johnson, F.D.; Burns, D.L. Molecular Characterization of an Operon Required for Pertussis Toxin Secretion. *Proc. Natl. Acad. Sci. USA* **1993**, *90*, 2970–2974. [CrossRef] [PubMed]
4. Armstrong, G.D.; Howard, L.A.; Peppler, M.S. Use of Glycosyltransferases to Restore Pertussis Toxin Receptor Activity to Asialoagalactofetuin. *J. Biol. Chem.* **1988**, *263*, 8677–8684. [PubMed]
5. Witvliet, M.H.; Burns, D.L.; Brennan, M.J.; Poolman, J.T.; Manclark, C.R. Binding of Pertussis Toxin to Eucaryotic Cells and Glycoproteins. *Infect. Immun.* **1989**, *57*, 3324–3330. [CrossRef]
6. Plaut, R.D.; Carbonetti, N.H. Retrograde Transport of Pertussis Toxin in the Mammalian Cell. *Cell. Microbiol.* **2008**, *10*, 1130–1139. [CrossRef]
7. el Bayâ, A.; Linnemann, R.; von Olleschik-Elbheim, L.; Robenek, H.; Schmidt, M.A. Endocytosis and Retrograde Transport of Pertussis Toxin to the Golgi Complex as a Prerequisite for Cellular Intoxication. *Eur. J. Cell Biol.* **1997**, *73*, 40–48.

8. Burns, D.L.; Manclark, C.R. Adenine Nucleotides Promote Dissociation of Pertussis Toxin Subunits. *J. Biol. Chem.* **1986**, *261*, 4324–4327.
9. Hazes, B.; Boodhoo, A.; Cockle, S.A.; Read, R.J. Crystal Structure of the Pertussis Toxin-ATP Complex: A Molecular Sensor. *J. Mol. Biol.* **1996**, *258*, 661–671. [CrossRef]
10. Plaut, R.D.; Scanlon, K.M.; Taylor, M.; Teter, K.; Carbonetti, N.H. Intracellular Disassembly and Activity of Pertussis Toxin Require Interaction with ATP. *Pathog Dis* **2016**, *74*, ftw065. [CrossRef]
11. Banerjee, T.; Cilenti, L.; Taylor, M.; Showman, A.; Tatulian, S.A.; Teter, K. Thermal Unfolding of the Pertussis Toxin S1 Subunit Facilitates Toxin Translocation to the Cytosol by the Mechanism of Endoplasmic Reticulum-Associated Degradation. *Infect. Immun.* **2016**, *84*, 3388–3398. [CrossRef]
12. Pande, A.H.; Moe, D.; Jamnadas, M.; Tatulian, S.A.; Teter, K. The Pertussis Toxin S1 Subunit Is a Thermally Unstable Protein Susceptible to Degradation by the 20S Proteasome. *Biochemistry* **2006**, *45*, 13734–13740. [CrossRef]
13. Worthington, Z.E.V.; Carbonetti, N.H. Evading the Proteasome: Absence of Lysine Residues Contributes to Pertussis Toxin Activity by Evasion of Proteasome Degradation. *Infect. Immun.* **2007**, *75*, 2946–2953. [CrossRef]
14. Ernst, K.; Eberhardt, N.; Mittler, A.-K.; Sonnabend, M.; Anastasia, A.; Freisinger, S.; Schiene-Fischer, C.; Malešević, M.; Barth, H. Pharmacological Cyclophilin Inhibitors Prevent Intoxication of Mammalian Cells with Bordetella Pertussis Toxin. *Toxins* **2018**, *10*, 181. [CrossRef]
15. Ernst, K.; Mittler, A.-K.; Winkelmann, V.; Kling, C.; Eberhardt, N.; Anastasia, A.; Sonnabend, M.; Lochbaum, R.; Wirsching, J.; Sakari, M.; et al. Pharmacological Targeting of Host Chaperones Protects from Pertussis Toxin in Vitro and in Vivo. *Sci. Rep.* **2021**, *11*, 5429. [CrossRef]
16. Kellner, A.; Taylor, M.; Banerjee, T.; Britt, C.B.T.; Teter, K. A Binding Motif for Hsp90 in the A Chains of ADP-Ribosylating Toxins That Move from the Endoplasmic Reticulum to the Cytosol. *Cell. Microbiol.* **2019**, *21*, e13074. [CrossRef]
17. Kellner, A.; Cherubin, P.; Harper, J.K.; Teter, K. Proline Isomerization as a Key Determinant for Hsp90-Toxin Interactions. *Front. Cell. Infect. Microbiol.* **2021**, *11*, 771653. [CrossRef]
18. Ernst, K. Requirement of Peptidyl-Prolyl Cis/Trans Isomerases and Chaperones for Cellular Uptake of Bacterial AB-Type Toxins. *Front. Cell. Infect. Microbiol.* **2022**, *12*, 938015. [CrossRef]
19. Bokoch, G.M.; Katada, T.; Northup, J.K.; Hewlett, E.L.; Gilman, A.G. Identification of the Predominant Substrate for ADP-Ribosylation by Islet Activating Protein. *J. Biol. Chem.* **1983**, *258*, 2072–2075.
20. Katada, T.; Ui, M. Direct Modification of the Membrane Adenylate Cyclase System by Islet-Activating Protein Due to ADP-Ribosylation of a Membrane Protein. *Proc. Natl. Acad. Sci. USA* **1982**, *79*, 3129–3133.
21. Scanlon, K.; Skerry, C.; Carbonetti, N. Association of Pertussis Toxin with Severe Pertussis Disease. *Toxins* **2019**, *11*, 373. [CrossRef] [PubMed]
22. Toyota, T.; Kakizaki, M.; Kimura, K.; Yajima, M.; Okamoto, T.; Ui, M. Islet Activating Protein (IAP) Derived from the Culture Supernatant Fluid of Bordetella Pertussis: Effect on Spontaneous Diabetic Rats. *Diabetologia* **1978**, *14*, 319–323. [CrossRef] [PubMed]
23. Andreasen, C.; Carbonetti, N.H. Pertussis Toxin Inhibits Early Chemokine Production to Delay Neutrophil Recruitment in Response to Bordetella Pertussis Respiratory Tract Infection in Mice. *Infect. Immun.* **2008**, *76*, 5139–5148. [CrossRef]
24. Kirimanjeswara, G.S.; Agosto, L.M.; Kennett, M.J.; Bjornstad, O.N.; Harvill, E.T. Pertussis Toxin Inhibits Neutrophil Recruitment to Delay Antibody-Mediated Clearance of Bordetella Pertussis. *J. Clin. Investig.* **2005**, *115*, 3594–3601. [CrossRef]
25. Spangrude, G.J.; Sacchi, F.; Hill, H.R.; Van Epps, D.E.; Daynes, R.A. Inhibition of Lymphocyte and Neutrophil Chemotaxis by Pertussis Toxin. *J. Immunol.* **1985**, *135*, 4135–4143. [CrossRef] [PubMed]
26. Warnock, R.A.; Askari, S.; Butcher, E.C.; Andrian, U.H. von Molecular Mechanisms of Lymphocyte Homing to Peripheral Lymph Nodes. *J. Exp. Med.* **1998**, *187*, 205–216. [CrossRef]
27. Schenkel, A.R.; Pauza, C.D. Pertussis Toxin Treatment In Vivo Reduces Surface Expression of the Adhesion Integrin Leukocyte Function Antigen-1 (LFA-1). *Cell Adhes. Commun.* **1999**, *7*, 183–193. [CrossRef]
28. Mattoo, S.; Cherry, J.D. Molecular Pathogenesis, Epidemiology, and Clinical Manifestations of Respiratory Infections Due to Bordetella Pertussis and Other Bordetella Subspecies. *Clin. Microbiol. Rev.* **2005**, *18*, 326–382. [CrossRef]
29. Carbonetti, N.H. Contribution of Pertussis Toxin to the Pathogenesis of Pertussis Disease. *Pathog. Dis.* **2015**, *73*, ftv073. [CrossRef]
30. Surridge, J.; Segedin, E.R.; Grant, C.C. Pertussis Requiring Intensive Care. *Arch. Dis. Child* **2007**, *92*, 970–975. [CrossRef]
31. Yeung, K.H.T.; Duclos, P.; Nelson, E.A.S.; Hutubessy, R.C.W. An Update of the Global Burden of Pertussis in Children Younger than 5 Years: A Modelling Study. *Lancet Infect. Dis.* **2017**, *17*, 974–980. [CrossRef]
32. WHO Immunization Coverage. Available online: https://www.who.int/news-room/fact-sheets/detail/immunization-coverage (accessed on 15 June 2023).
33. Locht, C.; Antoine, R. The History of Pertussis Toxin. *Toxins* **2021**, *13*, 623. [CrossRef]
34. Connelly, C.E.; Sun, Y.; Carbonetti, N.H. Pertussis Toxin Exacerbates and Prolongs Airway Inflammatory Responses during Bordetella Pertussis Infection. *Infect. Immun.* **2012**, *80*, 4317–4332. [CrossRef]
35. Kling, C.; Pulliainen, A.T.; Barth, H.; Ernst, K. Human Peptides α-Defensin-1 and -5 Inhibit Pertussis Toxin. *Toxins* **2021**, *13*, 480. [CrossRef]
36. Cederlund, A.; Gudmundsson, G.H.; Agerberth, B. Antimicrobial Peptides Important in Innate Immunity. *FEBS J.* **2011**, *278*, 3942–3951. [CrossRef]
37. Romero-Molina, S.; Ruiz-Blanco, Y.B.; Harms, M.; Münch, J.; Sanchez-Garcia, E. PPI-Detect: A Support Vector Machine Model for Sequence-Based Prediction of Protein–Protein Interactions. *J. Comput. Chem.* **2019**, *40*, 1233–1242. [CrossRef]

38. Evans, R.; O'Neill, M.; Pritzel, A.; Antropova, N.; Senior, A.; Green, T.; Žídek, A.; Bates, R.; Blackwell, S.; Yim, J.; et al. Protein Complex Prediction with AlphaFold-Multimer. *bioRxiv* **2021**, arXiv:2021.10.04.463034.
39. Sakari, M.; Tran, M.T.; Rossjohn, J.; Pulliainen, A.T.; Beddoe, T.; Littler, D.R. Crystal Structures of Pertussis Toxin with NAD+ and Analogs Provide Structural Insights into the Mechanism of Its Cytosolic ADP-Ribosylation Activity. *J. Biol. Chem.* **2022**, *298*, 101892. [CrossRef]
40. Ashok, Y.; Miettinen, M.; de Oliveira, D.K.H.; Tamirat, M.Z.; Näreoja, K.; Tiwari, A.; Hottiger, M.O.; Johnson, M.S.; Lehtiö, L.; Pulliainen, A.T. Discovery of Compounds Inhibiting the ADP-Ribosyltransferase Activity of Pertussis Toxin. *ACS Infect. Dis.* **2020**, *6*, 588–602. [CrossRef]
41. Ernst, K. Novel Strategies to Inhibit Pertussis Toxin. *Toxins* **2022**, *14*, 187. [CrossRef]
42. Altunaiji, S.; Kukuruzovic, R.; Curtis, N.; Massie, J. Antibiotics for Whooping Cough (Pertussis). *Cochrane Database Syst. Rev.* **2007**, *3*, CD004404. [CrossRef]
43. De Graaf, H.; Ibrahim, M.; Hill, A.R.; Gbesemete, D.; Vaughan, A.T.; Gorringe, A.; Preston, A.; Buisman, A.M.; Faust, S.N.; Kester, K.E.; et al. Controlled Human Infection with Bordetella Pertussis Induces Asymptomatic, Immunizing Colonization. *Clin. Infect. Dis.* **2020**, *71*, 403–411. [CrossRef] [PubMed]
44. Lehrer, R.I.; Barton, A.; Daher, K.A.; Harwig, S.S.; Ganz, T.; Selsted, M.E. Interaction of Human Defensins with Escherichia Coli. Mechanism of Bactericidal Activity. *J. Clin. Investig.* **1989**, *84*, 553–561. [CrossRef] [PubMed]
45. Kim, C.; Gajendran, N.; Mittrücker, H.-W.; Weiwad, M.; Song, Y.-H.; Hurwitz, R.; Wilmanns, M.; Fischer, G.; Kaufmann, S.H.E. Human α-Defensins Neutralize Anthrax Lethal Toxin and Protect against Its Fatal Consequences. *Proc. Natl. Acad. Sci. USA* **2005**, *102*, 4830–4835. [CrossRef] [PubMed]
46. Kim, C.; Slavinskaya, Z.; Merrill, A.R.; Kaufmann, S.H.E. Human α-Defensins Neutralize Toxins of the Mono-ADP-Ribosyltransferase Family. *Biochem. J.* **2006**, *399*, 225–229. [CrossRef] [PubMed]
47. Korbmacher, M.; Fischer, S.; Landenberger, M.; Papatheodorou, P.; Aktories, K.; Barth, H. Human α-Defensin-5 Efficiently Neutralizes Clostridioides Difficile Toxins TcdA, TcdB, and CDT. *Front. Pharmacol.* **2020**, *11*, 1204. [CrossRef]
48. Fischer, S.; Ückert, A.-K.; Landenberger, M.; Papatheodorou, P.; Hoffmann-Richter, C.; Mittler, A.-K.; Ziener, U.; Hägele, M.; Schwan, C.; Müller, M.; et al. Human Peptide α-Defensin-1 Interferes with Clostridioides Difficile Toxins TcdA, TcdB, and CDT. *FASEB J.* **2020**, *34*, 6244–6261. [CrossRef]
49. Fischer, S.; Popoff, M.R.; Barth, H. Human Alpha-Defensin-1 Protects Cells from Intoxication with Clostridium Perfringens Iota Toxin. *Pathog. Dis.* **2018**, *76*, fty022. [CrossRef]
50. Kudryashova, E.; Quintyn, R.; Seveau, S.; Lu, W.; Wysocki, V.H.; Kudryashov, D.S. Human Defensins Facilitate Local Unfolding of Thermodynamically Unstable Regions of Bacterial Protein Toxins. *Immunity* **2014**, *41*, 709–721. [CrossRef]
51. Castagnini, M.; Picchianti, M.; Talluri, E.; Biagini, M.; Del Vecchio, M.; Di Procolo, P.; Norais, N.; Nardi-Dei, V.; Balducci, E. Arginine-Specific Mono ADP-Ribosylation in Vitro of Antimicrobial Peptides by ADP-Ribosylating Toxins. *PLoS ONE* **2012**, *7*, e41417. [CrossRef]
52. Paone, G.; Wada, A.; Stevens, L.A.; Matin, A.; Hirayama, T.; Levine, R.L.; Moss, J. ADP Ribosylation of Human Neutrophil Peptide-1 Regulates Its Biological Properties. *Proc. Natl. Acad. Sci. USA* **2002**, *99*, 8231–8235. [CrossRef]
53. Lee, A.C.-L.; Harris, J.L.; Khanna, K.K.; Hong, J.-H. A Comprehensive Review on Current Advances in Peptide Drug Development and Design. *Int. J. Mol. Sci.* **2019**, *20*, E2383. [CrossRef]
54. Bosso, M.; Ständker, L.; Kirchhoff, F.; Münch, J. Exploiting the Human Peptidome for Novel Antimicrobial and Anticancer Agents. *Bioorg. Med. Chem.* **2018**, *26*, 2719–2726. [CrossRef]
55. Hazrati, E.; Galen, B.; Lu, W.; Wang, W.; Ouyang, Y.; Keller, M.J.; Lehrer, R.I.; Herold, B.C. Human α- and β-Defensins Block Multiple Steps in Herpes Simplex Virus Infection1. *J. Immunol.* **2006**, *177*, 8658–8666. [CrossRef]
56. Arnett, E.; Lehrer, R.I.; Pratikhya, P.; Lu, W.; Seveau, S. Defensins Enable Macrophages to Inhibit the Intracellular Proliferation of Listeria Monocytogenes. *Cell. Microbiol.* **2011**, *13*, 635–651. [CrossRef]
57. Romero-Molina, S.; Ruiz-Blanco, Y.B.; Green, J.R.; Sanchez-Garcia, E. ProtDCal-Suite: A Web Server for the Numerical Codification and Functional Analysis of Proteins. *Protein Sci.* **2019**, *28*, 1734–1743. [CrossRef]
58. Wei, G.; de Leeuw, E.; Pazgier, M.; Yuan, W.; Zou, G.; Wang, J.; Ericksen, B.; Lu, W.-Y.; Lehrer, R.I.; Lu, W. Through the Looking Glass, Mechanistic Insights from Enantiomeric Human Defensins. *J. Biol. Chem.* **2009**, *284*, 29180–29192. [CrossRef]
59. Szyk, A.; Wu, Z.; Tucker, K.; Yang, D.; Lu, W.; Lubkowski, J. Crystal Structures of Human α-Defensins HNP4, HD5, and HD6. *Protein Sci.* **2006**, *15*, 2749–2760. [CrossRef]
60. MacKerell, A.D., Jr.; Bashford, D.; Bellott, M.; Dunbrack, R.L., Jr.; Evanseck, J.D.; Field, M.J.; Fischer, S.; Gao, J.; Guo, H.; Ha, S.; et al. All-Atom Empirical Potential for Molecular Modeling and Dynamics Studies of Proteins. *J. Phys. Chem. B* **1998**, *102*, 3586–3616. [CrossRef]
61. Huang, J.; MacKerell Jr, A.D. CHARMM36 All-Atom Additive Protein Force Field: Validation Based on Comparison to NMR Data. *J. Comput. Chem.* **2013**, *34*, 2135–2145. [CrossRef]
62. Haug, E.J.; Arora, J.S.; Matsui, K. A Steepest-Descent Method for Optimization of Mechanical Systems. *J. Optim. Theory Appl.* **1976**, *19*, 401–424. [CrossRef]
63. Verlet, L. Computer "Experiments" on Classical Fluids. I. Thermodynamical Properties of Lennard-Jones Molecules. *Phys. Rev.* **1967**, *159*, 98–103. [CrossRef]
64. Bussi, G.; Donadio, D.; Parrinello, M. Canonical Sampling through Velocity Rescaling. *J. Chem. Phys.* **2007**, *126*, 014101. [CrossRef] [PubMed]

65. Bernetti, M.; Bussi, G. Pressure Control Using Stochastic Cell Rescaling. *J. Chem. Phys.* **2020**, *153*, 114107. [CrossRef]
66. Hess, B.; Bekker, H.; Berendsen, H.J.C.; Fraaije, J.G.E.M. LINCS: A Linear Constraint Solver for Molecular Simulations. *J. Comput. Chem.* **1997**, *18*, 1463–1472. [CrossRef]
67. Darden, T.; York, D.; Pedersen, L. Particle Mesh Ewald: An N·log(N) Method for Ewald Sums in Large Systems. *J. Chem. Phys.* **1993**, *98*, 10089–10092. [CrossRef]
68. Abraham, M.J.; Murtola, T.; Schulz, R.; Páll, S.; Smith, J.C.; Hess, B.; Lindahl, E. GROMACS: High Performance Molecular Simulations through Multi-Level Parallelism from Laptops to Supercomputers. *SoftwareX* **2015**, *1–2*, 19–25. [CrossRef]
69. Daura, X.; Gademann, K.; Jaun, B.; Seebach, D.; van Gunsteren, W.F.; Mark, A.E. Peptide Folding: When Simulation Meets Experiment. *Angew. Chem. Int. Ed.* **1999**, *38*, 236–240. [CrossRef]
70. Vicente, F.E.M.; González-Garcia, M.; Diaz Pico, E.; Moreno-Castillo, E.; Garay, H.E.; Rosi, P.E.; Jimenez, A.M.; Campos-Delgado, J.A.; Rivera, D.G.; Chinea, G.; et al. Design of a Helical-Stabilized, Cyclic, and Nontoxic Analogue of the Peptide Cm-P5 with Improved Antifungal Activity. *ACS Omega* **2019**, *4*, 19081–19095. [CrossRef]

Disclaimer/Publisher's Note: The statements, opinions and data contained in all publications are solely those of the individual author(s) and contributor(s) and not of MDPI and/or the editor(s). MDPI and/or the editor(s) disclaim responsibility for any injury to people or property resulting from any ideas, methods, instructions or products referred to in the content.

3 Summary

Pertussis, also known as whooping cough, is a contagious respiratory disease, caused by a bacterial infection with *Bordetella pertussis*. Pertussis is characterized by paroxysmal coughing, which can lead to severe complications and even death, especially in newborns and infants. Pertussis toxin (PT), secreted by the bacteria, plays a crucial role in causing the disease and particularly in driving its more severe manifestations. As an AB-type toxin, the B-subunit facilitates binding of PT to cellular receptors, followed by receptor-mediated endocytosis. Inside the cell, PT follows a retrograde vesicular transport through the Golgi into the ER. There, the A-subunit PTS1 dissociates from the holotoxin and is translocated into the cytosol. In the cytosol, PTS1 enzymatically transfers an ADP-ribose moiety to its substrate Gαi, an inhibitory α-subunit of G-protein, regulating the adenylyl cyclase. Thus, PT intoxication leads to disturbed cellular cAMP signaling. Current therapy of pertussis includes symptomatic treatment, which cannot tackle the underlying cause of the disease, the toxins. Furthermore, antibiotics are administered to eradicate the bacteria, yet the already secreted toxins still carry out their toxic effects. Therefore, this thesis aimed at identifying and characterizing novel approaches to inhibit PT as a major virulence factor causing the disease. On the one hand, cellular chaperones and protein folding helper enzymes were investigated, as they are hypothesized to support the cellular uptake of different toxins. The specific pharmacological small molecule inhibitors of Hsp90, Hsp70, Cyps and FKBPs, which are Rad, VER, CsA and FK506 were found to protect cells from PT intoxication, most likely by preventing the translocation step of PTS1 from the ER into the cytosol. On the other hand, defensins, which are antimicrobial peptides, were investigated as novel inhibitors of PT. The human peptides α-defensin-1 and -5 were demonstrated to protect cells from PT intoxication, employing distinct mechanisms of inhibition. While α-defensin-5 prevents uptake of PT into cells, α-defensin-1 inhibits the ADP-ribosylation of Gαi inside the cells. These different classes of inhibitors and modes of inhibition have the potential to complement each other in a therapeutic context. Taken together, this thesis provides a stepping stone and paves the way for the optimization and development of novel therapeutic strategies against the life-threatening disease pertussis.

4 References

Althouse, B. M., & Scarpino, S. V. (2015). Asymptomatic transmission and the resurgence of Bordetella pertussis. *BMC Medicine*, *13*.

Altunaiji, S., Kukuruzovic, R., Curtis, N., & Massie, J. (2007). Antibiotics for whooping cough (pertussis). *Cochrane Database of Systematic Reviews*, *3*.

Andreasen, C., & Carbonetti, N. H. (2008). Pertussis toxin inhibits early chemokine production to delay neutrophil recruitment in response to Bordetella pertussis respiratory tract infection in mice. *Infection and Immunity*, *76*, 5139–5148.

Armstrong, G. D., Howard, L. A., & Peppler, M. S. (1988). Use of Glycosyltransferases to Restore Pertussis Toxin Receptor Activity to Asialoagalactofetuin. *The Journal of Biological Chemistry*, *263*, 8677–8684.

Arndt, V., Rogon, C., & Höhfeld, J. (2007). To be, or not to be - Molecular chaperones in protein degradation. *Cellular and Molecular Life Sciences*, *64*, 2525–2541.

Banerjee, T., Cilenti, L., Taylor, M., Showman, A., Tatulian, S. A., & Teter, K. (2016). Thermal unfolding of the pertussis toxin S1 subunit facilitates toxin translocation to the cytosol by the mechanism of endoplasmic reticulum-associated degradation. *Infection and Immunity*, *84*, 3388–3398.

Barthold, L., Heber, S., Schmidt, C. Q., Gradl, M., Weidinger, G., Barth, H., & Fischer, S. (2022). Human α-Defensin-6 Neutralizes Clostridioides difficile Toxins TcdA and TcdB by Direct Binding. *International Journal of Molecular Sciences*, *23*, 4509.

Biebl, M. M., & Buchner, J. (2019). Structure, function, and regulation of the hsp90 machinery. *Cold Spring Harbor Perspectives in Biology*, *11*, a034017.

Bokoch, G. M., Katada, T., Northup, J. K., Hewlett, E. L., & Gilman, A. G. (1983). Identification of the predominant substrate for ADP-ribosylation by islet activating protein. *Journal of Biological Chemistry*, *258*, 2072–2075.

Bosso, M., Ständker, L., Kirchhoff, F., & Münch, J. (2018). Exploiting the human peptidome for novel antimicrobial and anticancer agents. *Bioorganic and Medicinal Chemistry*, *26*, 2719–2726.

Burns, D. L., & Manclark, C. R. (1986). Adenine nucleotides promote dissociation of pertussis toxin subunits. *Journal of Biological Chemistry*, *261*, 4324–4327.

Burress, H., Kellner, A., Guyette, J., Tatulian, S. A., & Teter, K. (2019). HSC70 and HSP90 chaperones perform complementary roles in translocation of the cholera toxin A1 subunit from the endoplasmic reticulum to the cytosol. *Journal of Biological Chemistry*, *294*, 12122–12131.

Burress, H., Taylor, M., Banerjee, T., Tatulian, S. A., & Teter, K. (2014). Co- and post-translocation roles for HSP90 in cholera intoxication. *Journal of Biological Chemistry*, *289*, 33644–33654.

Carbonetti, N. H. (2010). Pertussis toxin and adenylate cyclase toxin: Key virulence factors of Bordetella pertussis and cell biology tools. *Future Microbiology*, *5*, 455–469.

Carbonetti, N. H. (2015). Contribution of pertussis toxin to the pathogenesis of pertussis disease. *Pathogens and Disease*, *73*, ftv073.

Carbonetti, N. H. (2016). Bordetella pertussis: New concepts in pathogenesis and treatment. *Current Opinion in Infectious Diseases*, *29*, 287–294.

Cardot-Martin, E., Casalegno, J. S., Badiou, C., Dauwalder, O., Keller, D., Prévost, G., Rieg, S., Kern, W. V., Cuerq, C., Etienne, J., Vandenesch, F., Lina, G., & Dumitrescu, O. (2015). alpha-Defensins partially protect human neutrophils against Panton-Valentine leukocidin produced by *Staphylococcus aureus*. *Letters in Applied Microbiology*, *61*, 158–164.

Cederlund, A., Gudmundsson, G. H., & Agerberth, B. (2011). Antimicrobial peptides important in innate immunity. *FEBS Journal*, *278*, 3942–3951.

Chiappini, E., Stival, A., Galli, L., & de Martino, M. (2013). Pertussis re-emergence in the post-vaccination era. *BMC Infectious Diseases*, *13*.

Clerico, E., Tilitsky, J., Meng, W., & Gierasch, L. (2015). How Hsp70 molecular machines interact with their substrates to mediate diverse physiological functions. *Journal of Molecular Biology*, *427*, 1575–1588.

Connelly, C. E., Sun, Y., & Carbonetti, N. H. (2012). Pertussis toxin exacerbates and prolongs airway inflammatory responses during bordetella pertussis infection. *Infection and Immunity*, *80*, 4317–4332.

de Graaf, H., Ibrahim, M., Hill, A. R., Gbesemete, D., Vaughan, A. T., Gorringe, A., Preston, A., Buisman, A. M., Faust, S. N., Kester, K. E., Berbers, G. A. M., Diavatopoulos, D. A., & Read, R. C. (2020). Controlled human infection with Bordetella pertussis induces asymptomatic, immunizing colonization. *Clinical Infectious Diseases*, *71*, 403–411.

Dhingra, K., Valero, V., Gutierrez, L., Theriault, R., Booser, D., Holmes, F., Buzdar, A., Fraschini, G., & Hortobagyi, G. (1994). Phase II study of deoxyspergualin in metastatic breast cancer. *Investigational New Drugs.*, *12*, 235–241.

Dmochewitz, L., Lillich, M., Kaiser, E., Jennings, L. D., Lang, A. E., Buchner, J., Fischer, G., Aktories, K., Collier, R. J., & Barth, H. (2011). Role of CypA and Hsp90 in membrane translocation mediated by anthrax protective antigen. *Cellular Microbiology*, *13*, 359–373.

el Bayâ, A., Linnemann, R., von Olleschik-Elbheim, L., Robenek, H., & Schmidt, M. (1997). Endocytosis and retrograde transport of pertussis toxin to the Golgi complex as a prerequisite for cellular intoxication. *European Journal of Cell Biology*, *73*, 40–48.

Ernst, K. (2022a). Novel Strategies to Inhibit Pertussis Toxin. *Toxins*, *14*, 187.

Ernst, K. (2022b). Requirement of Peptidyl-Prolyl Cis/Trans isomerases and chaperones for cellular uptake of bacterial AB-type toxins. *Frontiers in Cellular and Infection Microbiology*, *12*, 938015.

Ernst, K., Eberhardt, N., Mittler, A. K., Sonnabend, M., Anastasia, A., Freisinger, S., Schiene-Fischer, C., Malešević, M., & Barth, H. (2018). Pharmacological cyclophilin inhibitors prevent intoxication of mammalian cells with Bordetella pertussis toxin. *Toxins*, *10*, 181.

Ernst, K., Kling, C., Landenberger, M., & Barth, H. (2018). Combined Pharmacological Inhibition of Cyclophilins, FK506-Binding Proteins, Hsp90, and Hsp70 Protects Cells From Clostridium botulinum C2 Toxin. *Frontiers in Pharmacology*, *9*, 1287.

Ernst, K., Langer, S., Kaiser, E., Osseforth, C., Michaelis, J., Popoff, M. R., Schwan, C., Aktories, K., Kahlert, V., Malesevic, M., Schiene-Fischer, C., & Barth, H. (2015). Cyclophilin-facilitated membrane translocation as pharmacological target to prevent intoxication of mammalian cells by binary clostridial actin ADP-ribosylated toxins. *Journal of Molecular Biology*, *427*, 1224–1238.

Ernst, K., Liebscher, M., Mathea, S., Granzhan, A., Schmid, J., Popoff, M. R., Ihmels, H., Barth, H., & Schiene-Fischer, C. (2016). A novel Hsp70 inhibitor prevents cell intoxication with the actin ADP-ribosylating Clostridium perfringens iota toxin. *Scientific Reports*, *6*, 1–17.

Ernst, K., Mittler, A. K., Winkelmann, V., Kling, C., Eberhardt, N., Anastasia, A., Sonnabend, M., Lochbaum, R., Wirsching, J., Sakari, M., Pulliainen, A. T., Skerry, C., Carbonetti, N. H., Frick, M., & Barth, H. (2021). Pharmacological targeting of host chaperones protects from pertussis toxin in vitro and in vivo. *Scientific Reports*, *11*, 5429.

Ernst, K., Sailer, J., Braune, M., & Barth, H. (2021). Intoxication of mammalian cells with binary clostridial enterotoxins is inhibited by the combination of pharmacological chaperone inhibitors. *Naunyn-Schmiedeberg's Archives of Pharmacology*, *394*, 941–954.

Ernst, K., Schmid, J., Beck, M., Hägele, M., Hohwieler, M., Hauff, P., Ückert, A., Anastasia, A., Fauler, M., Jank, T., Aktories, K., Popoff, M. R., Schiene-Fischer, C., Kleger, A., Müller, M., Frick, M., & Barth, H. (2017). Hsp70 facilitates trans-membrane transport of bacterial ADP-ribosylating toxins into the cytosol of mammalian cells. *Scientific Reports*, *7*, 1–16.

Ernst, K., Schnell, L., & Barth, H. (2017). Host cell chaperones Hsp70/Hsp90 and peptidyl-prolyl cis/trans isomerases are required for the membrane translocation of bacterial ADP-ribosylating toxins. *Curr Top Microbiol Immunol.*, *406*, 163–198.

Fischer, S., Popoff, M. R., & Barth, H. (2018). Human alpha-defensin-1 protects cells from intoxication with Clostridium perfringens iota toxin. *Pathogens and Disease*, *76*, 1–10.

Fischer, S., Ückert, A. K., Landenberger, M., Papatheodorou, P., Hoffmann-Richter, C., Mittler, A. K., Ziener, U., Hägele, M., Schwan, C., Müller, M., Kleger, A., Benz, R., Popoff, M. R., Aktories, K., & Barth, H. (2020). Human peptide α-defensin-1 interferes with Clostridioides difficile toxins TcdA, TcdB, and CDT. *FASEB Journal*, *34*, 6244–6261.

Fruman, D. A., Burakoff, S. J., & Bierer, B. E. (1994). Immunophilins in protein folding and immunosuppression. *FASEB J.*, *8*, 391–400.

Ganz, T. (2003). Defensins: Antimicrobial peptides of innate immunity. *Nature Reviews Immunology*, *3*, 710–720.

Ganz, T., Selsted, M. E., Szklarek, D., Harwig, S. S., Daher, K., Bainton, D. F., & Lehrer, R. I. (1985). Defensins. Natural peptide antibiotics of human neutrophils. *Journal of Clinical Investigation*, *76*, 1427–1435.

Giesemann, T., Guttenberg, G., & Aktories, K. (2008). Human α-Defensins Inhibit Clostridium difficile Toxin B. *Gastroenterology*, *134*, 2049–2058.

Göthel, S. F., & Marahiel, M. A. (1999). Peptidyl-prolyl cis-trams isomerases, a superfamily of ubiquitous folding catalysts. *Cellular and Molecular Life Sciences*, *55*, 423–436.

Handschuhmacher, R., Harding, M., Rice, J., Drugge, R., & Speicher, D. (1984). Cyclophilin: A Specific Cytosolic Binding Protein for Cyclosporin A. *Science*, *226*, 544–547.

Harding, M. W., Galat, A., Uehling, D. E., & Schreiber, S. L. (1989). A receptor for the immuno-suppressant FK506 is a cis–trans peptidyl-prolyl isomerase. *Nature*, *341*, 758–760.

Haug, G., Aktories, K., & Barth, H. (2004). The Host Cell Chaperone Hsp90 Is Necessary for Cytotoxic Action of the Binary Iota-Like Toxins. *Infection and Immunity*, *72*, 3066–3068.

Haug, G., Leemhuis, J., Tiemann, D., Meyer, D. K., Aktories, K., & Barth, H. (2003). The host cell chaperone Hsp90 is essential for translocation of the binary Clostridium botulinum C2 toxin into the cytosol. *Journal of Biological Chemistry*, *278*, 32266–32274.

Hausman, S. Z., & Burns, D. L. (1993). Binding of pertussis toxin to lipid vesicles containing glycolipids. *Infection and Immunity*, *61*, 335–337.

Hazes, B., Boodhoo, A., Cockle, S. A., & Read, R. J. (1996). Crystal Structure of the Pertussis Toxin-ATP Complex: A Molecular Sensor. *Journal of Molecular Biology*, *258*, 661–671.

Jia, J., Braune-Yan, M., Lietz, S., Wahba, M., Pulliainen, A. T., Barth, H., & Ernst, K. (2023). Domperidone Inhibits Clostridium botulinum C2 Toxin and Bordetella pertussis Toxin. *Toxins*, *15*, 412.

Kaiser, E., Böhm, N., Ernst, K., Langer, S., Schwan, C., Aktories, K., Popoff, M., Fischer, G., & Barth, H. (2012). FK506-binding protein 51 interacts with Clostridium botulinum C2 toxin and FK506 inhibits membrane translocation of the toxin in mammalian cells. *Cellular Microbiology*, *14*, 1193–1205.

Kaiser, E., Kroll, C., Ernst, K., Schwan, C., Popoff, M., Fischer, G., Buchner, J., Aktories, K., & Barth, H. (2011). Membrane translocation of binary actin-ADP-ribosylating toxins from Clostridium difficile and Clostridium perfringens Is facilitated by Cyclophilin A and Hsp90. *Infection and Immunity*, *79*, 3913–3921.

Kaiser, E., Pust, S., Kroll, C., & Barth, H. (2009). Cyclophilin A facilitates translocation of the Clostridium botulinum C2 toxin across membranes of acidified endosomes into the cytosol of mammalian cells. *Cellular Microbiology*, *11*, 780–795.

Katada, T., & Ui, M. (1982). Direct modification of the membrane adenylate cyclase system by islet-activating protein due to ADP-ribosylation of a membrane protein. *Proceedings of the National Academy of Sciences of the United States of America*, *79*, 3129–3133.

Kellner, A., Cherubin, P., Harper, J. K., & Teter, K. (2021). Proline Isomerization as a Key Determinant for Hsp90-Toxin Interactions. *Frontiers in Cellular and Infection Microbiology*, *11*, 771653.

Kellner, A., Taylor, M., Banerjee, T., Britt, C. B. T., & Teter, K. (2019). A binding motif for Hsp90 in the A chains of ADP-ribosylating toxins that move from the endoplasmic reticulum to the cytosol. *Cellular Microbiology*, *21*, e13074.

Kilgore, P. E., Salim, A. M., Zervos, M. J., & Schmitt, H. (2016). Pertussis : Microbiology , Disease , Treatment , and Prevention. *Clinical Microbiology Reviews*, *29*, 449–486.

Kim, C., Gajendran, N., Mittrü, H.-W., Weiwad, M., Song, Y.-H., Hurwitz, R., Wilmanns, M., Fischer, G., & Kaufmann, S. H. E. (2005). Human-defensins neutralize anthrax lethal toxin and protect against its fatal consequences. *Proceedings of the National Academy of Sciences of the United States of America*, *102*, 4830–4835. www.pnas.orgcgidoi10.1073pnas.0500508102

Kim, C., Slavinskaya, Z., Merrill, A. R., & Kaufmann, S. H. E. (2006). Human α-defensins neutralize toxins of the mono-ADP- ribosyltransferase family. *Biochemical Journal*, *399*, 225–229.

Kirimanjeswara, G. S., Agosto, L. M., Kennett, M. J., Bjornstad, O. N., & Harvill, E. T. (2005). Pertussis toxin inhibits neutrophil recruitment to delay antibody-mediated clearance of Bordetella pertussis. *Journal of Clinical Investigation*, *115*, 3594–3601.

Kling, C., Pulliainen, A. T., Barth, H., & Ernst, K. (2021). Human Peptides α-Defensin-1 and -5 Inhibit Pertussis Toxin. *Toxins*, 1–12.

Kling, C., Sommer, A., Almeida-Hernandez, Y., Rodríguez, A., Perez-Erviti, J. A., Bhadane, R., Ständker, L., Wiese, S., Barth, H., Pupo-Meriño, M., Pulliainen, A. T., Sánchez-García, E., & Ernst, K. (2023). Inhibition of Pertussis Toxin by Human α-Defensins-1 and -5: Differential Mechanisms of Action. *International Journal of Molecular Sciences*, *24*, 10557.

Korbmacher, M., Fischer, S., Landenberger, M., Papatheodorou, P., Aktories, K., & Barth, H. (2020). Human α-Defensin-5 Efficiently Neutralizes Clostridioides difficile Toxins TcdA, TcdB, and CDT. *Frontiers in Pharmacology*, *11*, 1–10.

Kovalainen, M., Mönkäre, J., Riikonen, J., Pesonen, U., Vlasova, M., Salonen, J., Lehto, V.-P., Järvinen, K., & Herzig, K.-H. (2015). Novel Delivery Systems for Improving the Clinical Use of Peptides. *Pharmacological Reviews*, *67*, 541–561.

Kudryashova, E., Quintyn, R., Seveau, S., Lu, W., Wysocki, V. H., & Kudryashov, D. S. (2014). Human defensins facilitate local unfolding of thermodynamically unstable regions of bacterial protein toxins. *Immunity*, *41*, 709–721.

Kudryashova, E., Seveau, S. M., & Kudryashov, D. S. (2017). Targeting and inactivation of bacterial toxins by human defensins. *Biological Chemistry*, *398*, 1069–1085.

Kügler, S., Böcker, K., Heusipp, G., Greune, L., Kim, K. S., & Schmidt, M. A. (2007). Pertussis toxin transiently affects barrier integrity, organelle organization and transmigration of monocytes in a human brain microvascular endothelial cell barrier model. *Cellular Microbiology*, *9*, 619–632.

Lau, J. L., & Dunn, M. K. (2018). Therapeutic peptides: Historical perspectives, current development trends, and future directions. *Bioorganic and Medicinal Chemistry*, *26*, 2700–2707.

Lee, A. C. L., Harris, J. L., Khanna, K. K., & Hong, J. H. (2019). A comprehensive review on current advances in peptide drug development and design. *International Journal of Molecular Sciences*, *20*, 2383.

Lehrer, R. I., Jung, G., Ruchala, P., Wang, W., Micewicz, E. D., Waring, A. J., Gillespie, E. J., Bradley, K. A., Ratner, A. J., Rest, R. F., & Lu, W. (2009). Human α-defensins inhibit hemolysis mediated by cholesterol-dependent cytolysins. *Infection and Immunity*, *77*, 4028–4040.

Li, J., & Buchner, J. (2013). Structure, Function and Regulation of the Hsp90 Machinery. *Biomedical Journal*, *36*, 106–117.

Li, J., Soroka, J., & Buchner, J. (2012). The Hsp90 chaperone machinery: Conformational dynamics and regulation by co-chaperones. *Biochimica et Biophysica Acta - Molecular Cell Research*, *1823*, 624–635.

Liu, J., Farmer, J. D., Lane, W. S., Friedman, J., Weissman, I., & Schreiber', S. L. (1991). Calcineurin Is a Common Target of Cyclophilin-Cyclosporin A and FKBP-FK506 Complexes. *Cell*, *66*, 807–815.

Locht, C. (2021). The path to new pediatric vaccines against pertussis. *Vaccines*, *9*, 1–13.

Locht, C., & Antoine, R. (2021). The history of pertussis toxin. *Toxins*, *13*.

Locht, C., Coutte, L., & Mielcarek, N. (2011). The ins and outs of pertussis toxin. *FEBS Journal*, *278*, 4668–4682.

Long, S. S., Welkon, C. J., & Clark, J. L. (1990). Widespread Silent Transmission of Pertussis in Families: Antibody Correlates of Infection and Symptomatology. *The Journal of Infectious Diseases*, *161*, 480–486. https://academic.oup.com/jid/article/161/3/480/2190492

Mattar, E. H., Almehdar, H. A., Yacoub, H. A., Uversky, V. N., & Redwan, E. M. (2016). Antimicrobial potentials and structural disorder of human and animal defensins. *Cytokine and Growth Factor Reviews*, *28*, 95–111.

Mattoo, S., & Cherry, J. D. (2005). Molecular pathogenesis, epidemiology, and clinical manifestations of respiratory infections due to Bordetella pertussis and other Bordetella subspecies. *Clinical Microbiology Reviews*, *18*, 326–382.

Nigro, P., Pompilio, G., & Capogrossi, M. C. (2013). Cyclophilin A: A key player for human disease. *Cell Death and Disease*, *4*, e888-10.

Pachón-Ibáñez, M. E., Smani, Y., Pachón, J., & Sánchez-Céspedes, J. (2017). Perspectives for clinical use of engineered human host defense antimicrobial peptides. *FEMS Microbiology Reviews*, *41*, 323–342.

Paddock, C. D., Sanden, G. N., Cherry, J. D., Gal, A. A., Langston, C., Tatti, K. M., Wu, K. H., Goldsmith, C. S., Greer, P. W., Montague, J. L., Eliason, M. T., Holman, R. C., Guarner, J., Shieh, W. J., & Zaki, S. R. (2008). Pathology and pathogenesis of fatal Bordetella pertussis infection in infants. *Clinical Infectious Diseases*, *47*, 328–338.

Pande, A. H., Moe, D., Jamnadas, M., Tatulian, S. A., & Teter, K. (2006). The Pertussis Toxin S1 Subunit Is a Thermally Unstable Protein Susceptible to Degradation by the 20S Proteasome. *Biochemistry*, *45*, 13734–13740.

Pande, A. H., Scaglione, P., Taylor, M., Nemec, K. N., Tuthill, S., Moe, D., Holmes, R. K., Tatulian, S. A., & Teter, K. (2007). Conformational Instability of the Cholera Toxin A1 Polypeptide. *Journal of Molecular Biology*, *374*, 1114–1128.

Paramonov, V. M., Sahlgren, C., Rivero-Müller, A., & Pulliainen, A. T. (2020). IGIST - A Kinetic Bioassay for Pertussis Toxin Based on Its Effect on Inhibitory GPCR Signaling. *ACS Sensors*, *5*, 3438–3448.

Plaut, R. D., Scanlon, K. M., Taylor, M., Teter, K., & Carbonetti, N. H. (2016). Intracellular disassembly and activity of pertussis toxin require interaction with ATP. *Pathogens and Disease*, *74*, 1–9.

Pratt, W. B., & Toft, D. O. (1997). Steroid receptor interactions with heat shock protein and immunophilin chaperones. *Endocrine Reviews*, *18*, 306–360.

Punnonen, E.-L., Ryhänen, K., & Marjomi, V. S. (1998). At reduced temperature, endocytic membrane traffic is blocked in multivesicular carrier endosomes in rat cardiac myocytes. *European Journal of Cell Biology*, *75*, 344–352.

Ratajczak, T., Carello, A., Mark, P. J., Warner, B. J., Simpson, R. J., Moritz, R. L., & House, A. K. (1993). The cyclophilin component of the unactivated estrogen receptor contains a tetratricopeptide repeat domain and shares identity with p59 (FKBP59). *Journal of Biological Chemistry*, *268*, 13187–13192.

Ratts, R., Zeng, H., Berg, E. A., Blue, C., McComb, M. E., Costello, C. E., VanderSpek, J. C., & Murphy, J. R. (2003). The cytosolic entry of diphtheria toxin catalytic domain requires a host cell cytosolic translocation factor complex. *Journal of Cell Biology*, *160*, 1139–1150.

RKI. (2020). *Infektionsepidemiologisches Jahrbuch meldepflichtiger Krankheiten für 2020*.

Rodas, P. I., Álamos-Musre, A. S., Álvarez, F. P., Escobar, A., Tapia, C. V., Osorio, E., Otero, C., Calderón, I. L., Fuentes, J. A., Gil, F., Paredes-Sabja, D., & Christodoulides, M. (2016). The NarE protein of neisseria gonorrhoeae catalyzes ADP-ribosylation of several ADP-ribose acceptors despite an N-terminal deletion. *FEMS Microbiology Letters*, *363*, fnw181.

Roe, S. M., Prodromou, C., O'Brien, R., Ladbury, J. E., Piper, P. W., & Pearl, L. H. (1999). Structural basis for inhibition of the Hsp90 molecular chaperone by the antitumor antibiotics radicicol and geldanamycin. *Journal of Medicinal Chemistry*, *42*, 260–266.

Rosenwirth, E., Billich, A., Datema, R., Donatsch, P., Hammerschmid, F., Harrison, R., Hiestand, P., Jaksche, H., Mayer, P., Peichl, P., Quesniaux, V., Schatz, F., Schuurman, H., Traber, R., Wenger, R., Wolff, B., Zenke, G., & Zurini, M. (1994). Inhibition of Human Immunodeficiency Virus Type 1 Replication by SDZ NIM 811, a Nonimmunosuppressive Cyclosporine Analog. *Antimicrobial Agents and Chemotherapy*, *38*, 1763–1772.

Scanlon, K., Skerry, C., & Carbonetti, N. (2019a). Association of pertussis toxin with severe pertussis disease. *Toxins*, *11*, 373.

Scanlon, K., Skerry, C., & Carbonetti, N. (2019b). Role of Major Toxin Virulence Factors in Pertussis Infection and Disease Pathogenesis. In *Advances in Experimental Medicine and Biology* (Vol. 1183, pp. 35–51).

Scheufler, C., Brinker, A., Bourenkov, G., Pegoraro, S., Moroder, L., Bartunik, H., Hartl, F. U., & Moarefi, I. (2000). Structure of TPR domain-peptide complexes: Critical elements in the assembly of the Hsp70-Hsp90 multichaperone machine. *Cell*, *101*, 199–210.

Schlecht, R., Scholz, S. R., Dahmen, H., Wegener, A., Sirrenberg, C., Musil, D., Bomke, J., Eggenweiler, H. M., Mayer, M. P., & Bukau, B. (2013). Functional analysis of Hsp70 inhibitors. *PLoS ONE*, *8*, e78443.

Schmid, S. L., & Smythe, E. (1991). Stage-specific assays for coated pit formation and coated vesicle budding in vitro. *The Journal of Cell Biology*, *114*, 869–880.

Schuster, M., Schnell, L., Feigl, P., Birkhofer, C., Mohr, K., Roeder, M., Carle, S., Langer, S., Tippel, F., Buchner, J., Fischer, G., Hausch, F., Frick, M., Schwan, C., Aktories, K., Schiene-Fischer, C.,

& Barth, H. (2017). The Hsp90 machinery facilitates the transport of diphtheria toxin into human cells. *Scientific Reports*, *7*, 1–14.

Schütz, D., Ruiz-Blanco, Y. B., Münch, J., Kirchhoff, F., Sanchez-Garcia, E., & Müller, J. A. (2020). Peptide and peptide-based inhibitors of SARS-CoV-2 entry. *Advanced Drug Delivery Reviews*, *167*, 47–65.

Spangrude, G. J., Sacchi, F., Hill, H. R., Van Epps, D. E., & Daynes, R. A. (1985). Inhibition of lymphocyte and neutrophil chemotaxis by pertussis toxin. *The Journal of Immunology*, *135*, 4135–4143.

Stein, P. E., Boodhoo, A., Armstrong, G. D., Cockle, S. A., Klein, M. H., & Read, R. J. (1994). The crystal structure of pertussis toxin. *Structure*, *2*, 45–57.

Surridge, J., Segedin, E. R., & Grant, C. C. (2007). Pertussis requiring intensive care. *Archives of Disease in Childhood*, *92*, 970–975.

Tamura, M., Nogimori, K., Murai, S., Yajima, M., Ito, K., Katada, T., Ui, M., & Ishii, S. (1982). Subunit structure of islet-activating protein, pertussis toxin, in conformity with the A-B model. *Biochemistry*, *21*, 5516–5522.

Taylor, M., Navarro-Garcia, F., Huerta, J., Burress, H., Massey, S., Ireton, K., & Teter, K. (2010). Hsp90 is required for transfer of the cholera toxin A1 subunit from the endoplasmic reticulum to the cytosol. *Journal of Biological Chemistry*, *285*, 31261–31267.

Teter, K. (2019). Intracellular trafficking and translocation of pertussis toxin. *Toxins*, *11*, 1–12.

Tong, M., & Jian, Y. (2015). FK506-Binding Proteins and Their Diverse Functions. *Current Molecular Pharmacology*, *9*, 48–65.

Wang, A., Chen, F., Wang, Y., Shen, M., Xu, Y., Hu, J., Wang, S., Geng, F., Wang, C., Ran, X., Su, Y., Cheng, T., & Wang, J. (2013). Enhancement of Antiviral Activity of Human Alpha-Defensin 5 against Herpes Simplex Virus 2 by Arginine Mutagenesis at Adaptive Evolution Sites. *Journal of Virology*, *87*, 2835–2845.

Wang, C., Shen, M., Gohain, N., Tolbert, W. D., Chen, F., Zhang, N., Yang, K., Wang, A., Su, Y., Cheng, T., Zhao, J., Pazgier, M., & Wang, J. (2015). Design of a Potent Antibiotic Peptide Based on the Active Region of Human Defensin 5. *Journal of Medicinal Chemistry*, *58*, 3083–3093.

Wei, G., de Leeuw, E., Pazgier, M., Yuan, W., Zou, G., Wang, J., Ericksen, B., Lu, W. Y., Lehrer, R. I., & Lu, W. (2009). Through the looking glass, mechanistic insights from enantiomeric human defensins. *Journal of Biological Chemistry*, *284*, 29180–29192.

Wei, G., Pazgier, M., de Leeuw, E., Rajabi, M., Li, J., Zou, G., Jung, G., Yuan, W., Lu, W.-Y., Lehrer, R. I., & Lu, W. (2010). Trp-26 Imparts Functional Versatility to Human α-Defensin HNP1. *Journal of Biological Chemistry*, *285*, 16275–16285.

Weiss, A. A., & Goodwin, S. M. (1989). Lethal Infection by Bordetella pertussis Mutants in the Infant Mouse Model. *Infection and Immunity*, *57*, 3757–3764.

Weiss, A. A., Hewlett, E. L., Myers, G. A., & Falkow, S. (1984). Pertussis Toxin and Extracytoplasmic Adenylate Cyclase as Virulence Factors of Bordetella pertussis. *The Journal of Infectious Diseases*, *150*, 219–222.

WHO. (2016). Pertussis vaccines: WHO position paper, August 2015-Recommendations. *Vaccine*, *34*, 1423–1425.

WHO Immunization Coverage. (n.d.). *WHO Immunization Coverage*. Available Online: Https://Www.Who.Int/News-Room/Fact-Sheets/Detail/Immunization-Coverage (Accessed on 15 June 2023).

Wilkinson, K., Righolt, C., Elliott, L., Fanella, S., & Mahmud, S. (2021). Pertussis vaccine effectiveness and duration of protection - A systematic review and meta-analysis. *Vaccine*, *39*, 3120–3130.

Williamson, D. S., Borgognoni, J., Clay, A., Daniels, Z., Drysdale, M. J., Foloppe, N., Francis, G. L., J, C., Howes, R., Macias, A. T., Murray, J. B., Parsons, R., Shaw, T., Surgenor, A. E., Terry, L., Wang, Y., Wood, M., Massey, A. J., Dokurno, P., & Graham, C. J. (2009). Novel Adenosine-Derived Inhibitors of 70 kDa Heat Shock Through Structure-Based Design. *Journal of Medicinal Chemistry*, *52*, 1510–1513.

Witvliet, M. H., Burns, D. L., Brennan, M. J., Poolman, J. T., & Manclark, C. R. (1989). Binding of pertussis toxin to eucaryotic cells and glycoproteins. *Infection and Immunity*, *57*, 3324–3330.

Worthington, Z. E. V., & Carbonetti, N. H. (2007). Evading the proteasome: Absence of lysine residues contributes to pertussis toxin activity by evasion of proteasome degradation. *Infection and Immunity*, *75*, 2946–2953.

Xu, Y., & Barbieri, J. T. (1995). Pertussis toxin-mediated ADP-ribosylation of target proteins in Chinese hamster ovary cells involves a vesicle trafficking mechanism. *Infection and Immunity*, *63*, 825–832.

Xu, Y., & Barbieri, J. T. (1996). Pertussis toxin-catalyzed ADP-ribosylation of Gi-2 and Gi-3 in CHO cells is modulated by inhibitors of intracellular trafficking. *Infection and Immunity*, *64*, 593–599.

Yeung, K. H. T., Duclos, P., Nelson, E. A. S., & Hutubessy, R. C. W. (2017). An update of the global burden of pertussis in children younger than 5 years: a modelling study. *The Lancet Infectious Diseases*, *17*, 974–980.

Zhao, L., & Lu, W. (2014). Defensins in innate immunity. *Current Opinion in Hematology*, *21*, 37–42.

Zhu, X., Zhu, Y., Ye, S., Wang, Q., Xu, W., Su, S., Sun, Z., Yu, F., Liu, Q., Wang, C., Zhang, T., Zhang, Z., Zhang, X., Xu, J., Du, L., Liu, K., Lu, L., Zhang, R., & Jiang, S. (2015). Improved Pharmacological and Structural Properties of HIV Fusion Inhibitor AP3 over Enfuvirtide: Highlighting Advantages of Artificial Peptide Strategy. *Scientific Reports*, *5*, 13028.

5 Statutory Declaration

I hereby declare that I wrote the present dissertation with the topic:

"Characterization of new approaches to inhibit Pertussis toxin based on human peptides and cellular chaperone inhibitors"

independently and used no other aids that those cited. In each individual case, I have clearly identified the source of the passages that are taken word for word or paraphrased from other works.

I also hereby declare that I have carried out my scientific work according to the principles of good scientific practice in accordance with the current „Satzung der Universität Ulm zur Sicherung guter wissenschaftlicher Praxis" [Rules of the University of Ulm for Assuring Good Scientific Practice].

Ulm,

Carolin Kling